Fall 12-17-2011

Identification of Power System Stability Using Relevant Modes

Rogers Whitlock Jr
University of New Orleans, rwhitloc@uno.edu

Identification of Power System Stability Using Relevant Modes

A Thesis

Submitted to the Graduate Faculty of the
University of New Orleans
in partial fulfillment of the
requirements for the degree of

Master of Science
in
Engineering

by

Rogers Whitlock Jr

B.S. Southern University A&M College, 2004

December 2011

Table of Contents

List of Figures

Abstract

The purpose of this investigation is to identify appropriate location of capacitor banks and sources of reactive power by studying power system stability in the vicinity of system equilibrium states. The locations for reactive power sources are determined by identifying those modes of the system that participate most in the system behavior in general and in dictating the final state of the system after experiencing faults or disturbances. To identify the relevant modes of the system that participate most in the system dynamic, we shall make use of modal and participation analysis for different system conditions. We also apply modal and participation analysis to a system in order to identify the components of greatest impact that result in the most efficient system control. The ideas developed in this study are used to analyze and identify weak boundaries of the IEEE 39- Bus system that contribute to the system's instability.

Keywords: simulation, dynamics, computing, load flow, reactive power, power transmission, small signal stability, modal analysis, eigenvalues

Chapter 1

Introduction and objective

Small Signal Stability

Power System Stability – Small Signal Stability: Historical Review

1.1 Power Systems

We begin with a general discussion that answers the questions, "What is a power system and what is small signal stability?" Power systems as a whole are comprised of the means of generating power, transferring said power to desired destinations and the loads that will make use of the generated power. In reality, power systems often incorporate much more as the size and complexity of the system grows, but this generalized framework shall suffice as our precursor into small signal stability. Concerning the first component of a power system, power generation, there are numerous ways this is currently done. Power can be generated on a large scale from materials such as coal, natural gas, oil, nuclear sources, water and wind. For coal, natural gas and petroleum, the byproducts of combustion are utilized to provide mechanical power, which in turn powers a turbine to produce energy. For nuclear power, nuclear fission takes advantage of the extreme heat produced during such a reaction. This heat is used in conjunction with cooling water to produce steam that drives a turbine much the same way as fossil fuel plants. Hydroelectric power generation utilizes the kinetic energy of descending water to power turbines that turn mechanical energy into electrical energy. Wind power works much the same way as hydroelectric with the power source being wind as opposed to moving water. Many other power generation methods are in use and take advantage of varying sources such as solar power, tidal waves, ocean thermal energy conversion and many others. No matter what type of power generation is considered, they all operate on the principle idea of converting one type of energy into another. The means may differ, the methods, efficiency and system needed may differ, but the postulate of energy conversion (taking one type of energy and turning it into electrical energy) remains. The next component of power systems are the means by which the generated power is transferred to a desired destination. These transmission and distribution systems vary but have limitations, safety and reliability aspects to consider. Simply put, the transmission of generated electric power is the transfer of electricity down insulated conductors. The control of this transfer is where the distribution aspect of the system comes in but oftentimes mimics the transmission system on a smaller scale. The interconnected power systems of the U.S. are broken down into large areas (Western Systems Coordinating Council, North American Power Systems Interconnection, etc.) which aides in system structure and reliability. From these large interconnected areas, the transmission and distribution system continues with horizontally integrated companies responsible for different aspects of the system (generation, transmission, distribution). The equipment involved in this area of power systems include substations, switchgear, motor control centers, transformers, capacitor banks and a host of other components that work in unison to distribute power to a variety of end users. Finally, we complete our overview of power systems with mention of the end users that drive the need for generated power in the first place. End users vary from large industrial manufacturing plants to small individual households. As a result, the power demand for various users also differs significantly. Despite the amount required, making reliable energy available is the end result of any and every power system.

As mentioned earlier, reliability of a power system is of major concern. As a result, it is easy to see why having a working understanding of every aspect of the power system, its operation and behavior is of utmost importance. In addition to reliability, other considerations warrant power system analysis. These include safety, planning of new and expanding systems,

maintenance of power systems and dealing with disturbances both within and outside of the system.

1.2 Power system stability

Power system stability is no new subject, having been established as a field of study as early as the 1920's. As with any technical arena, the early stages were of much less complexity and revolved around electric generation supplying areas over long transmission systems. These power systems met instability of fewer types due to simpler system design and operation. The main problems were synchronization that was addressed by how robust the transmission system was designed to be. With much less knowledge of the detailed models behind these systems and with much less computational power available, the economical efficiency and reliability of these systems was limited. As calculative ability and newer analysis techniques were developed, analysis improved but there were still many simplifying assumptions being made to allow this. Positive damping is one example as well as the idea of treating systems as two-machine systems. This cycle of new analysis techniques continued leading to the evolution of power systems and their application. By the 1930's interconnection of different systems and scaled physical models were introduced to the field. Interconnection obviously adds to the complexity of system analysis that was however somewhat alleviated due to the fact that the physical models expanded system analysis to include multi-machine systems. Despite these improvements in system study, the limitation of large, complicated calculation efforts thwarted further development and restricted the overall emphasis of analysis to the network as opposed to the inner workings of the machines involved. Simple model components were used for the voltage sources and loads instead of more detailed representations. The next wave of progression came by way of performance enhancement. Stability of systems was improved by faster protection devices and the increased capability of regulation components within the system. As with every action, the equal and opposite reaction of these advents was decreased damping resulting in problems from oscillation becoming more widespread. Again, the analysis of these newer trends was limited by complexity of their calculation. It wasn't until the 1950's that crude computers allowed more than just the system behavior to be scrutinized. With this increased evaluation capacity, individual components of equipment characteristics could also be evaluated. At about the 1960's two main trends started to dominate system analysis. Interconnection of systems became an increasingly larger concern as transient stability also became more of a focal point. All of the improvements mentioned above continued; new analytical methods, increased computational ability due to computers, increasingly detailed modeling, new and more complicated testing and higher performance levels of system components all continued to take place and shape the world of power system stability to what it has become today.

With the progression of power system stability now reviewed, we ask, "So what exactly is stability?" According to Kundur [1], Power System Stability is defined as that property of a power system that enables it to remain in a state of operating equilibrium under normal operating conditions and to regain an acceptable state of equilibrium after being subjected to a disturbance. This definition goes a long way in shaping the aspects of power systems that each technique and methodology must address. This equilibrium to be maintained both before and after disturbances incorporates several aspects and is dependent upon a number of system parameters. Synchronization of the machines within the system and voltage stability are of primary concern and the components that govern these characteristics are heavily scrutinized as they form the

building blocks of stability analysis. One of the chief components of synchronization is rotor angle. Rotor angle, in essence, is the angle between a machine's rotor axis and stator axis; and all of the synchronous machines within a power system must maintain a synchronized state of equilibrium between their rotor angles. As a result, rotor angle and the stability thereof is one of the fundamental concerns of analysis. Another important aspect of system stability that involves the rotors of the machines is the power-rotor angle relationship that is involved. This complex, non-linear correlation not only accounts for the amount of power transferred but also the ability of the system to return to equilibrium after a disturbance. The third major component of power system stability is rotor speed. The change in rotor speed upon experiencing some type of disturbance can have significant effects on the damping characteristics of the system. As a result, oscillatory stability becomes a key point of emphasis.

Having explained stability and the chief components involved, we now delve into the two designations of disturbances involved in stability analysis. These two divisions are small-signal stability analysis of small disturbances and transient stability analysis of large disturbances. Indicative of its nomenclature, small-signal stability is the study of system response to small disturbances. These disturbances result in the system having to cope with synch issues from rotor angle displacement or oscillation problems from insufficient damping. Synch issues often involve application of voltage regulation but oscillation problems comprise the majority of instability events and are more complex due to having several different modes of oscillation to deal with. Generally speaking, small signal stability involves the analysis of power systems around an equilibrium point. This eliminates non-linearities and complex dynamics of the system; thus stability is examined for small disturbances using a simplified system model. The purpose and usefulness of small signal stability analysis is to generate characteristics of system behavior with minimal error while significantly decreasing both the complexity and scale of computation involved. With the size and complexity of power systems ever increasing, the computational effort involved can easily surpass feasible limits even when utilizing computers and other speed processing equipment. As a result, simplified techniques can be used to yield rather precise and useful characteristics of a system that in turn, indicate system response and behavior, all while greatly reducing the effort involved. The term "small signal" reflects the minor disturbances used to evaluate the simplified system model. Small disturbances within a system are common and refer to disturbances that allow representation of the nonlinear system as a linearized model. These disturbances can include load changes, and various oscillations and resonance within a power system. So what is the general idea behind small signal stability? As mentioned earlier, small signal stability takes a power system relation involving complex nonlinearities and analyzes a stable system around an equilibrium point as it experiences small perturbations. This is done by linearizing the system around a point or utilizing other techniques that eliminate complex dynamics. This effectively takes a nonlinear system and transforms it into a linear system where many assumptions and simplifications can be made. It is important to note that the linear approximation is only made at a certain point and changes at each different point in time.

Conversely, transient stability analysis refers to the analysis of power systems accounting for the non linear dynamics of the modeled system. Larger disturbances justify analysis of the system's response at different operating points as the system characteristics change. Transient stability analysis differs in the type and degree of disturbance but can often decompose into a state similar to small signal instability. Concerning transient instability, synchronization issues

can result from first swing issues or long term end state instability can result from growing oscillations.

1.3 Thesis Contributions

The purpose of this study is to introduce power systems and small signal stability then analyze a system using modal analysis as we explore the effect and relationship of small signal stability and voltage stability of the system. While determining the different modes of oscillation, special attention will be paid to the impact and effect specific changes have on the power system. This will enable us to more clearly see how power systems operate, understand the advantages gained using certain power system analysis techniques and quantitatively determine the most effective way to achieve optimal results in system correction. The remainder of the thesis is devoted to:

Chapter 2: The second chapter of this literary work is devoted to establishing a mathematical foundation behind small signal stability and modal analysis techniques. A literature review is conducted to explain and explore the derivations of the numerical methods used by the simulation software to analyze the power system. The small signal stability areas addressed include linearization of non-linear differential equations that model a power system, modal analysis via state space representation, eigenvalue analysis, eigenvectors, phase portraits and participation factor analysis. Upon completion of Chapter 2, a thorough understanding of the small signal stability analysis process should be obtained.

Chapter 3: The third chapter is devoted to introducing both the power system that is used in the research and the simulation software used to conduct that analysis. The IEEE 39 bus system is presented along with all of the system data inputs that are necessary to model and analyze system operation. These inputs include voltage magnitude and angle, real and reactive power, impedance, admittance, and component data for the system buses, generators, loads, shunt capacitors, transformers and transmission lines. In addition, the simulation software PSS/E and NEVA are present. Software information that is detailed includes the capabilities and calculative processes involved in system analysis. Examples are then shown of the results yielded by PSS/E and NEVA and explanations are given as to the interpretation and significance of the charts and graphs.

Chapter 4: The fourth chapter is devoted to presenting the simulation results and the analysis thereof. A methodology is also outlined as to the approach taken during the research. The results published in this chapter include system eigenvalues, mode distribution, voltage stability analysis using load flow, and participation analysis using the modal analysis results.

Chapter 5: The fifth chapter is devoted to discussing the conclusions that are to be drawn from the research results and future work. These conclusions include system stability, the interconnection between modal stability of the system and voltage stability, and the system component that participates most in modal stability.

Following Chapter 5, an Appendix is included containing all of the modal analysis simulation results that were not directly addressed in Chapter 4. This information can be drawn upon when

a more detailed account of the modal stability of the various system configurations is needed. Finally, a list of references and a Vita about the author completes the thesis work.

Chapter 2

Literature Review

Small Signal Stability

2.1 Small signal stability

As in most engineering analysis, the process begins with modeling the system you wish to analyze. This allows you to mathematically quantify the system response to whatever stimulus is injected. Only then can detailed portraits of system behavior be drawn upon which design methodology is based. As stated earlier, small signal stability analysis is characterized by the linear nature of the model equations used to represent the system. As a result, the initial step in system analysis is to take the non-linear system equations and linearize them around an equilibrium point. The general formulation method used is state-space representation. This representation format quantifies the system into the simplest of terms while still holding the true characteristics needed to outline the behavior of the system. The components that make up this representation are the state variables of the power system itself and it is the combination of these variables along with system inputs that determine how the system performs. For any given system there exists a singular behavior pattern for that system given a set of inputs. However, there are often nonexclusive state space representations for that system, as differing state variables can often be chosen to accurately represent the system.

The equilibrium points around which the analysis takes place basically takes a snapshot of the system's response to a given input at a specific instant of time. This is found by setting all of the derivatives to zero and solving, which graphically represents zero velocity. Linear systems only have one equilibrium point and satisfy the equation $f(x_0) = 0$ and therefore contain information about the system's stability.

Linear systems possess the nature of having stability, or lack thereof, independent of the input. Whether or not a system is stable depends solely on the system itself. As a result any system that is stable will return to that stable state assuming zero input. The stable states of a linearized system can be categorized two different ways. A system is asymptotically stable if it returns to the same equilibrium point after a small disturbance. Local stability bespeaks the return of a system to some other equilibrium after a small disturbance, all the while remaining within a small region around the original equilibrium point.

The state space representation and subsequent linearization of a power system begins with the description of the corresponding nonlinear differential equations. These differential equations are those, such as the popular swing equation, that numerically model the operation of the different components of the system. In the instance of the generator models, the angular dynamics between the rotor and stator axis depend on the angular difference:

$$\theta(t) = (\omega_o + \theta_o) + \Delta\theta(t) \tag{2.1}$$

Note; ω is the rotary angle that determines the frequency.

Using the classical model, the essential differential equation (swing equation) for modeling the dynamic behavior of synchronous machine, is provided by Equation 2.2.

$$M\ddot{\delta}(t) + D\dot{\delta}(t) + P_G(\delta) = P_M^O \tag{2.2}$$

Note; δ is the angle of generator and P_M is the mechanical power that is converted to electrical power.

From these types of basic equations, state space representation is initiated with the desired variable (i.e. rotor angle) defined as the independent input variable $\dot{x}_i$. Thus yielding the form of Equation 2.3

$$\dot{x}_i = f_i(x_1, x_2, ...x_n; u_1, u_2, ..., u_r; t) \quad i = 1,2,....,n) \tag{2.3}$$

From Equation 2.3, a vector-matrix notation is conceived that is comprised of a state vector, input vector and function relating the two where the function and variable vectors are of the form in Equation 2.4.

$$x = \begin{bmatrix} x_1 \\ x_2 \\ \vdots \\ x_n \end{bmatrix} \qquad u = \begin{bmatrix} u_1 \\ u_2 \\ \vdots \\ u_r \end{bmatrix} \qquad f = \begin{bmatrix} f_1 \\ f_2 \\ \vdots \\ f_n \end{bmatrix} \tag{2.4}$$

This relation in turn, governs the response of the system as outside inputs are added. An output vector is also created describing what is observed involving the same state and input variables used in the state vector of Equation 2.5

$$y = g(x,u) \tag{2.5}$$

Where y and g are defined as the vectors in equation 2.6

$$y = \begin{bmatrix} y_1 \\ y_2 \\ \vdots \\ y_m \end{bmatrix} \qquad g = \begin{bmatrix} g_1 \\ g_2 \\ \vdots \\ g_m \end{bmatrix} \tag{2.6}$$

Next, we specify initial state and input vectors x_0 and u_0 and utilize the zero velocity characteristic mentioned earlier in order to linearize the system.

$$\dot{x}_0 = f(x_0, u_0) = 0 \tag{2.7}$$

A small disturbance is then added in the form of deviations Δx and Δu . This allows utilization of Taylor series expansion with the higher order terms removed resulting in linearized equations.

$$\dot{x} = x_0 + \Delta x = f\left[\left(\dot{x}_0 + \Delta x\right), \left(u_0 + \Delta u\right)\right] \tag{2.8}$$

$$\dot{x}_i = \dot{x}_{i0} + \Delta\dot{x}_i = f_i\left[(x_0 + \Delta x),(u_0 + \Delta u)\right] = f_i(x_0,u_0) + \frac{\partial f_i}{\partial x_1}\Delta x_1 + ... + \frac{\partial f_i}{\partial x_n}\Delta x_n + \frac{\partial f_i}{\partial u_1}\Delta u_1 + ... + \frac{\partial f_i}{\partial u_r}\Delta u_r \tag{2.9}$$

$$\Delta\dot{x}_i = \frac{\partial f_i}{\partial x_1}\Delta x_1 + ... + \frac{\partial f_i}{\partial x_n}\Delta x_n + \frac{\partial f_i}{\partial u_1}\Delta u_1 + ... + \frac{\partial f_i}{\partial u_r}\Delta u_r \tag{2.10}$$

$$\Delta\dot{y}_i = \frac{\partial g_i}{\partial x_1}\Delta x_1 + ... + \frac{\partial g_i}{\partial x_n}\Delta x_n + \frac{\partial g_i}{\partial u_1}\Delta u_1 + ... + \frac{\partial g_i}{\partial u_r}\Delta u_r \tag{2.11}$$

These can be more conveniently grouped into the form shown in Equations 2.12 and 2.13.

$$\Delta\dot{x} = A\Delta x + B\Delta u \tag{2.12}$$

$$\Delta y = C\Delta x + D\Delta u \tag{2.13}$$

A, B, C, and D are vectors defined in Equation 2.14.

$$A = \begin{bmatrix} \frac{\partial f_1}{\partial x_1} & \cdots & \frac{\partial f_1}{\partial x_n} \\ \cdots & \ddots & \cdots \\ \frac{\partial f_n}{\partial x_1} & \cdots & \frac{\partial f_n}{\partial x_n} \end{bmatrix} B = \begin{bmatrix} \frac{\partial f_1}{\partial u_1} & \cdots & \frac{\partial f_1}{\partial u_r} \\ \cdots & \ddots & \cdots \\ \frac{\partial f_n}{\partial u_1} & \cdots & \frac{\partial f_n}{\partial u_r} \end{bmatrix}$$
$$C = \begin{bmatrix} \frac{\partial g_1}{\partial x_1} & \cdots & \frac{\partial g_1}{\partial x_n} \\ \cdots & \ddots & \cdots \\ \frac{\partial g_m}{\partial x_1} & \cdots & \frac{\partial g_m}{\partial x_n} \end{bmatrix} D = \begin{bmatrix} \frac{\partial g_1}{\partial u_1} & \cdots & \frac{\partial g_1}{\partial u_r} \\ \cdots & \ddots & \cdots \\ \frac{\partial g_m}{\partial u_1} & \cdots & \frac{\partial g_m}{\partial u_r} \end{bmatrix} \tag{2.14}$$

The A matrix from above is the most important as it presents a numerical view of the system in which its inherent characteristics can be drawn out. This A matrix is also equivalent to the Jacobian matrix evaluated at the equilibrium point. In order to extract the valuable information stored within the A matrix (State matrix), we must calculate the eigenvalues. This is performed by solving the A matrix's relation to the identity matrix that results in the Characteristic Equation 2.15.

$$\left|\lambda I - A = 0\right| \tag{2.15}$$

Depending on the nature of the resulting values, relevant information about the system can be derived. Consulting Lyapunov's theories, we know a system is asymptotically stable if its

characteristic equation yields eigenvalues of Equation 2.16 with negative real parts. If at least one eigenvalue has a positive real part, the system is unstable. Eigenvalues having real parts of zero yield no conclusive determination. In addition, real and complex eigenvalues differ in oscillatory nature. Real eigenvalues represent non oscillatory modes that decay if the value is negative. If the real eigenvalue is positive, it means the system has aperiodic instability. No matter the sign, magnitude corresponds to the level of behavior in that, the larger the value the heavier the effect. For complex values (that always exist in pairs), oscillation is confirmed. This then enables us to calculate the damping value and frequency of the complex eigenvalues. The amount and tendency of damping is given by the real part of the complex eigenvalue. Negative real parts mean damped oscillation and positive real parts mean growing oscillation. The frequency of oscillation is a function of the imaginary part as shown in Equation 2.17.

$$\lambda = \sigma \pm j\omega \tag{2.16}$$

$$f = \frac{\omega}{2\pi} \tag{2.17}$$

The damping ratio is given by Equation 2.18.

$$\xi = \frac{-\sigma}{\sqrt{\sigma^2 + \omega^2}} \tag{2.18}$$

Lastly, amplitude decay can be found using the damping ratio of Equation 2.19.

$$\varphi = \frac{1}{\sigma} \tag{2.19}$$

Having found the eigenvalues of the system, eigenvectors can then be calculated to specify other aspects of the system's behavior such as mode contribution and shape. Eigenvectors exist as right and left column and row vectors (respectively) that correspond to each eigenvalue. The column vector satisfying Equation 2.20 gives the right eigenvector for each eigenvalue and yields the mode shape.

$$AV_i = \lambda_i V_i \tag{2.20}$$

Conversely, the row vector that represents the left eigenvector is satisfied by Equation 2.21 and gives the contribution of each eigenvalue to its particular mode.

$$V_i A = \lambda_i V_i \tag{2.21}$$

The discerning distinction between right and left eigenvectors is their orthogonality for the multiplication of vectors from differing eigenvalues and a constant result for the multiplication of vectors from the same eigenvalue. The left and right eigenvectors then form Equation 2.22.

$$R = \left[\underline{r_1} \vdots \underline{r_2} \vdots \underline{r_3} \vdots \ldots \vdots \underline{r_n}\right] L = \left[l_1^T \vdots l_2^T \vdots l_3^T \vdots \ldots \vdots l_n^T\right]^T \tag{2.22}$$

A diagonal matrix of the eigenvalues is created as shown in Equation 2.23.

$$\Lambda = \begin{bmatrix} \lambda_1 & 0 & 0 & 0 \\ 0 & \lambda_2 & 0 & 0 \\ 0 & 0 & \ddots & 0 \\ 0 & 0 & 0 & \lambda_n \end{bmatrix} \tag{2.23}$$

Next, we analyze the transformation of the original state variables, such that each variable is linked to only one mode as opposed to each variable being the linear combination of all the modes of the system. This again can yield valuable information about the system as we will then be able to gauge individual participation levels. We begin with Equations 2.24 and 2.25 and form a new state equation of Equation 2.26

$$\Delta x = Rz \tag{2.24}$$

$$R\dot{\boldsymbol{Z}} = ARz \tag{2.25}$$

$$\dot{\boldsymbol{Z}} = R^{-1}ARz \tag{2.26}$$

This new state equation then reduces to Equation 2.27.

$$\dot{\boldsymbol{Z}} = \Lambda z \tag{2.27}$$

Given the time sensitive solution of Equation 2.28, we arrive at the expression in Equation 2.29.

$$z_i(t) = z_i(0)e^{\lambda_i t} \tag{2.28}$$

$$\Delta x(t) = Rz(t) \quad = [R_1 \quad R_2 \quad \cdots \quad R_n] \begin{bmatrix} z_1(t) \\ z_2(t) \\ \vdots \\ z_n(t) \end{bmatrix} \tag{2.29}$$

Using the relations in Equations 2.30 and 2.31, we see the response of any particular variable simplifies to the expression in Equation 2.32

$$\Delta x(t) = \sum_{i=1}^{n} R_i z_i(0)e^{\lambda_i t} \tag{2.30}$$

$$z(t) = R^{-1}\Delta x(t) = L\Delta x(t) \tag{2.31}$$

$$\Delta x_i(t) = R_{i1}c_1e^{\lambda_1 t} + R_{i2}c_2e^{\lambda_2 t} + ... + R_{in}c_ne^{\lambda_n t} \tag{2.32}$$

Note; c_i is known as the magnitude of excitation and is defined as Equation 2.33.

$$c_i = L_i\Delta x(0) \tag{2.33}$$

Using the eigenvector expressions to plot the trajectory we see there exist several possible types for eigenvalues of the form $\lambda_{1,2} = \sigma \pm j\omega$. The trajectory, also known as a phase portrait, is a graphical representation of the stability of the system. In the phase portrait, the trajectory of the eigenvalues are plotted in the phase plane and show stability as well as the oscillation of the mode. Figures 1-6 show common phase portraits exemplified by power systems [14]:

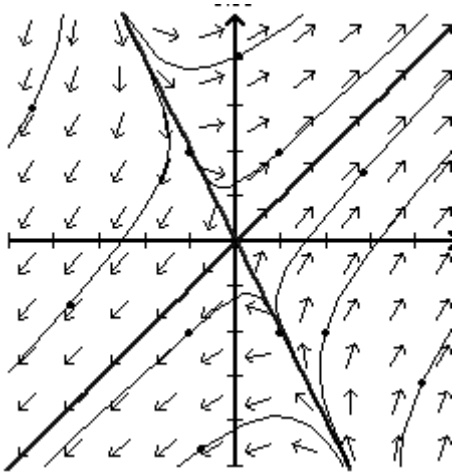

Fig 1 : Saddle node $\left(\lambda_{1,2} = \pm\sigma\right)$

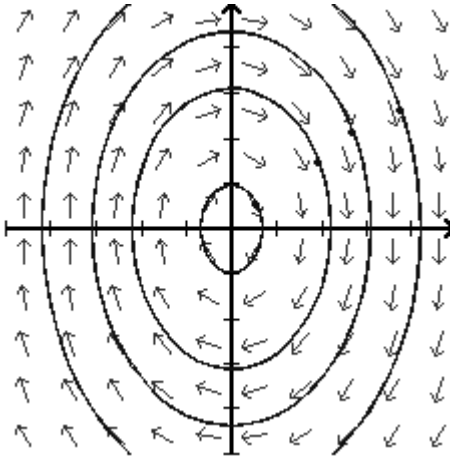

Fig 2 : Vortex $\left(\lambda_{1,2} = \pm j\omega\right)$

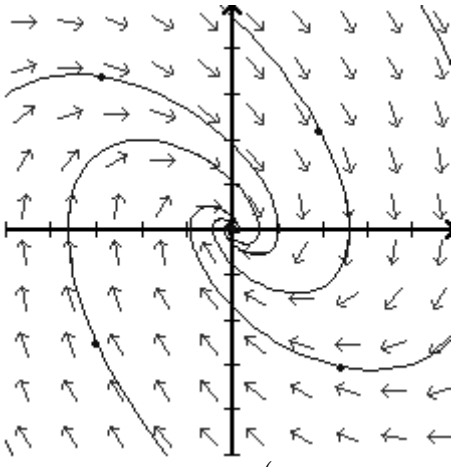

Fig 3 : Stable focus $\left(\lambda_{1,2} = -\sigma \pm j\omega\right)$

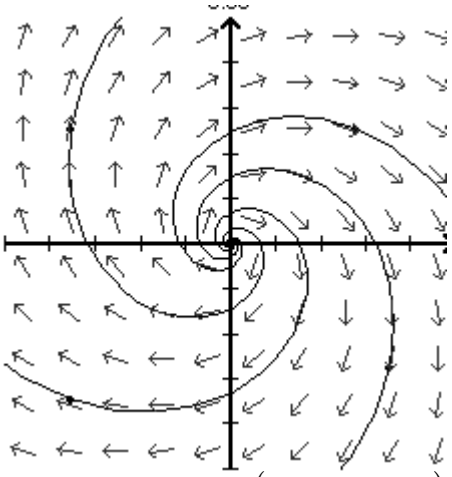

Fig 4: Unstable focus $\left(\lambda_{1,2} = \sigma \pm j\omega\right)$

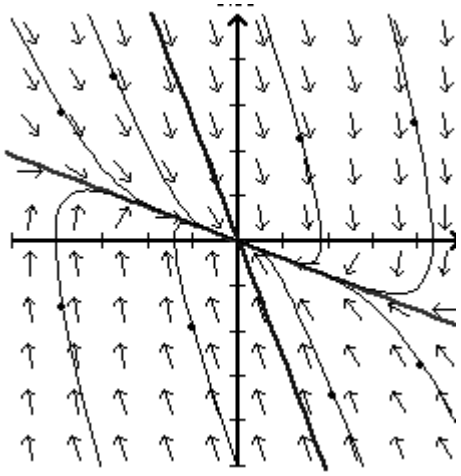

Fig 5 : Stable node $(\lambda = -\sigma)$

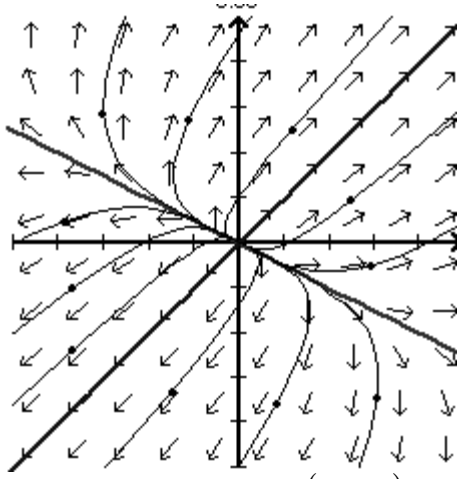

Fig 6: Unstable node $(\lambda = \sigma)$

Now we move to the analysis of the sensitivity an eigenvalues to the state matrix (and its individual components) and participation factors. The sensitivity of an eigenvalue to a particular component within the A matrix is easily computed by differentiating the A matrix by the component as in Equation 2.34

$$\frac{\partial A}{\partial a_{kj}} R_i + A \frac{\partial R_i}{\partial a_{kj}} = \frac{\partial \lambda_i}{\partial a_{kj}} R_i + \lambda_i \frac{\partial R_i}{\partial a_{kj}} \tag{2.34}$$

Then using the left and right eigenvector relationships of Equations 2.35 and 2.36, we can clearly show exactly how controlled each eigenvlaue by a certain component using the formulations in Equations 2.37 and 2.38

$$L_i R_i = 1 \tag{2.35}$$

$$L_i (A - \lambda_i I) = 0 \tag{2.36}$$

$$L_i \frac{\partial A}{\partial a_{kj}} R_i = \frac{\partial \lambda_i}{\partial a_{kj}} \tag{2.37}$$

$$\frac{\partial \lambda_i}{\partial a_{kj}} = L_{ik} R_{ji} \tag{2.38}$$

Next we look into participation factor analysis. In participation factor analysis, a participation matrix is created in which each matrix element is a measurement of the state/mode relationship.

The participation matrix is shown in Equation 2.39; where each element within the matrix is of the form listed in Equation 2.40.

$$P = [\, p_1 \;\; p_2 \;\cdots\; p_n \,] \tag{2.39}$$

$$p_i = \begin{bmatrix} p_{1i} \\ p_{2i} \\ \vdots \\ p_{ni} \end{bmatrix} = \begin{bmatrix} R_{1i} L_{i1} \\ R_{2i} L_{i2} \\ \vdots \\ R_{ni} L_{in} \end{bmatrix} \tag{2.40}$$

Eigenvalue sensitivity can then be related to the diagonal element of the state matrix as shown in Equation 2.41.

$$p_{ki} = R_{ki} L_{ik} = \frac{\partial \lambda_i}{\partial a_{kk}} \tag{2.41}$$

This concludes the mathematical derivations of the equations involved in modal analysis of power system. From the modal analysis process, eigenvalues, eigenvectors and the participation matrix can be derived to detail the characteristics, stability and sensitivity of the power system.

2.2 Methods of solution

We now cover several existing methods of solution concerning the analysis of large power systems. The general idea behind each method is similar in the sense that the aim is to minimize the amount of information being considered. In order to accomplish this, it is important to identify what information must be addressed and what eigenvalues must be focused on.

2.2.1 AESOPS

Analysis of Essentially Spontaneous Oscillations in Power Systems (AESOPS) is the first method presented. AESOPS is an algorithm that minimizes the complexity of computation by focusing on certain eigenvalues of the system. These eigenvalues are those involved in the rotor angle modes of the system. This iterative process begins with an educated guess of what the eigenvalue may be. A torque value is generated from this intial eigenvalue and applied to the rotor of one particular generator. Next, the complex frequency response as a result of the applied torque is determined which yields a linear system response. From this response a new eigenvalue can be calculated. This new value then results in a new torque value that is applied and the process continues until the eiegenvalue converges. Once the desired level of convergence is reached, it is understood that the final value is associated with a certain mode of oscillation that the generator participates in heavily. [2] [4]

2.2.2 MAM

Modified Arnoldi Method (MAM) is approach is another way of determining system characteristics efficiently using a particular reduction method. This method takes a starting vector and composes a matrix called the upper Hessenberg matrix that has the same eigenvalues as the original state matrix A. This upper Hessenberg matrix is a reduced version of the A matrix with certain properties that allow eigenvalues of A that pertain to a specific point can be focused upon. An iterative process can be implemented to increase accuracy and other processes must be carried out during the procedure to ensure a reduction of the accumulated errors. [4]

2.2.3 PEALS

Program for Eigenvalue Analysis of Large Systems (PEALS) is a method that actually uses two of the aforementioned techniques in conjunction; AESOPS and the modified Arnoldi method. These two techniques are used together because they work cohesively as an analysis method if altered to conjoin. The AESOP portion of PEALS determines the eigenvalues involved in the rotor angle modes. [2]

2.2.4 SMA

Selective Modal Analysis (SMA) is a process that deals with the task of analysis through modal order reductions. It is an iterative reduction technique utilizing eigenvalue matrix analysis to converge the original system down to a more concise representation of state contribution. The state variables of motor speed, rotor angle and flux linkage are used to provide a look into the sensitivity and relationships of the state variables, modes and participation factors. The process converges to the more active modes while separating out the less relevant modes of the system. The limitations of SMA in the analysis of power systems revolve around its impracticality on very large power systems. This is due to the sheer size of the matrices the eigenvalue analysis must be applied. With three state variables per generator, thus a matrix three times the number of generators in the system, very large systems drastically increase the difficulty of applying SMA. [3] [4] [9]

2.2.5 S-Method

The S-method is an analytical method that takes advantage of the state matrix by transforming the eigenvalues from one plane to another. Instead of relating the eigenvalues as existing in the s plane, they are converted over into the z plane. This has a profound effect as this transformation now places the eigenvalues into a circumferential axis as opposed the the vertical imaginary axis of the s plane. The corresponding left imaginary axis/right imaginary axis designation in the z plane is the area inside of the circle and outside of the circle. In essence, this is a graphically based tool similar to other techniques that differs in eigenvalue presentation. [2]

2.2.6 Q-R transformation

The Q-R transformation technique is similar to those listed above. In this approach, the A matrix of the system is decomposed into a product of two matrices; Q and R. The Q matrix is a unit matrix and the R matrix is a triangular matrix. Solving for the unknown variables using these matrices yields the eigenvalues in an iterative process, where the solution converges to each eigenvalue of the system.

Chapter 2 has presented the mathematical framework involved in the small signal stability of power systems. The calculative process for modal analysis and eigenvalue determination was covered as well as the left and right eigenvectors that can be found using the eigenvalues. Phase portraits of a power system were introduced, including the numerical forumulas and examples of the most common trajectories encountered in power systems. Participation analysis was also covered, showing how to calculate the sensitivity of a mode to an individual variable. Lastly, brief outlines were provided for several of the most common analysis techniques that utilize the modal and eigenvalue analysis equations that were presented. These techniques included AESOPS, MAM, PEALS, SMA, the S-Method and Q-R transformation.

Now that a general understanding has been presented as to what small signal stability is and how to conduct the small signal stability analysis of a power system, we move on to the presentation of the actual power system that shall be used in this research. The system and the system inputs that are listed in the next chapter are those that shall be analyzed according to the processes outlined in Chapter 2. In addition, the simulation software used to make the analysis of the power system feasible will also be introduced.

Chapter 3

System Model

IEEE 39-bus system

The power system used during the project analysis and modeled in the PSS/E software was the popular IEEE 39-bus test system; also called the New England test system. This system is a reduced equivalent of the 345 kv network that is located in the northeast region of the United States. This system consists of 10 generators, 12 transformers and 19 loads, as pictured in Figure 7.

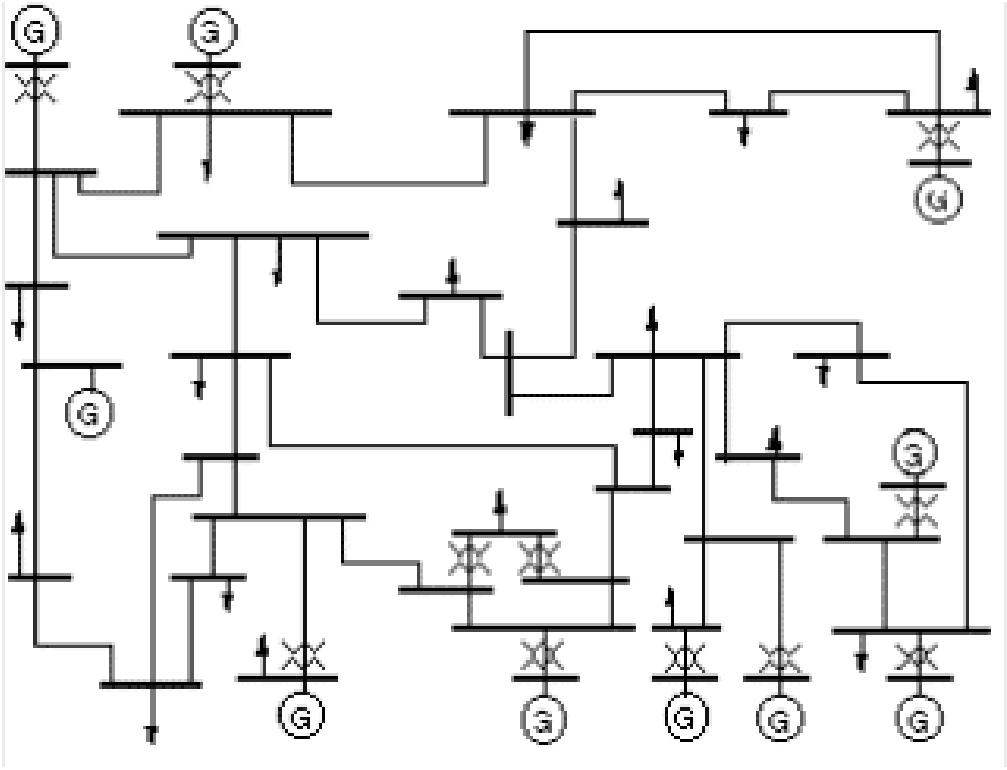

Fig 7: IEEE 39 bus system [15]

This system can be modeled in a certain way where some generators are assumed to represent numerous generators. In this test system, one generator is selected as the slack bus; the infinite bus that serves as both the reference node and balancing bus. For this test system, bus 1 was selected as the slack bus and its characteristics will display as such. Below is the presentation of system characteristics and general descriptions for the various parameters needed by PSS/E to properly model the test system.

3.1 Bus data

The bus data in Table 1 for the specified system includes basic data by which the software determines the system operation. The first set of parameters specified for each bus includes the bus voltage in per unit kv and the bus voltage phase angle in degrees. In addition to this the bus type must also be specified. The options for bus type include 1 – a load bus with no generator boundary condition, 2 – a generator or plant bus that either regulates voltage or has fixed reactive

power. In this type, if and when the generator reaches its reactive power limit, it will no longer control voltage. It only holds reactive power at its limit. 3 – a swing/slack bus and has no power or reactive limits. It regulates voltage at a fixed reference angle. 4 – a bus that is disconnected or isolated.

Table 1: 39 bus system bus data [16]

Bus Number	Base KV	Code	Voltage (pu)	Angle (deg)
1	1	1	1.0455	-9.43
2	1	1	1.0436	-6.86
3	1	1	1.0204	-9.74
4	1	1	0.9978	-10.57
5	1	1	0.9936	-9.34
6	1	1	0.9965	-8.62
7	1	1	0.9408	-10.76
8	1	1	0.9546	-11.37
9	1	1	1.0111	-11.18
10	1	1	1.0086	-6.2
11	1	1	1.0033	-7.03
12	1	1	0.9906	-7.04
13	1	1	1.0051	-6.93
14	1	1	1.001	-8.63
15	1	1	0.9939	-9.01
16	1	1	1.006	-7.52
17	1	1	1.0135	-8.59
18	1	1	1.0147	-9.47
19	1	1	1.0404	-2.81
20	1	1	0.9857	-4.26
21	1	1	1.0136	-5.04
22	1	1	1.0401	-0.49
23	1	1	1.0347	-0.69
24	1	1	1.0138	-7.4
25	1	1	1.0518	-5.47
26	1	1	1.0376	-6.7
27	1	1	1.0205	-8.75
28	1	1	1.0344	-3.08
29	1	1	1.0341	-0.24
30	1	2	1.0475	-4.43
31	1	2	1.04	-1.59
32	1	2	0.9831	1.86
33	1	2	0.9972	2.43
34	1	2	1.0123	0.95
35	1	2	1.0493	4.52
36	1	2	1.0635	7.23
37	1	2	1.0278	1.34
38	1	2	1.0265	6.89
39	1	3	1.03	-10.96

3.2 Generator and Plant data

Concerning the modeling of generators in the PSS/E software as listed in Table 2, there are a number of parameters and characteristics that must be inputted. These include:

- Active power that is supplied by the generator, in MW.
- Maximum and minimum active power values of the generator. If the generator is a fixed output or non-regulating generator then these values must be equal to the active power value.
- Reactive power that is supplied by the generator, in Mvar.
- Maximum and minimum reactive power values of the generator. If the generator is a fixed output or non-regulating generator then these values must be equal to the reactive power value.
- Regulated voltage in per unit kv.
- Base units of Mva that is associated with each generator
- Complex machine impedance, in per unit of the base Mva. This information must be specified if dynamic simulations like fault analysis are to be conducted. In such simulations, this is the unsaturated subtransient impedance of the generator if it is to be modeled by subtransient level machine models. It is the unsaturated transient impedance for classical and transient level models.
- Step up transformer impedance in per unit of the base Mva.
- Step up transformer off nominal turns ratio in per unit.

Table 2: 39 bus system generator data [16]

Bus Number	Code	Pgen	Qgen	Qmax	Qmin	Vsched (pu)	Voltage (pu)	RMPCT
30	2	250	175.2	800	-500	1.0475	1.0475	100
31	2	572.9	774.4	800	-500	1.04	1.04	100
32	2	650	244.8	800	-500	0.9831	0.9831	100
33	2	632	172.2	800	-500	0.9972	0.9972	100
34	2	508	196.3	400	-300	1.0123	1.0123	100
35	2	650	282.2	800	-500	1.0493	1.0493	100
36	2	560	140.7	800	-500	1.0635	1.0635	100
37	2	540	25.3	800	-500	1.0278	1.0278	100
38	2	830	124.9	800	-500	1.0265	1.0265	100
39	3	1005.7	165.9	1500	-1000	1.03	1.03	100

Bus Number	Code	Vsched (pu)	Pgen (MW)	Pmax (MW)	Pmin (MW)	Qgen (Mvar)
30	2	1.0475	250	9999.9	0	175.207
31	2	1.04	572.93	9999.9	0	774.372
32	2	0.9831	650	9999.9	0	244.778
33	2	0.9972	632	9999.9	0	172.224

Table 2: 39 bus system generator data [16]

34	2	1.0123	508	9999.9	0	196.316
35	2	1.0493	650	9999.9	0	282.187
36	2	1.0635	560	9999.9	0	140.745
37	2	1.0278	540	9999.9	0	25.322
38	2	1.0265	830	9999.9	0	124.892
39	3	1.03	1005.729	9999.9	0	165.907

Qmax (Mvar)	Qmax (Mvar)	Mbase (MVA)	R source (pu)	X source (pu)	Rtran (pu)	Xtran (pu)	Gentap (pu)
800	-500	1000	0.0014	0.2	0	0	1
800	-500	1000	0.027	0.2	0	0	1
800	-500	1000	0.00386	0.2	0	0	1
800	-500	1000	0.00222	0.2	0	0	1
400	-300	1000	0.0014	0.2	0	0	1
800	-500	1000	0.0615	0.2	0	0	1
800	-500	1000	0.00268	0.2	0	0	1
800	-500	1000	0.00686	0.2	0	0	1
800	-500	1000	0.003	0.2	0	0	1
1500	-1000	1000	0.001	0.02	0	0	1

3.3 Load data

The parameters inputted into PSS/E for each load are listed in Table 3 and depend on what type of load is present. There can be a constant MVA load, a constant current load or a constant admittance load. As such, the possible parameters include the active power component for for constant Mva (entered in MW), reactive power component value for constant MVA (entered in Mvar), active power value for a constant current load in MW at one per unit voltage, reactive power value for a constant current load in Mvar at one per unit voltage, active power value for a constant admittance load in MW at one per unit voltage, or the reactive power value for a constant admittance load in Mvar at one per unit voltage. As noted in the following load data, all the loads represented in this system are constant MVA loads.

Table 3: 39 bus system load data [16]

Bus Number	Pload (MW)	Qload (Mvar)	Ipload (MW)	Ypload (MW)	Yqload (Mvar)
1	0	0	0	0	0
2	0	0	0	0	0
3	322	2.4	0	0	0

Table 3: 39 bus system load data [16]

4	500	184	0	0	0
5	0	0	0	0	0
6	0	0	0	0	0
7	234	839.9999	0	0	0
8	522	176	0	0	0
9	0	0	0	0	0
10	0	0	0	0	0
11	0	0	0	0	0
12	8.5	88	0	0	0
13	0	0	0	0	0
14	0	0	0	0	0
15	320	153	0	0	0
16	329	323	0	0	0
17	0	0	0	0	0
18	158	30	0	0	0
19	0	0	0	0	0
20	680	103	0	0	0
21	274	115	0	0	0
22	0	0	0	0	0
23	248	84.6	0	0	0
24	309	-92.2	0	0	0
25	224	47.2	0	0	0
26	139	17	0	0	0
27	281	75.5	0	0	0
28	206	27.6	0	0	0
29	284	126.9	0	0	0
31	9.2	4.6	0	0	0
39	1104	250	0	0	0

3.4 Fixed shunt data

The parameters in Table 4 for the shunts include the active and reactive component of the shunt admittance to ground. Also, listed in the plant data section the total percentage of the total Mvar required to hold the voltage at the bus controlled voltage is also needed if there is a valid remote bus and there is more than one local or remote voltage controlling device.

Table 4: 39 bus system fixed shunt data [16]

Bus Number	Bus Name	Id	In Service	G-shunt (MW)	B-shunt (Mvar)
4	1	1	1	0	100
5	1	1	1	0	200

3.5 Branch data

For the branch data shown in Table 5, (all non-transformer branches with shunts connected), the information needed for the equivalent pi line model construction includes the branch resistance in per unit, the branch reactance in per unit, total charging susceptance in per unit, and the complex admittance values in per unit of the buses connected on both sides. These complex admittance values can be positive or negative depending on whether the line connects a reactor or capacitor.

Table 5: 39 bus system branch data [16]

From Bus #	To Bus #	Line R (pu)	Line X (pu)	Charging (pu)	Line G from (pu)	Line B from (pu)	Line G to (pu)	Line B to (pu)
1	2	0.0035	0.0411	0.6987	0	0	0	0
1	39	0.001	0.025	0.75	0	0	0	0
2	3	0.0013	0.0151	0.2572	0	0	0	0
2	25	0.007	0.0086	0.146	0	0	0	0
3	4	0.0013	0.0213	0.2214	0	0	0	0
3	18	0.0011	0.0133	0.2138	0	0	0	0
4	5	0.0008	0.0128	0.1342	0	0	0	0
4	14	0.0008	0.0129	0.1382	0	0	0	0
5	6	0.0002	0.0026	0.0434	0	0	0	0
5	8	0.0008	0.0112	0.1476	0	0	0	0
6	7	0.0006	0.0092	0.113	0	0	0	0
6	11	0.0007	0.0082	0.1389	0	0	0	0
7	8	0.0004	0.0046	0.078	0	0	0	0
8	9	0.0023	0.0363	0.3804	0	0	0	0
9	39	0.001	0.025	1.2	0	0	0	0
10	11	0.0004	0.0043	0.0729	0	0	0	0
10	13	0.0004	0.0043	0.0729	0	0	0	0
13	14	0.0009	0.0101	0.1723	0	0	0	0
14	15	0.0018	0.0217	0.366	0	0	0	0
15	16	0.0009	0.0094	0.171	0	0	0	0
16	17	0.0007	0.0089	0.1342	0	0	0	0
16	19	0.0016	0.0195	0.304	0	0	0	0
16	21	0.0008	0.0135	0.2548	0	0	0	0
16	24	0.0003	0.0059	0.068	0	0	0	0
17	18	0.0007	0.0082	0.1319	0	0	0	0
17	27	0.0013	0.0173	0.3216	0	0	0	0
21	22	0.0008	0.014	0.2565	0	0	0	0
22	23	0.0006	0.0096	0.1846	0	0	0	0
23	24	0.0022	0.035	0.361	0	0	0	0
25	26	0.0032	0.0323	0.513	0	0	0	0
26	27	0.0014	0.0147	0.2396	0	0	0	0

Table 5: 39 bus system branch data [16]

26	28	0.0043	0.0474	0.7802	0	0	0	0
26	29	0.0057	0.0625	1.029	0	0	0	0
28	29	0.0014	0.0151	0.249	0	0	0	0

3.6 Two winding transformer data

All of the transformers modeled in this system are two winding transformers and the device parameters exhibit as such. The parameters needed to model the transformers are listed in Table 6 and include:

- the winding I/O code which defines the units in which the turns ratio are specified (the units of RMA, and RMI are also governed by CW). Is 1 for off-nominal turns ratio in per unit of winding bus base voltage, is 2 for winding voltage in kV, 3 for off nominal turns ratio in per unit of nominal winding voltage
- The magnetizing admittance I/O code that defines the units in which MAG1 and MAG2 are specified. Is 1 for complex admittance in per unit on system base quantities, 2 for 3 phase no load loss in watts and exciting current in per unit on winding one to two base MVA and nominal voltage
- The impedance data I/O code that defines the units in which the winding impedances R1-2, X1-2 are specified. Is 1 for resistance and reactance in per unit on system base quantities, 2 for resistance and reactance in per unit on a specified base MVA and winding bus base voltage, 3 for the transformer 3 phase load loss in watts and impedance magnitude in per unit on a specified base MVA and winding bus base voltage
- the magnetizing conductance and susceptance in per unit on system base quantities
- the measured impedance of the transformer between the buses to which its first and second windings are connected
- the winding one off nominal turns ratio in per unit of winding one base voltage

- the nominal (rated) winding 1 voltage in kv or zero to indicate that nominal winding one base voltage is to be taken as the base voltage of bus “I”. This is used in converting magnetizing data between per unit admittance values and physical units when CM is 2. This is also used in converting tap ratio data between values in per unit of nominal winding one voltage and values in per unit of winding one bus base voltage when CW is 3
- the winding one phase shift angle in degrees. This is positive when winding 2 leads the winding 1 side. Must be greater than –180 and less than or equal to 180
- the transformer control mode for automatic of the winding one tap or phase shift angle during power flow solutions. 0 for no control (fixed tap and phase shift), +/- 1 for voltage control, +/- 2 for reactive power flow control, +/- 3 for active power flow control, +/- 4 for control of a dc line quantity. If the number is positive automatic adjustments of the transformer winding is enabled when the corresponding adjustment is activated during power flow solutions. A negative number suppresses the automatic adjustment of the transformer winding

- the number of tap positions available
- the load drop compensation impedance for voltage controlling transformers in per unit on system base quantities
- the number of transformer impedance correction table if this transformer winding's impedance is to be a function of neither off nominal turns ratio or phase shift angle. 0 if no transformer impedance correction is to be applied to this transformer winding.
- the winding 2 off nominal turns ratio in per unit of winding 2 bus base voltage when CW =1. This is the actual winding 2 voltage in kv when CW is 2. This is equal to the bus base voltage of bus "J". This is the winding 2 off nominal turns ratio in per unit of nominal winding 2 voltage
- the nominal (rated) winding 2 voltage in kv, or zero to indicate that nominal winding 2 voltage is to be taken as the base voltage of bus "J". This is used in converting tap ratio data between values in per unit of nominal winding 2 voltage and values in per unit of winding 2 bus base voltage when CW is 3

Table 6: 39 bus system transformer data [16]

From Bus #	To Bus #	Metered	Winding 1 Side	Controlled Bus	Controlled Side	Tapped Positions
2	30	1	1	0	0	8
6	31	0	0	6	0	8
10	32	1	1	0	0	8
11	12	0	0	0	0	8
12	13	1	1	0	0	8
19	20	1	1	0	0	8
19	33	1	1	0	0	8
20	34	1	1	0	0	8
22	35	1	1	0	0	8
23	36	1	1	0	0	8
25	37	1	1	0	0	8
29	38	1	1	0	0	8

Control Mode	Auto Adjust	Winding I/O Code	Impedance I/O Code	Admittance I/O Code
None	1	Turns ratio (pu on bus base kV)	Zpu (system base)	Y pu (system base)
Voltage	1	Turns ratio (pu on bus base kV)	Zpu (system base)	Y pu (system base)
None	1	Turns ratio (pu on bus base kV)	Zpu (system base)	Y pu (system base)
None	1	Turns ratio (pu on bus base kV)	Zpu (system base)	Y pu (system base)
None	1	Turns ratio (pu on bus base kV)	Zpu (system base)	Y pu (system base)

Table 6: 39 bus system transformer data [16]

None	1	Turns ratio (pu on bus base kV)	Zpu (system base)	Y pu (system base)
None	1	Turns ratio (pu on bus base kV)	Zpu (system base)	Y pu (system base)
None	1	Turns ratio (pu on bus base kV)	Zpu (system base)	Y pu (system base)
None	1	Turns ratio (pu on bus base kV)	Zpu (system base)	Y pu (system base)
None	1	Turns ratio (pu on bus base kV)	Zpu (system base)	Y pu (system base)
None	1	Turns ratio (pu on bus base kV)	Zpu (system base)	Y pu (system base)
None	1	Turns ratio (pu on bus base kV)	Zpu (system base)	Y pu (system base)

Specified R (pu or watts)	Specified X	Rate A (MVA)	Rate B (MVA)	Rate C (MVA)
0	0.0181	0	0	0
0	0.025	0	0	0
0	0.02	0	0	0
0.0016	0.0435	0	0	0
0.0016	0.0435	0	0	0
0.0007	0.0138	0	0	0
0.0007	0.0142	0	0	0
0.0009	0.018	0	0	0
0	0.0143	0	0	0
0.0005	0.0272	0	0	0
0.0006	0.0232	0	0	0
0.0008	0.0156	0	0	0

Magnetizing G (pu or watts)	Magnetizing B	Winding MVA	Wnd 1 Ratio (pu or kv)	Wnd 1 Nominal kv	Wnd 1 Angle (degrees)
0	0	100	1.025	0	0
0	0	100	0.9	0	0
0	0	100	1.07	0	0
0	0	100	1.006	0	0
0	0	100	1.006	0	0
0	0	100	1.06	0	0
0	0	100	1.07	0	0
0	0	100	1.009	0	0
0	0	100	1.025	0	0
0	0	100	1	0	0
0	0	100	1.025	0	0
0	0	100	1.025	0	0

Table 6: 39 bus system transformer data [16]

Wnd 2 Ration (pu or kv)	Wnd 2 Nominal kv	Rmax (ratio or angle)	Rmin (ratio or angle)	Vmax (pu, kv, MW or Mvar)	Vmin (pu, kv, MW, Mvar)
1	0	1.2	0.8	1.2	0.8
1	0	1.2	0.8	1.17	0.98
1	0	1.2	0.8	1.2	0.8
1	0	1.2	0.8	1.2	0.8
1	0	1.2	0.8	1.2	0.8
1	0	1.2	0.8	1.2	0.8
1	0	1.2	0.8	1.2	0.8
1	0	1.2	0.8	1.2	0.8
1	0	1.2	0.8	1.2	0.8
1	0	1.2	0.8	1.2	0.8
1	0	1.2	0.8	1.2	0.8
1	0	1.2	0.8	1.2	0.8

Wnd Connect Angle	Load Drop Comp R (pu)	Load Drop Comp X (pu)	Impedance Table	R (table corrected pu or watts)	X (table corrected pu)
0	0	0	0	0	0
0	0	0	0	0	0
0	0	0	0	0	0
0	0	0	0	0	0
0	0	0	0	0	0
0	0	0	0	0	0
0	0	0	0	0	0
0	0	0	0	0	0
0	0	0	0	0	0
0	0	0	0	0	0
0	0	0	0	0	0
0	0	0	0	0	0

3.7 PSS/E software

In order to effectively and efficiently analyze the various IEEE 39 bus systems and characteristics, a simulation software program that encompasses much of the aforementioned analysis techniques is utilized. This software is PSS/E (Power System Simulator for Engineering) and a modular component of the software specific to modal analysis called NEVA (Netomac Eigenvalue Analysis). The description, capabilities and functionality of these systems as they pertain to the system analysis involved in this project are described as follows.

The power system stability analysis capabilities of PSS/E NEVA center around small signal stability using frequency domain modal analysis. As mentioned earlier, small signal stability revolves around understanding the reaction of a system that has reached a state of equilibrium to a small disturbance. There are other means of investigating the reaction and stability of a system after a disturbance that deal with large signals and involve nonlinear expressions and more

complex system dynamics. The focus of this study and NEVA linearizes systems around an operating point and calculates eigenvalues and eigenvectors to quantify system operation. Modeling a nonlinear system as a linear system around a specific operating point, or steady state condition allows for a simplified process of analysis. This inherent nature of modal analysis is apparent in the analysis steps. In time domain, a disturbance must be applied in order to observe the system response. In modal analysis, the system characteristics (and subsequent system response to a small disturbance) are contained in the calculated eigenvalues, therefore no disturbance needs be applied.

With a power system modeled in PSS/E that has all the necessary characteristics outlined in the previous section, a load flow simulation can be run. In this load flow simulation the system is basically stabilized at an operating point and modal analysis can be commenced. With the eigenvalues and eigenvectors produced from modal analysis the simulation ascertains information regarding the frequencies and damping of the system oscillations, as well as observability, controllability, and controller tuning. To aide in the understanding of the system's properties, charts displaying these characteristics allow for easy comparison. Local and interarea oscillations are easily distinguishable through these charts and graphs and increase the functionality and usefulness of the NEVA program. Also, with these specialized display of results, it is easy to distinguish the instability of a system.

Figure 8 is an example graph displaying the frequency results of each mode of a system that has been analyzed. In it, it is easy to observe the stability of the system in that all the modes (circles) are located to the left of the imaginary plane. Had there been any unstable modes, they would have been locate to the right of the imaginary plane. Degree of stability is also easy to detect. The farther away from the imaginary plane each mode is, the more stable the system is. And the closer a mode is to the imaginary plane, the closer to being unstable that mode is. Also, the placement of each mode yields information regarding the damping of that oscillation. Again, the farther away the mode is from the imaginary axis (the less steep the slope in respect to the point of origin), the larger the damping of that mode will be. Conversely, the closer the mode is to the imaginary axis (the steeper the slope in respect to the point of origin) the slower the damping of that particular mode.

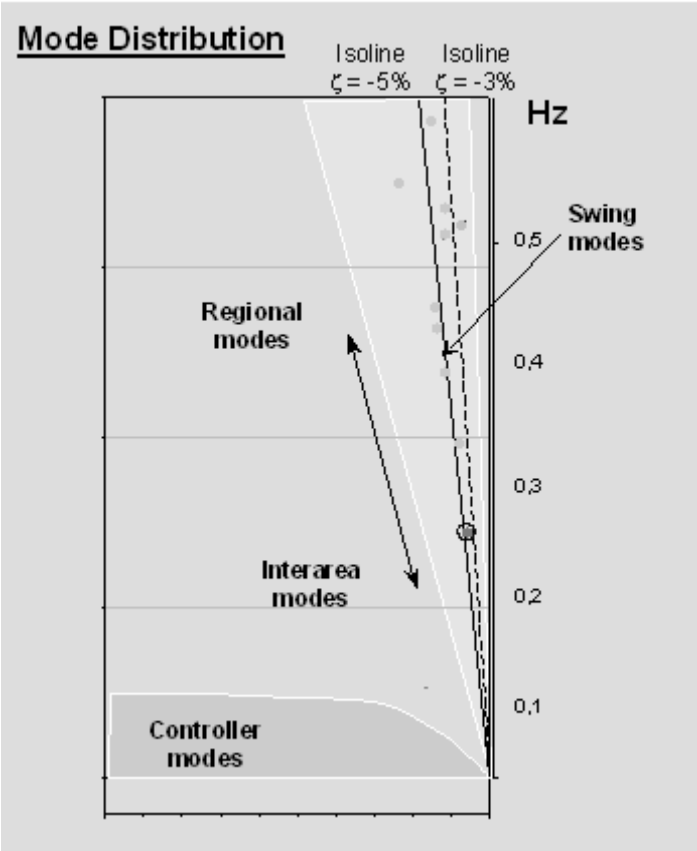

Fig 8: PSS/E – NEVA eigenvalue distribution graph [17]

Figure 9 shows some more examples of the display benefits yielded by NEVA. In these images, a modes that represent oscillations between generators within a certain area is compared to a mode that represents oscillations between generators in separate areas. As you can easily see, the results of the interarea mode is distinctly different from those from the local mode and this fact can be displayed and represented in a variety of ways. From such varying and simplistic data displays, the understanding of what is occurring within a power system from a functional standpoint can be grasped on a much more intimate level than would otherwise be possible. Also, the time necessary to comparatively analyze system data is drastically reduced adding to the simulation's efficiency.

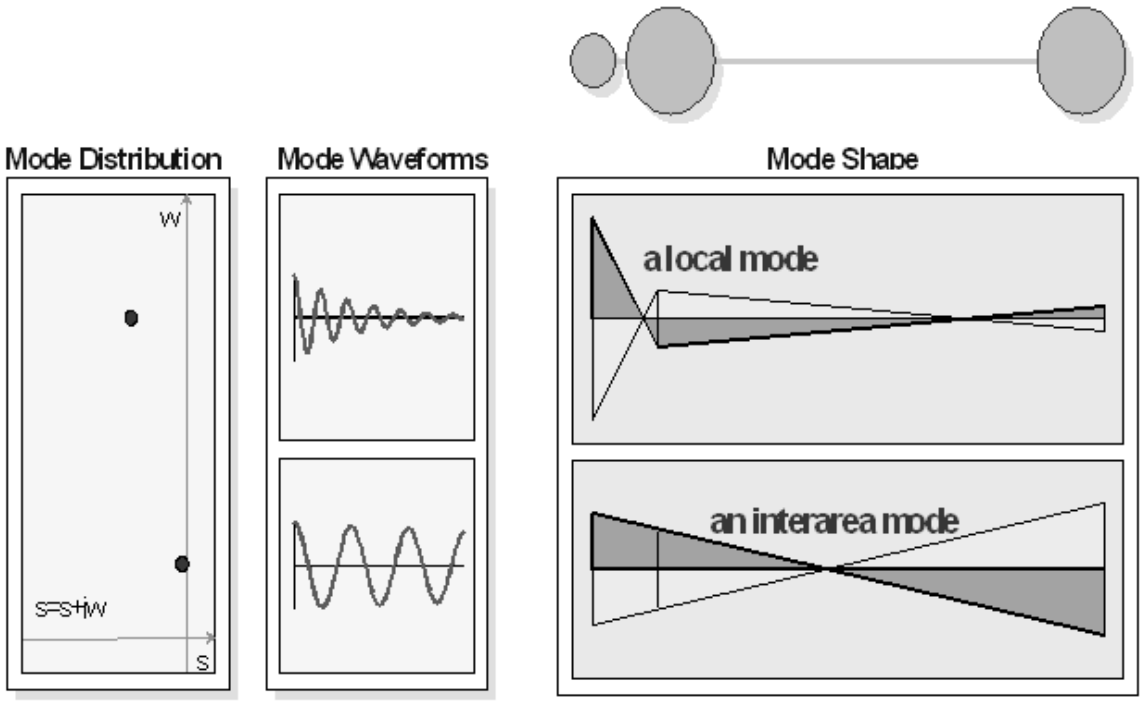

Fig 9: PSS/E – NEVA alternate eigenvalue distribution graphs [17]

With the overall methodology and capabilities of PSS/E NEVA outlined and sample results displayed, we now examine the core mathematical processes taken by the software to perform the various analyses mentioned earlier. These analyses all revolve around the eigenvalues that represent the system performance. In PSS/E NEVA, different techniques for calculating eigenvalues are taken depending on the size of the system being modeled and the amount of detail given for the particular system components. For systems less than 50 generators and systems that have between 50 and 100 generators with limited and simple details, full eigenvalue analysis is performed. This means, all eigenvalues for the system are calculated. For systems that have 50 to 100 generators with extensive detail and systems over 100 generators only partial eigenvalue analysis is performed. In other words, only eigenvalues that represent modes of interest are calculated. Although it is possible to miss unstable modes with partial eigenvalue analysis, the technique is robust enough to be considered dependable and any miniscule chance of missing unstable modes is warranted by the allowance of the analysis on a system of that size.

The calculation of eigenvalues within PSS/E is done by using matrix techniques and utilizing the QR transformation method then performing implicit inverse iterations to find the eigenvectors. As outlined in earlier sections, this method basically decomposes the state matrix that is already calculated into a product of an orthogonal matrix and a triangular matrix, then iterates until the matrix converges to the eigenvalues located in the triangular matrix.
In the case of partial eigenvalue analysis, initial values (essentially guesses) are given for all the eigenvalues. When the iterative techniques are used, they again converge to the final eigenvalues and the solution is complete. The methods used by PSS/E to accomplish the partial eigenvalue analysis include sub space iteration methods, eigenvalue refinement methods, dominant pole interation methods, and heuristic iteration methods.

Sub space iteration is an iterative technique of calculating eigenvalues relying on vector orthogonality. Where K and M are symmetric matrices of A, and X is the starting vector matrix,

the iterative process follows Equations 3.1 – 3.6 until convergence of the eigenvalues is achieved.

$$KV_i = \lambda MV_i \tag{3.1}$$

$$K\overline{X}_{K+1} = MX_K \tag{3.2}$$

$$K_{K+1} = \overline{X}^T_{K+1} K \overline{X}_{K+1} \tag{3.3}$$

$$M_{K+1} = \overline{X}^T_{K+1} M \overline{X}_{K+1} \tag{3.4}$$

$$K_{K+1} Q_{K+1} = M_{K+1} Q_{K+1} \Lambda_{K+1} \tag{3.5}$$

$$X_{K+1} = \overline{X}_{K+1} Q_{K+1} \tag{3.6}$$

Dominant pole iteration is another iterative technique that uses convergence from an initial guess or estimate to calculate the eigenvalues. Given the A matrix and an initial eigenvalue estimate of λ_i the calculation process begins with Equation 3.7.

$$\begin{bmatrix} \lambda_i I - A & -b \\ c^T & 0 \end{bmatrix} \begin{bmatrix} x(\lambda_i) \\ u(\lambda_i) \end{bmatrix} = \begin{bmatrix} 0 \\ 1 \end{bmatrix} \tag{3.7}$$

Solving Equation 3.7 then yields Equation 3.8

$$\begin{bmatrix} \lambda_i I - A^T & -c \\ b^T & 0 \end{bmatrix} \begin{bmatrix} v(\lambda_i) \\ u(\lambda_i) \end{bmatrix} = \begin{bmatrix} 0 \\ 1 \end{bmatrix} \tag{3.8}$$

λ_i converges to the eigenvalue λ_{i-1} as the input $u(\lambda_{i-1})$ approaches zero as shown in Equation 3.9

$$\lambda_i = \lambda_{i-1} + \frac{u(\lambda_{i-1})}{v^T(\lambda_{i-1}) \bullet x(\lambda_{i-1})} \tag{3.9}$$

In addition to solving for eigenvalues and eigenvectors that all exhibit the inherent properties of the system being modeled; there are a number of other characteristics that can be determined from these eigenvalues. In PSS/E NEVA these include damping, mode observability, mode controllability, participation factors, transfer function residues, controller location factors, frequency response, linear impulse and step response.

Concerning mode damping, PSSE/NEVA allows the user to observe the presence and level of damping associated with each mode of the system. Damping of course, plays a role in the stability of the system; and the more stable a system is the more quickly its modes of oscillation are damped out. As a result, it is easy to see why damping analysis is so important in system

evaluation. In the program, damping analysis is carried out using a damping ratio (or relative damping). Damping ratio combines the best features of two other indices to make the format more usable. Damping itself (σ) is simply the real part of the mode that is calculated. This real part can be associated with a time constant amplitude of decay that represents a 37% decay of the initial value. Mathematically, this is represented by Equation 3.10.

$$\tau_0 = \frac{1}{\sigma} \tag{3.10}$$

The index used in PSS/E combines the best of both methods by using a damping ratio. In the damping ratio, the rate of decay is calculated, thus giving an indication of the relationship between the number of oscillations and the amount of amplitude decay. Graphically speaking, this is the slope of the line drawn from the mode to the origin of the S axis, as shown in Figure 10. The steeper the slope the faster the damping of the mode is decayed. Mathematically, this is represented by Equation 3.11.

$$\xi = \cos\Psi = \frac{\sigma}{\sqrt{\sigma^2 + \omega^2}} \tag{3.11}$$

ψ is the angle between the line and the axis.

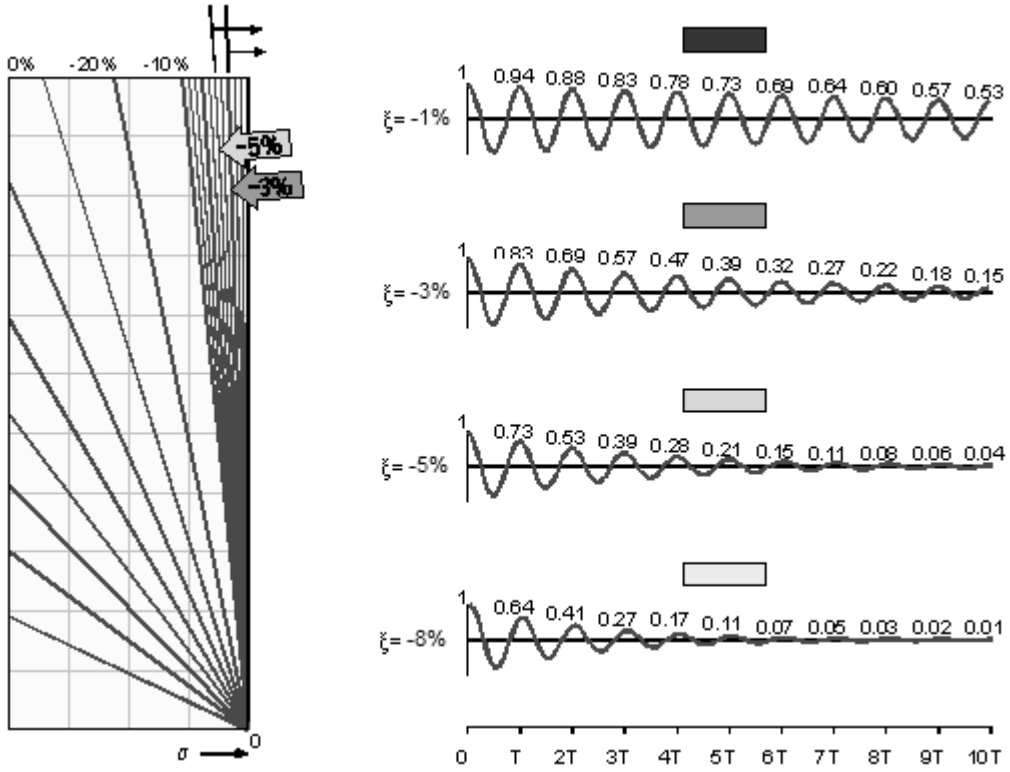

Fig 10: PSS/E – NEVA damping index graph [17]

Concerning mode observability, PSS/E uses the right eigenvector to calculate this. This value exhibits the activities of different system variables on the mode. These can include generator rotor angle, active power, and reactive power. In addition to several different inputs, there are different outputs that can be observed concerning network behavior. These can include voltage deviation of the buses in the system and power deviations of the transmission lines in the system.

Conversely, mode controllability utilizes the left eigenvectors of the system. This index represents the influences that different system variables have on the mode. Collectively, along with mode observability, the system can display which generator(s) swing against other generator(s), as well as how significant a role each generator (or group of generator) plays.

The participation factors, transfer function residues and controller indices revolve around optimum placement of power system stabilizers and controllers. The aspects are beyond the scope of this paper but it is important to note them while discussing the program capabilities.

Chapter 3 concludes the presentation of the background information and system data that will be used in the research of the power system. The IEEE 39 bust test system was identified as well as its inputs. The PSS/E NEVA software was also introduced, with a review of its calculative procedures pertaining to small signal stability. Example data was given to familiarize the reader with expected results and the interpretation of the results. Now we are ready to proceed with the research methodology that will be presented in Chapter 4.

Chapter 4

Simulation Results and Analysis

4.1 Methodology

With the electrical system and simulation software detailed, we now begin system analysis and simulation. Our analysis of the modes of the New England system with the aforementioned system characteristics will encompass several steps.

4.1.1 Base Case Modal Analysis

We will begin by analyzing the system stability of the different modes to get a general understanding of the system stability and behavioral response to changes. This will exhibit the basic modal analysis techniques that have previously been discussed and allow us to have a starting foundation in which to compare later results.

4.1.2 Stability Response to System Changes

Next we will change the make-up of the system with certain components to get a different picture of system behavior that we can then compare to the base case. This comparison will allow us to track the system response changes and quantify the difference. From these differences we can then make assumptions and prove what effects the modes of a system and how. The changes proposed to the base case include adding shunt capacitance of pure reactance to each of the load buses. With pure reactance (no resistive component), we symbolize capacitor banks that effect the bus voltage and subsequent power factor at the different buses of the system. This pure reactance will first be positive, then negative to analyze the change in stability.

4.1.3 Analysis of Stability and Mode Manipulation

Finally, computational analysis will be conducted to further analyze the system, and draw design and control conclusions that form the basis of participation factor analysis. We will look at the results of the base case and subsequent cases where we added purely reactive components. The differences in these results will allow us to draw conclusions and prove what effects this has on a power system, how much of an effect it has on a power system (participation), and how to optimize stability improvement in power systems by manipulating the system at points which cause the biggest shift in system stability.

The original 39 bust test system, with the previously listed system values yields a small signal system response that is stable and has 62 different modes of oscillation as shown in Figures 11 and 12. All of the modes are stable but the degree of stability varies with the different modes. In order to determine the state of each mode, the state matrix was first determined for the system. This outlines its behavior and response to varying component and system variables. Once determined, the eigenvalues were found for each mode around an equilibrium point.

The stability of the modes in this base case is easily determined by the negative (or near negative) real eigenvalue, denoted as sigma in the results. With the graphical output shown below, it is easy to see the mode stability, as well as the magnitude of damping and the differing degrees of stability. The most stable modes are farthest away from the origin of the x-axis. The

modes with the most damping are those highest on the y-axis (thus creating the steepest slope with the origin point).

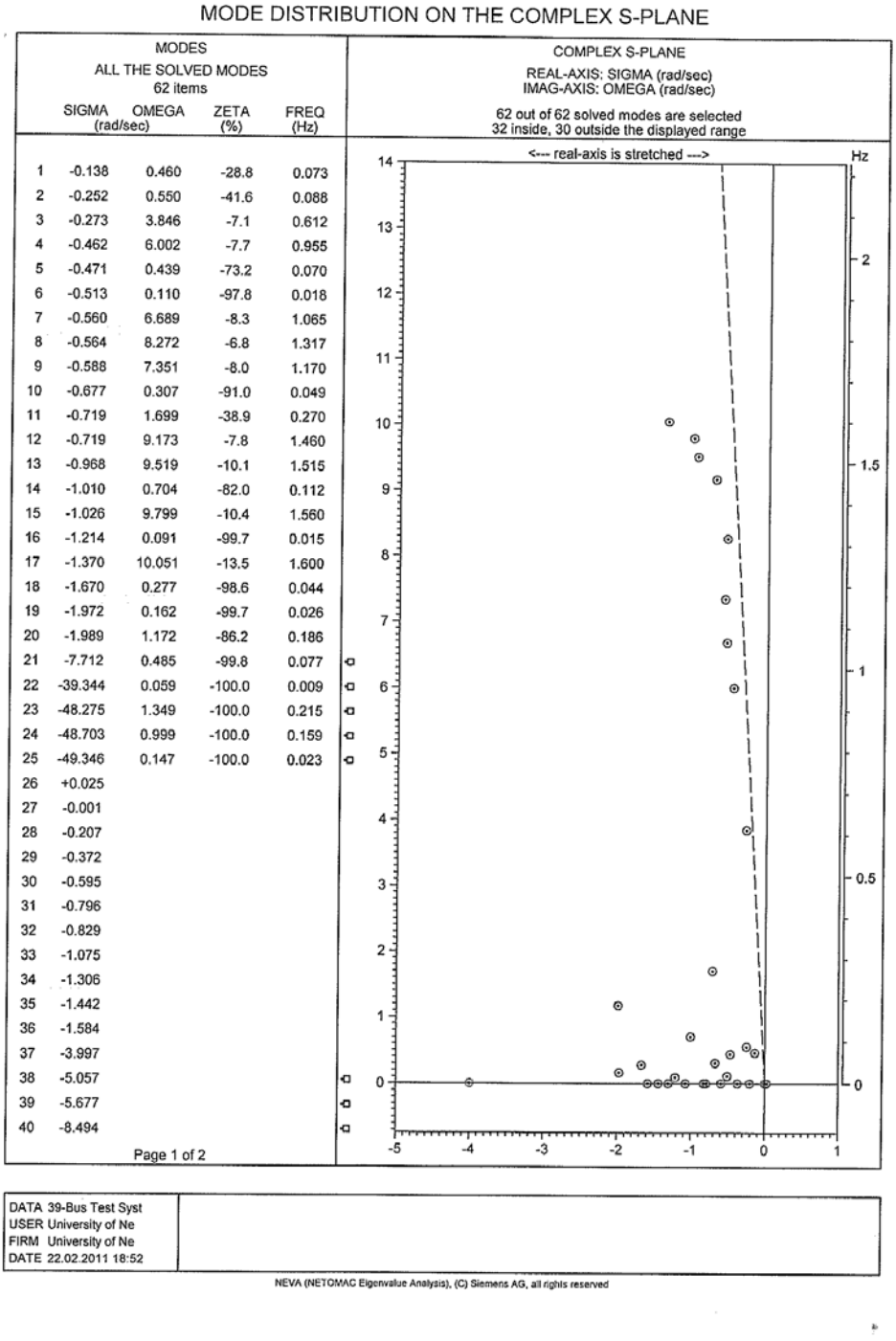

Fig 11: Modal analysis (eigenvalues) of base case 39 bus test system

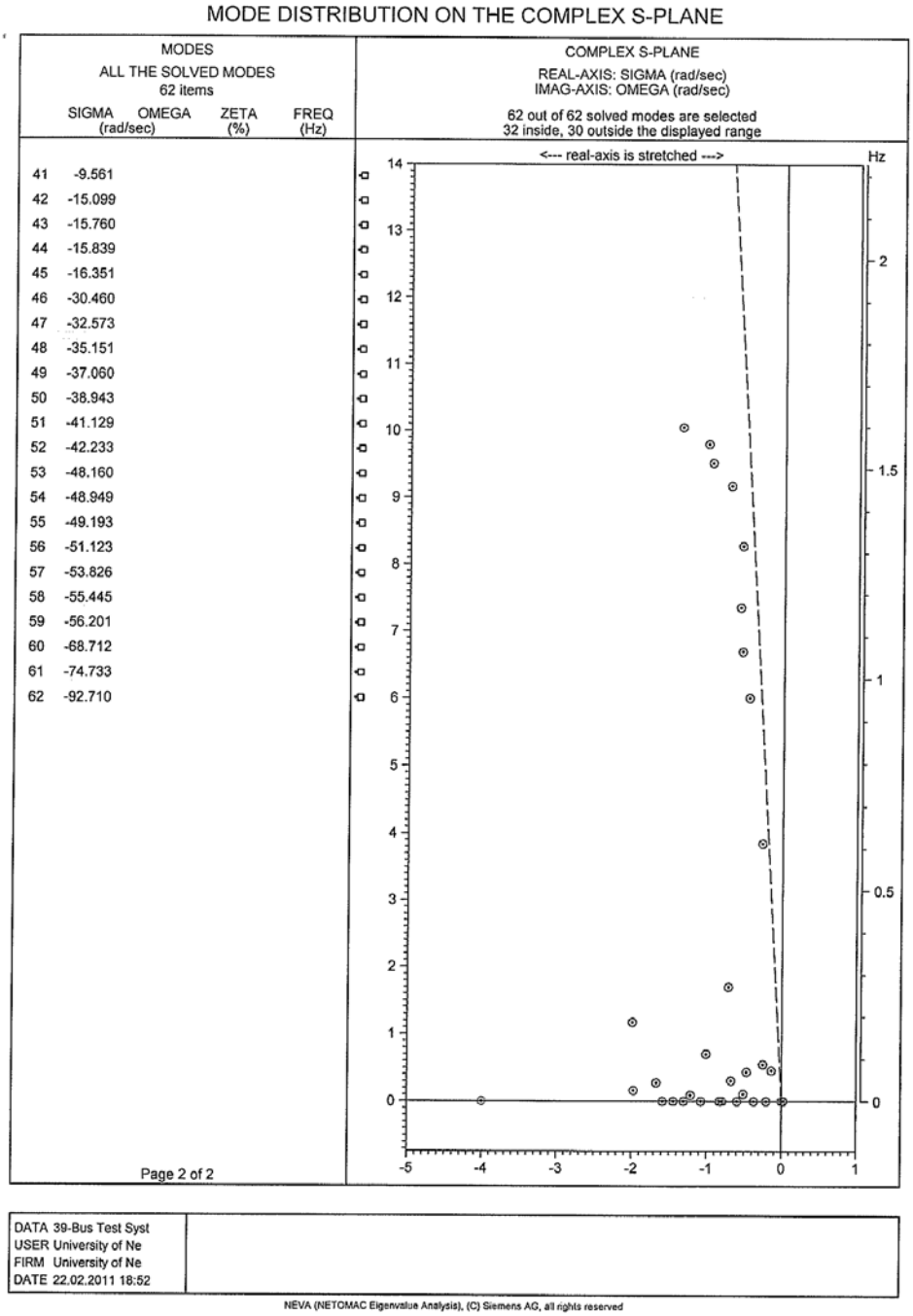

Fig 12: Modal analysis (eigenvalues) of base case 39 bus test system

Now that modal analysis has been completed to analyze power system stability for the base case, we move on to manipulating the system through load bus component variance and the addition of shunt capacitance in order to observe system response.

The first method of analysis aims to determine the correlation between voltage stability and mode stability by adjusting the real and reactive power values of the load bus with the lowest power factor. The load bus with the lowest power factor is chosen because it corresponds to the bus that will have the most input on voltage stability. As a result, we begin the first analysis by performing load flow analysis of the base case in PSS/E to determine the load bus with the lowest power factor (largest voltage instability). Table 7 lists the real and reactive power of each load bus, as well as the voltage and power factor. Bus 12 is shown to have the lowest power factor, thus will be used to manipulate the voltage stability of the base case system.

Table 7: Load flow results of base case 39 bus test system

Initial Case				
Load Bus	P (MW)	Q (Mvar)	P.F.	V
3	322	2.4	0.999972225	1.0199
4	500	184	0.938471234	0.9973
7	233.8	839.9999	0.26814073	0.9403
8	522	176	0.947588489	0.954
12	8.5	88	0.096143451	0.9901
15	320	153	0.902181928	0.9932
16	329.4	323	0.714009096	1.0053
18	158	30	0.98244725	1.0141
20	628	103	0.986815325	0.9859
21	274	115	0.922078195	1.0131
23	247.5	84.6	0.94624715	1.0345
24	308.6	-92.2	0.958150399	1.0132
25	224	47.2	0.97851269	1.0519
26	139	17	0.99260396	1.0375
27	281	75.5	0.965748365	1.0202
28	206	27.6	0.991143659	1.0343
29	283.5	126.9	0.91273296	1.034
31	9.2	4.6	0.894427191	1.04
39	1104	250	0.975306119	1.03

Next, we increase the real and reactive power values at base case load bus 12 in intervals of 50%, 100%, and 150% and perform new load flow calculations. Increasing P and Q simultaneously allows us to adjust voltage levels while keeping the power factor constant. The manipulation of the voltage level at the load bus will then allow us to perform mode analysis and determine the effect voltage stability has on each mode. Table 8 shows the load flow results of a

50% P and Q manipulation on bus 12. Table 9 shows the load flow results of a 100% P and Q manipulation and table 10 shows the load flow results of a 150% P and Q manipulation.

Table 8: Load flow of 39 bus test system with bus 12 P and Q increased by 50%

Increasing bus 12 P and Q by 50% of original case				
Load Bus	P (MW)	Q (Mvar)	P.F.	V
3	322	2.4	0.999972225	1.0183
4	500	184	0.938471234	0.9941
7	233.8	839.9999	0.26814073	0.9368
8	522	176	0.947588489	0.9507
12	12.75	132	0.961434506	0.9749
15	320	153	0.902181928	0.9912
16	329.4	323	0.714009096	1.0041
18	158	30	0.98244725	1.0128
20	628	103	0.986815325	0.9856
21	274	115	0.922078195	1.0123
23	247.5	84.6	0.94624715	1.034
24	308.6	-92.2	0.958150399	1.0121
25	224	47.2	0.97851269	1.0513
26	139	17	0.99260396	1.0368
27	281	75.5	0.965748365	1.0192
28	206	27.6	0.991143659	1.0339
29	283.5	126.9	0.91273296	1.0338
31	9.2	4.6	0.894427191	1.04
39	1104	250	0.975306119	1.03

Table 9: Load flow of 39 bus test system with bus 12 P and Q increased by 100%

Increasing bus 12 P and Q by 100% of original case				
Load Bus	P (MW)	Q (Mvar)	P.F.	V
3	322	2.4	0.999972225	1.0162
4	500	184	0.938471234	0.9898
7	233.8	839.9999	0.26814073	0.9318
8	522	176	0.947588489	0.9459
12	17	176	0.961434506	0.9582
15	320	153	0.902181928	0.9886
16	329.4	323	0.714009096	1.0025
18	158	30	0.98244725	1.0109
20	628	103	0.986815325	0.9853
21	274	115	0.922078195	1.0111
23	247.5	84.6	0.94624715	1.0333
24	308.6	-92.2	0.958150399	1.0106
25	224	47.2	0.97851269	1.0507
26	139	17	0.99260396	1.0359
27	281	75.5	0.965748365	1.0179
28	206	27.6	0.991143659	1.0334
29	283.5	126.9	0.91273296	1.0334
31	9.2	4.6	0.894427191	1.0372
39	1104	250	0.975306119	1.03

Table 10: Load flow of 39 bus test system with bus 12 P and Q increased by 150%

Increasing bus 12 P and Q by 150% of original case				
Load Bus	P (MW)	Q (Mvar)	P.F.	V
3	322	2.4	0.999972225	1.0137
4	500	184	0.938471234	0.9847
7	233.8	839.9999	0.26814073	0.9255
8	522	176	0.947588489	0.94
12	21.25	220	0.961434506	0.94
15	320	153	0.902181928	0.9856
16	329.4	323	0.714009096	1.0006
18	158	30	0.98244725	1.0088
20	628	103	0.986815325	0.9849
21	274	115	0.922078195	1.0098
23	247.5	84.6	0.94624715	1.0326
24	308.6	-92.2	0.958150399	1.0089
25	224	47.2	0.97851269	1.0498
26	139	17	0.99260396	1.0348
27	281	75.5	0.965748365	1.0165
28	206	27.6	0.991143659	1.0329
29	283.5	126.9	0.91273296	1.0331
31	9.2	4.6	0.894427191	1.0322
39	1104	250	0.975306119	1.03

As you can see, increasing both P and Q while keeping the power factor constant, decreases the voltage level at the load bus.

Now that we have successfully manipulated the voltage level at the most influential base case load bus, we perform modal analysis on the system for each different voltage level. Figures 13-18 show the NEVA modal analysis results for the 50%, 100%, and 150% system manipulations.

MODE DISTRIBUTION ON THE COMPLEX S-PLANE

MODES
ALL THE SOLVED MODES
62 items

	SIGMA (rad/sec)	OMEGA (rad/sec)	ZETA (%)	FREQ (Hz)
1	-0.139	0.460	-28.9	0.073
2	-0.253	0.551	-41.7	0.088
3	-0.272	3.845	-7.1	0.612
4	-0.461	6.002	-7.7	0.955
5	-0.481	0.435	-74.2	0.069
6	-0.514	0.111	-97.8	0.018
7	-0.559	6.692	-8.3	1.065
8	-0.563	8.273	-6.8	1.317
9	-0.586	7.352	-7.9	1.170
10	-0.677	0.307	-91.1	0.049
11	-0.714	9.184	-7.8	1.462
12	-0.720	1.699	-39.0	0.270
13	-0.968	9.520	-10.1	1.515
14	-1.011	0.703	-82.1	0.112
15	-1.028	9.801	-10.4	1.560
16	-1.212	0.090	-99.7	0.014
17	-1.370	10.053	-13.5	1.600
18	-1.670	0.278	-98.6	0.044
19	-1.981	0.126	-99.8	0.020
20	-1.988	1.173	-86.1	0.187
21	-7.719	0.483	-99.8	0.077
22	-39.355	0.029	-100.0	0.005
23	-48.280	1.349	-100.0	0.215
24	-48.701	1.000	-100.0	0.159
25	-49.346	0.147	-100.0	0.023
26	+0.023			
27	0.000			
28	-0.207			
29	-0.372			
30	-0.598			
31	-0.797			
32	-0.830			
33	-1.077			
34	-1.306			
35	-1.444			
36	-1.589			
37	-4.003			
38	-5.056			
39	-5.670			
40	-8.517			

Page 1 of 2

COMPLEX S-PLANE
REAL-AXIS: SIGMA (rad/sec)
IMAG-AXIS: OMEGA (rad/sec)

62 out of 62 solved modes are selected
32 inside, 30 outside the displayed range

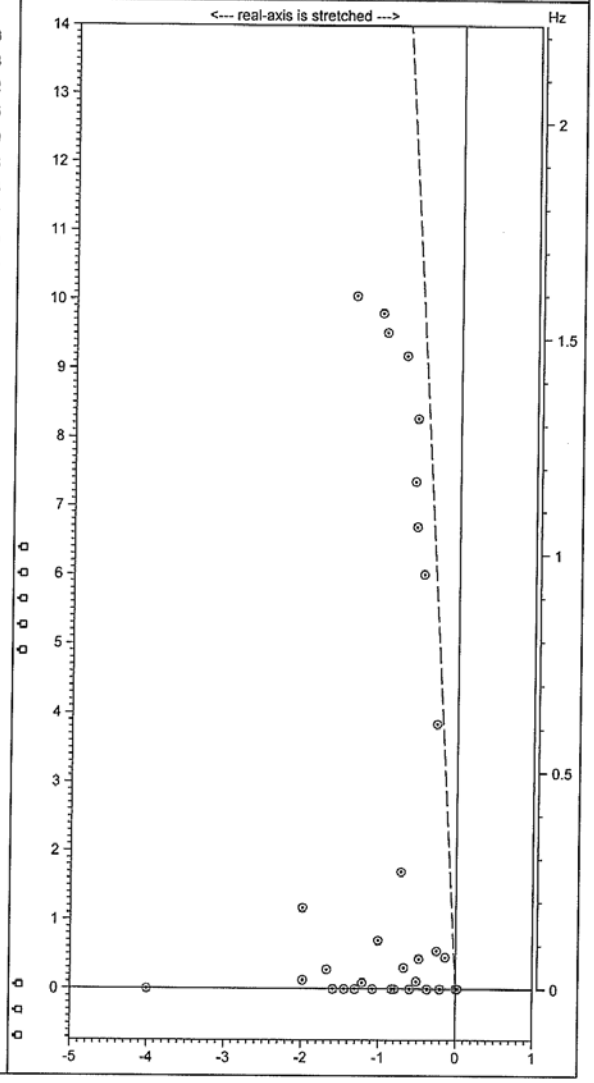

DATA 39-Bus Test Syst
USER University of Ne
FIRM University of Ne
DATE 22.02.2011 18:55

Fig 13: Modal analysis (eigenvalues) of 39 bus test system with bus 12 P and Q increased by 50%

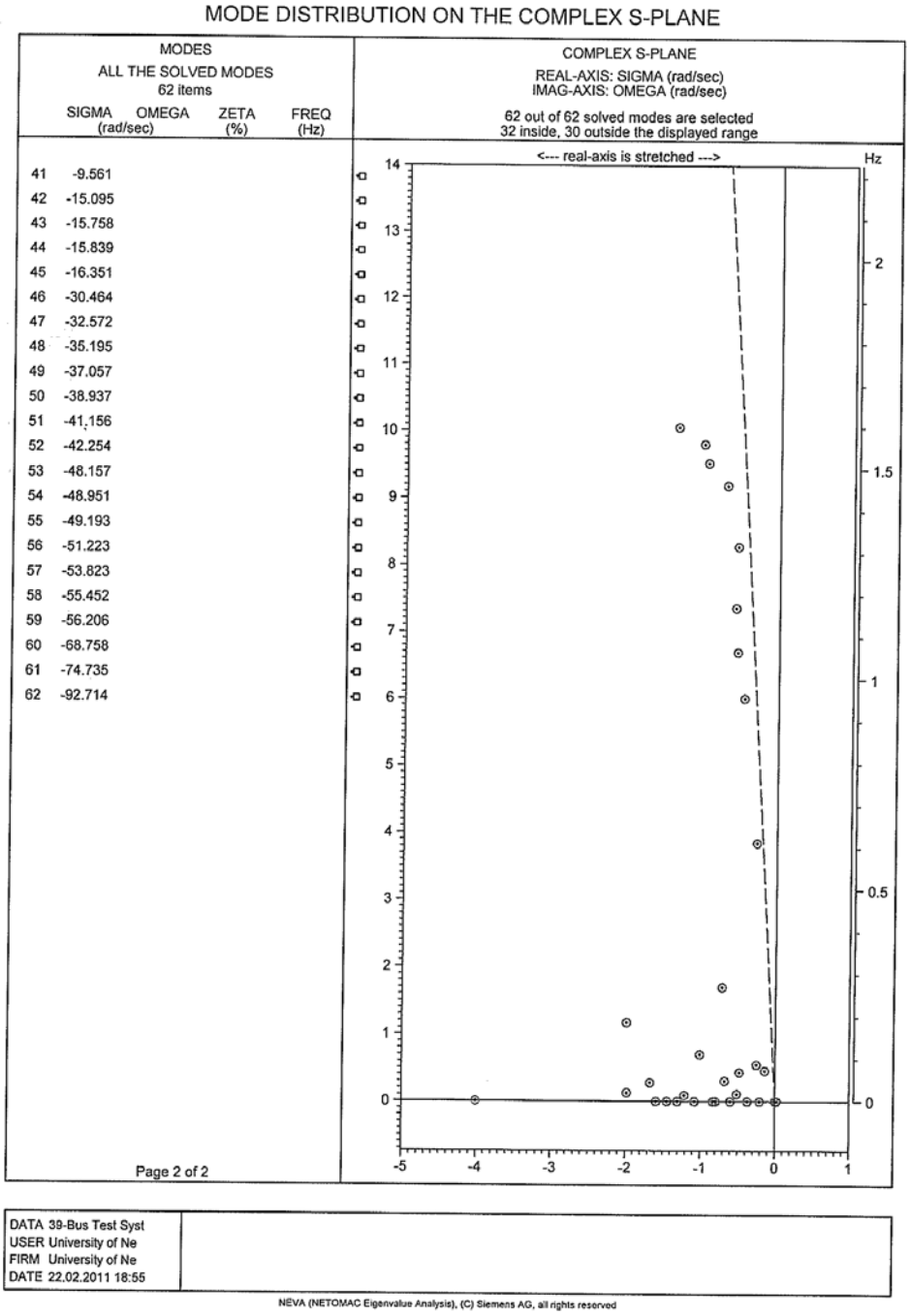

Fig 14: Modal analysis (eigenvalues) of 39 bus test system with bus 12 P and Q increased by 50%

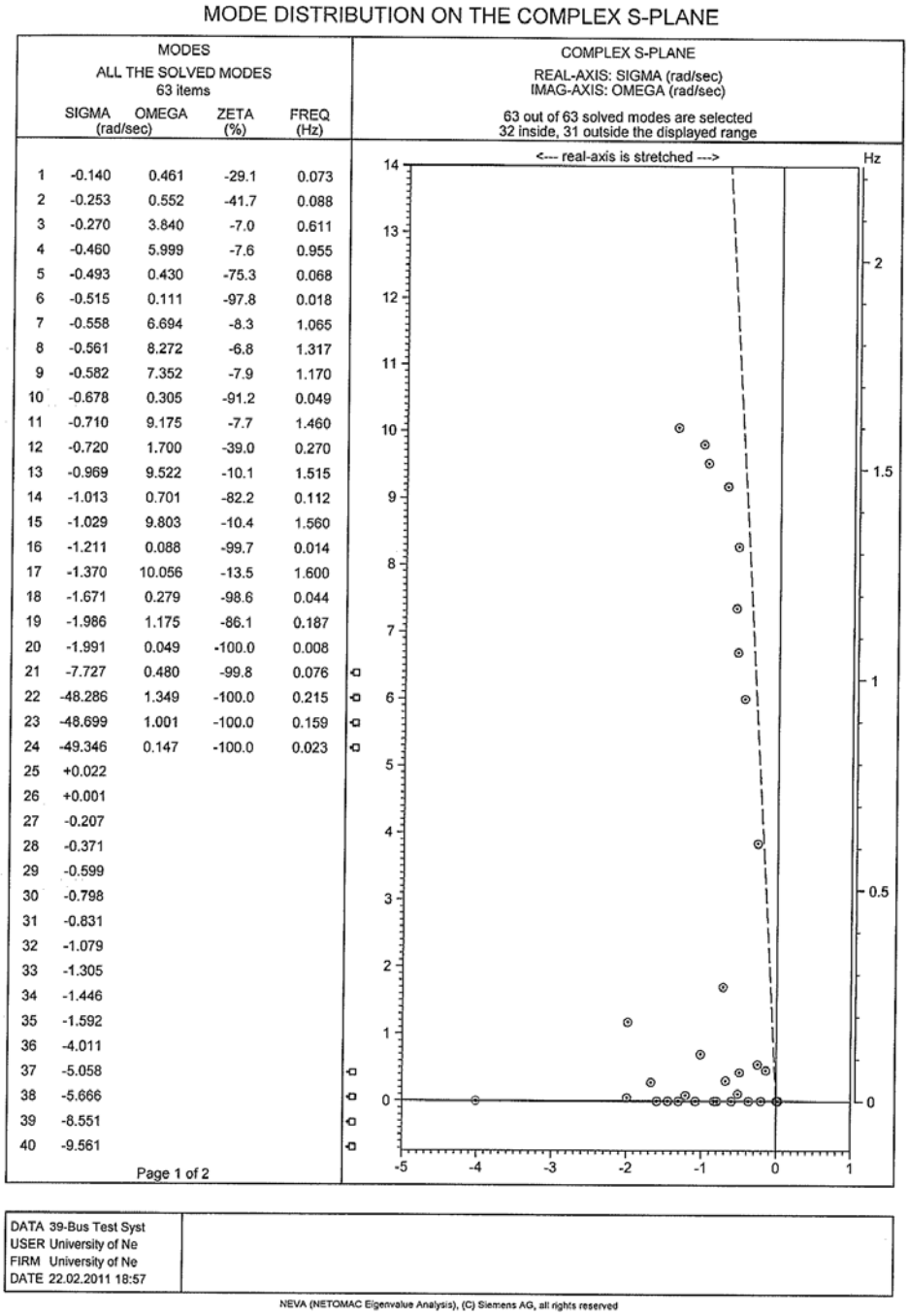

Fig 15: Modal analysis (eigenvalues) of 39 bus test system with bus 12 P and Q increased by 100%

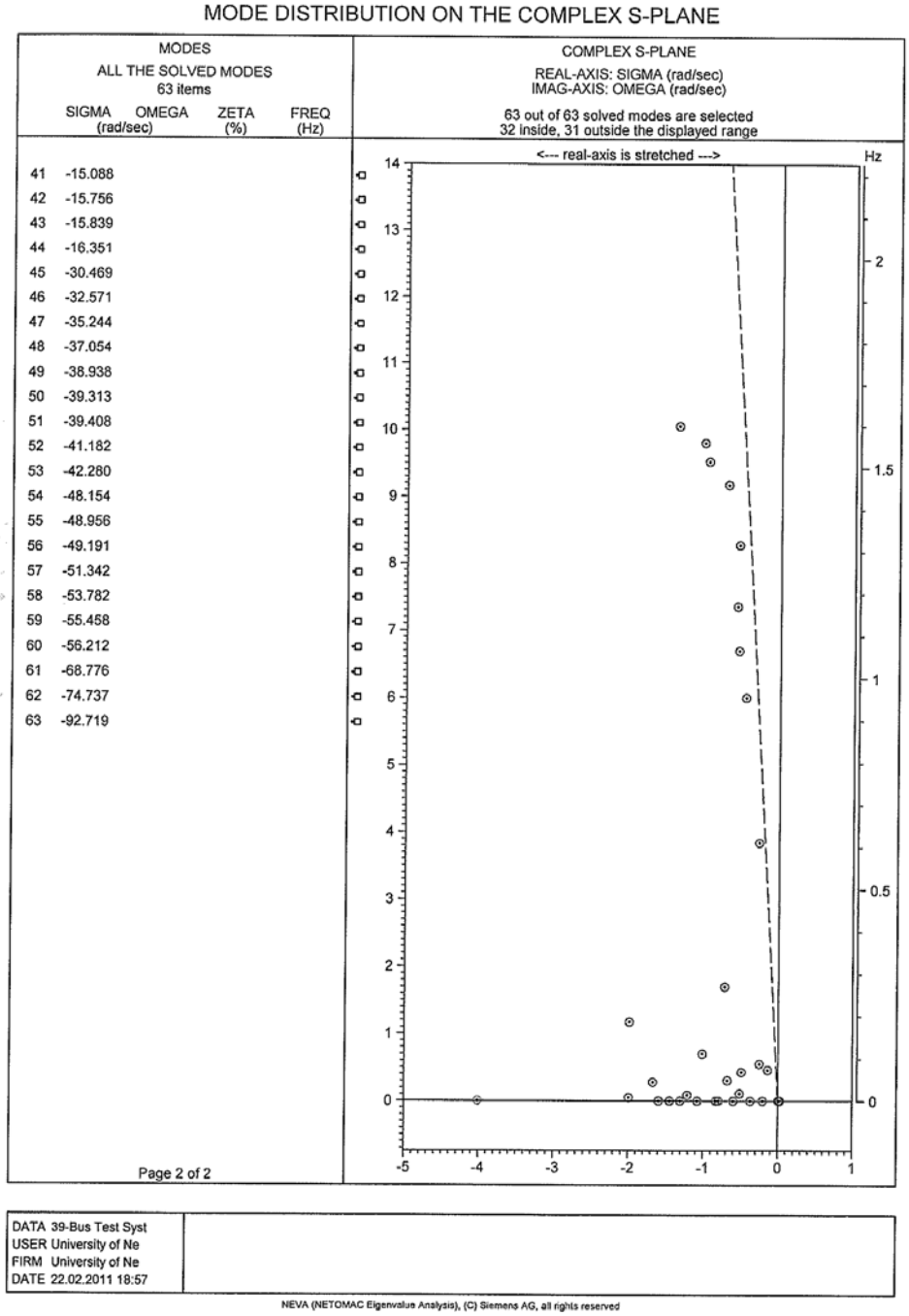

Fig 16: Modal analysis (eigenvalues) of 39 bus test system with bus 12 P and Q increased by 100%

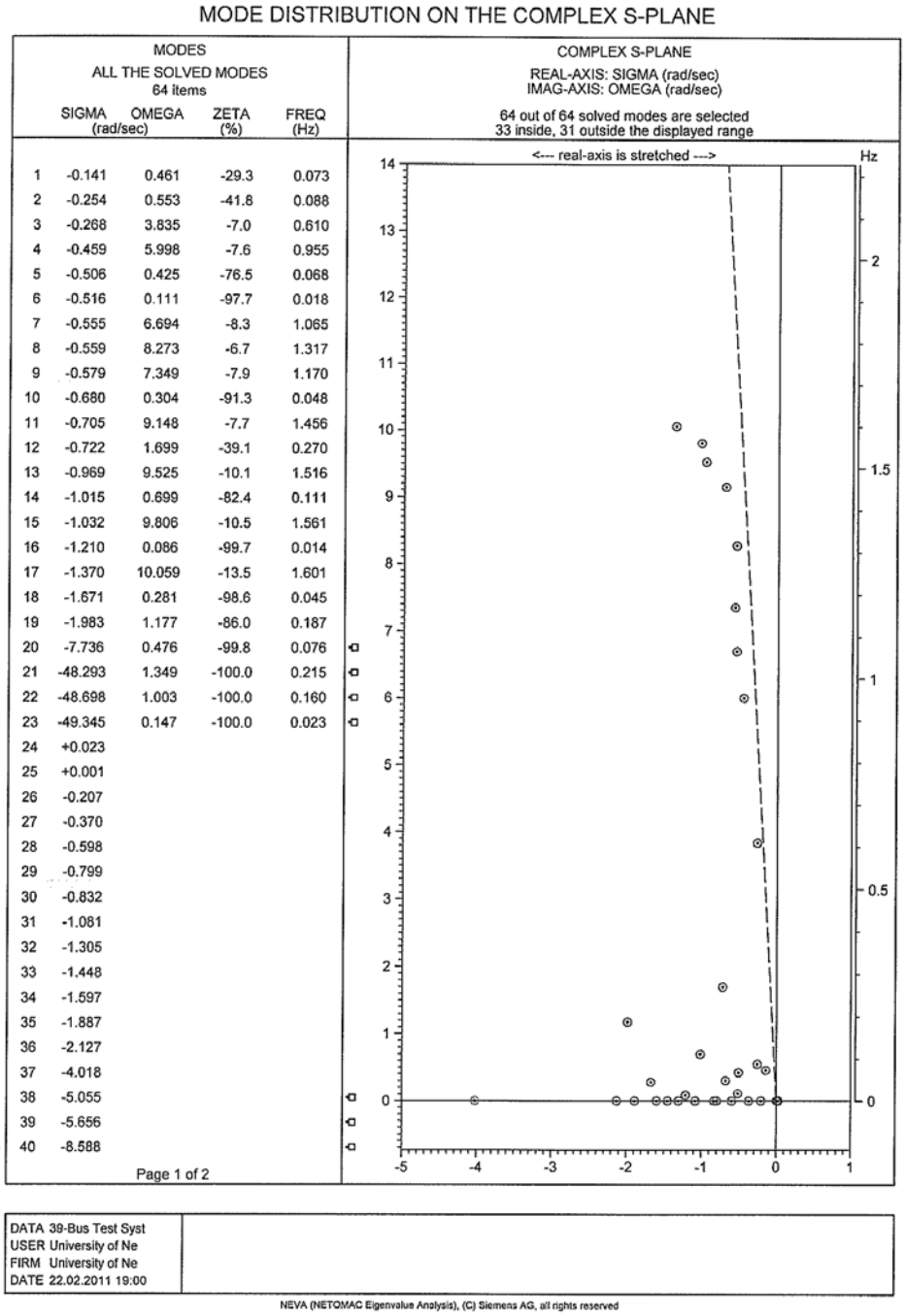

Fig 17: Modal analysis (eigenvalues) of 39 bus test system with bus 12 P and Q increased by 150%

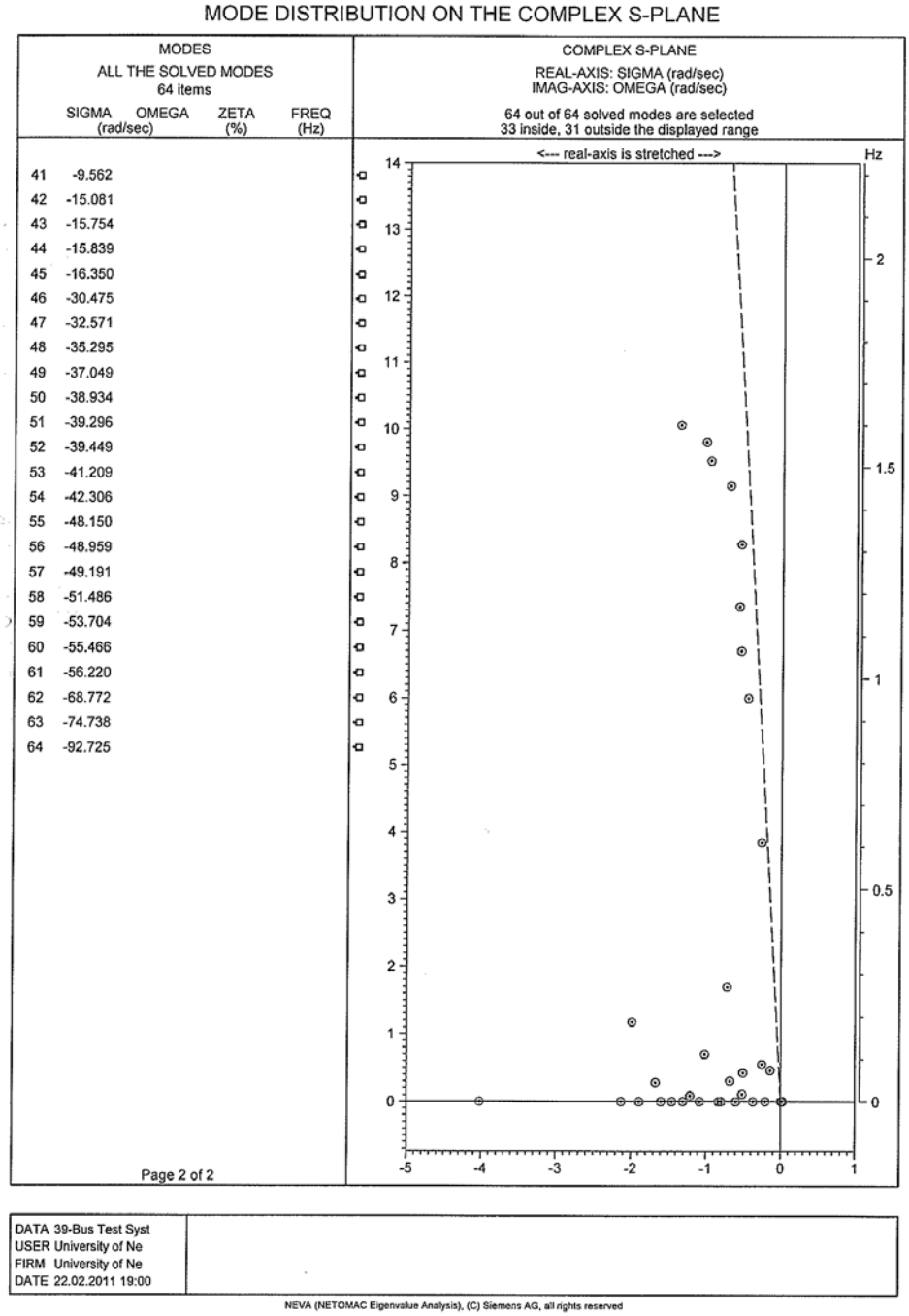

Fig 18: Modal analysis (eigenvalues) of 39 bus test system with bus 12 P and Q increased by 150%

From the modal analysis performed in NEVA we can now see that as we continuously decrease the voltage stability at bus 12, the modes of the system subsequently move closer and closer to the origin. These results prove the connection between voltage stability at the load bus and modal stability. As the voltage becomes more unstable, the modes of the system become more unstable. The opposite is also true, as the voltage becomes more stable, the modes of the system become more stable.

A second analysis is now performed to further investigate the aforementioned discovery that as voltage stability is improved, modes of the system also become more stable. In this analysis, we add purely reactive shunt capacitance to each load bus and observe the modes of the system. In looking at the power triangle that relates real, reactive and complex power we would expect that as the positive reactive power is decreased, the power factor moves closer to 1.0, and the voltage stability of the system will increase. We would then expect the modes of the system to become more stable. In this exercise, the base case load bus voltages were adjusted to provide more unstable modes. For this unstable case, a purely reactive shunt capacitance with B= +/- 1000 is added and modal analysis is performed. Table 11 shows the pertinent information from the case in which a shunt capacitance with B = -1000 was added to load bus 3. This case exemplifies the results found in every other case for which a shunt capacitor with B = -1000 was added and.

Table 11: Modal analysis results of Load Bus 3 manipulation case as compared to Base Case

Mode	Sigma value of Base Case	Sigma value of system with B = -1000 shunt capacitor at Load Bus 3
1	-0.138	-0.183
3	-0.273	-0.276
5	-0.471	-0.526
10	-0.677	-0.679
13	-0.968	-0.978
20	-1.989	-7.895
22	-39.344	-48.748

The results of the original system manipulation cases are now verified. In each case where a shunt capacitor was added with B = 1000 (ADDING to the reactive power of the bus) the modes were moved closer to the imaginary axis; thus making the modes more unstable. In each case where a shunt capacitor was added with B = -1000 (SUBTRACTING from the reactive power of the bus) the modes were moved farther away from the imaginary axis; thus making the modes more stable. As a result, our initial results about the effects of voltage stability and power factor are proven correct. As voltage stability increases, the modes of the system are made more stable. Also, as the power factor is increased toward unity, the modes of the system are made more stable.

Finally, we analyze mode participation and impact as it pertains to improving system stability. In the past analyses we showed the correlation between voltage stability and modal stability. We also proved the positive effects of adding shunt capacitors to the system load banks. Now we use

the same cases to analyze the participation and impact of such system stabilization that assists in the design of stable power systems.

In order to have the most impact on a system (stabilize the system the most) one would desire that modes with the largest real parts (i.e. closest to the imaginary axis) were moved farthest away from that imaginary axis and made more negative. To analyze which load bank had the most participation, impact and control on system stability when the shunt capacitor was added, we will take each case and analyze the ten most unstable modes from the base case (the modes with the smallest negative sigma or largest positive sigma). Once the 10 most unstable modes are identified for the base case, we identify the 10 most unstable modes from each case in which the shunt capacitor with B =-1000 was added. Now we have the sample data in which to analyze which load bus shunt capacitor had the greatest impact on stabilizing the system. In order to compare the 10 most unstable modes from each case, we normalize each set by taking the square root of the sum of the square of each sigma value. This will yield positive values for each case. Once this is completed we analyze the effect the shunt capacitor had on each case by subtracting each normalized value from the base case normalized value. This difference then shows exactly how far the 10 most unstable modes of each shunt capacitor case were moved from the base case. The end result is data showing which shunt capacitor had the biggest impact. The cases with the largest difference had their modes moved the farthest away from the imaginary axis (thus were made the most stable). Below is the quantitative analysis:

Ten most unstable mode sigma values taken from the base modal analysis case and each case where a shunt capacitor was added to a load bus are shown in Table 12.

Table 12: 10 most unstable eigenvalue sigma values for each case where a shunt capacitor was added with B = -1000

Sigma no.	Base case value	Case 1 (LB 3)	Case 2 (LB 4)	Case 3 (LB 7)	Case 4 (LB 8)
sigma1	0.025	0.024	0.025	0.025	0.023
sigma2	-0.001	-0.001	-0.002	-0.001	0.001
sigma3	-0.138	-0.185	-0.168	-0.160	-0.160
sigma4	-0.207	-0.207	-0.208	-0.208	-0.209
sigma5	-0.252	-0.243	-0.240	-0.237	-0.236
sigma6	-0.273	-0.276	-0.275	-0.270	-0.270
sigma7	-0.372	-0.345	-0.354	-0.359	-0.359
sigma8	-0.462	-0.425	-0.432	-0.439	-0.440
sigma9	-0.471	-0.526	-0.489	-0.474	-0.477
sigma10	-0.513	-0.526	-0.530	-0.531	-0.531

Table 12: 10 most unstable eigenvalue sigma values for each case where a shunt capacitor was added with B = -1000

Sigma no.	Case 5 (LB 12)	Case 6 (LB 15)	Case 7 (LB 16)	Case 8 (LB 18)	Case 10 (LB 21)
sigma1	0.025	0.023	0.022	0.023	0.023
sigma2	-0.002	0.000	0.001	0.000	0.001
sigma3	-0.156	-0.164	-0.164	-0.180	-0.157
sigma4	-0.208	-0.207	-0.207	-0.207	-0.207
sigma5	-0.247	-0.240	-0.240	-0.240	-0.248
sigma6	-0.268	-0.359	-0.360	-0.351	-0.363
sigma7	-0.361	-0.424	-0.418	-0.414	-0.431
sigma8	-0.443	-0.515	-0.529	-0.530	-0.518
sigma9	-0.506	-0.541	-0.539	-0.532	-0.542
sigma10	-0.529	-0.550	-0.543	-0.542	-0.547

Sigma no.	Case 11 (LB 23)	Case 12 (LB 24)	Case 13 (LB 25)	Case 14 (LB 26)
sigma1	0.022	0.023	0.023	0.023
sigma2	0.001	0.000	-0.001	0.001
sigma3	-0.148	-0.162	-0.207	-0.196
sigma4	-0.207	-0.207	-0.261	-0.207
sigma5	-0.256	-0.243	-0.311	-0.243
sigma6	-0.276	-0.361	-0.429	-0.275
sigma7	-0.367	-0.422	-0.492	-0.353
sigma8	-0.445	-0.532	-0.503	-0.375
sigma9	-0.495	-0.535	-0.521	-0.504
sigma10	-0.546	-0.545	-0.523	-0.531

Sigma no.	Case 15 (LB 27)	Case 16 (LB 28)	Case 17 (LB 29)	Case 19 (LB 39)
sigma1	0.023	0.023	0.024	0.025
sigma2	0.000	0.000	-0.001	-0.001
sigma3	-0.185	-0.169	-0.169	-0.138
sigma4	-0.207	-0.207	-0.207	-0.222
sigma5	-0.243	-0.238	-0.237	-0.252
sigma6	-0.282	-0.266	-0.266	-0.258
sigma7	-0.354	-0.362	-0.324	-0.372
sigma8	-0.387	-0.368	-0.362	-0.462
sigma9	-0.515	-0.486	-0.486	-0.471
sigma10	-0.536	-0.505	-0.522	-0.513

Next we normalize each set in order to make our comparison. This is accomplished by taking the square root of the sum of the squares of each sigma value. This is defined as MMODE described in Equation 4.1. Table 13 then lists the MMODE results for the base case system and each system for which a capacitor with B = -1000.

$$MMODE = \sqrt{sigma_1^2 + sigma_2^2 + sigma_3^2 + ...} \tag{4.1}$$

Table 13: Mode of sigma values for each case where a shunt capacitor was added with B = -1000

MMODEBASE	1.017909623
MMODECASE1	1.03185561
MMODECASE2	1.017866887
MMODECASE3	1.012693438
MMODECASE4	1.014553104
MMODECASE5	1.030659498
MMODECASE6	1.138366813
MMODECASE7	1.138593431
MMODECASE8	1.133404164
MMODECASE10	1.143371768
MMODECASE11	1.040112975
MMODECASE12	1.141180091
MMODECASE13	1.196347358
MMODECASE14	1.008275756
MMODECASE15	1.02113858
MMODECASE16	0.977737184
MMODECASE17	0.970803791
MMODECASE19	1.017157805

Next we differentiate the magnitude of the modal impact for each shunt capacitor case by subtracting the normalized value of each case from the base case. We define this as DMODE shown in Equation 4.2. Table 14 then lists the DMODE results for each –B shunt capacitor case compared to the base case. The result is a determination that the load bus with the largest participation, impact and control on stabilizing the modes of the system when adding a capacitor of B = -1000 is load bus 13.

$$DMODE_n = MMODEBASE = MMODECASE_n \tag{4.2}$$

Table 14: Difference between the base mode and case modes

DMODE1	0.013945987
DMODE2	-4.27355E-05
DMODE3	-0.005216184
DMODE4	-0.003356519
DMODE5	0.012749875

Table 14: Difference between the base mode and case modes

DMODE6	0.12045719
DMODE7	0.120683808
DMODE8	0.115494542
DMODE10	0.125462145
DMODE11	0.022203352
DMODE12	0.123270468
DMODE13	0.178437735
DMODE14	-0.009633867
DMODE15	0.003228958
DMODE16	-0.040172439
DMODE17	-0.047105832
DMODE19	-0.000751818

In this chapter, we presented the small signal stability analysis results of an IEEE 39 bus system. In defining various system inputs including bus data, generator data, line data, and transformer data, we produced simulation results for the modal analysis of the system. Next we found the correlation between voltage stability and modal stability by manipulating the voltage at the load buses of the system. We were able to see that as voltage stability decreased, so did modal stability (and vice versa). Finally, we used the modal and voltage stability simulation results to find which load bus participated most in the modal stability of the system.

Chapter 5 will review these results and draw conclusions base on the data. The conclusions will include system stability, how voltage stability affects modal stability and the load bus that participates most. In addition, future work involved in continuing the research will be cited.

Chapter 5

Concluding Remarks and Future Works

5.1 Concluding Remarks

In summary, Chapter 1 presented the foundational building blocks of power systems and power system stability. While defining what each is, we delved into the progression, historically, of how each has grown and evolved into what we see today. The major components of a power system, generation, transmission and distribution were covered as examples of different types of power systems were explained. Power system stability and its different designations were then outlined. The linearizing approach of small signal stability to simplify the analysis and calculations of a system while identifying system characteristics and operation were explained as a contrast to the time varying, differential methodology of transient stability analysis. Finally, we introduced the contents of the thesis as pertaining to the expected contributions. From the introduction of Chapter 1, Chapter 2 followed with a mathematical and literary review of how small signal stability is performed. Equations that are used in small signal stability were derived and explanations of the significance were detailed. The computational derivations included utilizing state space representation to linearize a modeled power system, state matrix calculation and eigenvalue determination, left and right eigenvectors and participation matrix identification. After mathematically communicating the modal analysis process, summaries of several common techniques that make use of eigenvalue analysis equations were presented. These techniques include AESOPS, MAM, PEALS, SMA, S-Method and Q-R Transformation.

Chapter 3 builds on the foundation laid by Chapters 1 and 2, by introducing the IEEE 39 bus power system and simulation software that will utilize the numerical analysis techniques that have been established. The system inputs are presented and details are shown for exactly how the simulation software will analyze the system. Sample graphs and data reveal expected results that show system stability (or lack thereof), modes eigenvalues, oscillation, and damping. A deeper understanding of the analysis of a power system and the application of the eigenvalue analysis techniques can now be gained as a result of the example data yielded by the simulation software.

Chapter 4 bridges the background information provided in the first three chapters and the research results by first outlining the approach and methodology used in this endeavor. Modal analysis of an initial 39 bus system, that yields the eigenvalues of the system is used to determine whether the system is stable or not, at that particular equilibrium point. Once stability is determined, we turn our attention to performing modal analysis on the system while manipulating different aspects of the system in order to draw conclusion about the correlation between voltage stability and modal stability. To verify our results, this is performed two different ways; adjusting load bus real and reactive power to decrease voltage stability, and adding shunt capacitors to the load buses. Trends in the modal analysis results are now ready to be compared to voltage stability in order to draw conclusions. Finally, the modal and voltage stability results are used to determine the participation of each load bus in the system. Using the average of the 10 most unstable modes of each case, we were able to extract information on which load bus altered the system eigenvalues most; thus revealing the largest participation.

The first conclusion reached as a result of the data produced in this research, indicates that the original IEEE 39 bus test system is in fact stable around the equilibrium point of the system inputs. System stability is easily determined by the NEVA modal distribution plot due to the fact that the real parts of each eigenvalue is located on the left side of the vertical axis. With system stability now confirmed, the analysis of voltage stability versus modal stability begins by adjusting the voltage characteristics of the system and comparing the resulting mode changes.

This showes that as voltage stability decreased, the modes of the system also became more unstable; resulting in less system stability. This relationship is confirmed by performing modal analysis on the system after applying shunt capacitances that also affect voltage stability. Once again we observe the fact that as voltage stability decreased, so does the stability of the modes of the system. Our final investigative component was a design centered approach to quantitatively predict the participation level each bus has on modal stability. Using a weighted average technique we showed how a determination can be made as to which bus will yield the greatest control of system stability by manipulating its voltage stability. The affects of manipulating bus 13 provided the largest eigenvalue shift, on average. As a result, the conclusion is made that bus 13 has the largest participation in the modal stability of the 39 bus system presented.

5.2 Future Work

The research and methodology presented in this paper serve as a useful tool in solving real world power system problems. In large power systems, such as industrial facilities, the modal stability and participation factor analysis techniques can allow for a number of advantages. These advantages include stability determination and monitoring as systems grow and expand as well as achieving operational and stability improvement in the most efficient manner possible by focusing engineering efforts on the components that participate most. From this, large cost savings can be achieved as decreased power consumption yields lower utility costs, equipment can be operated more efficiently, stability control efforts are minimized, and equipment life cycles are prolonged. In addition, the evolution of Smart Grid technology allows for the application of these techniques in a more 'real time' fashion to achieve more continual system improvement that matches the dynamic nature of the power system. Again, this will result in increased reliability and efficiency in power systems that yield cost savings.

Going forward, future work includes expanding the investigative process by analyzing different systems using the same approach. In addition, detailed calculations of the participation matrix can also be performed to further analyze the approach used in this research. Utilizing different system inputs and analyzing the system at different equilibrium points will also help identify system behavior and its control.

Bibliography

[1] Kundur, P; “Power System Stability and Control,” McGraw0Hill, 1994

[2] Rogers, G. J, “Methods for Small Signal Analysis of Very Large Power Systems,” IEEE Proceedings on the 25th Conference on Decision and Control, pp. 393-398, 1987

[3] Barquin, J.; Rouco, L.; Vargas, H.R.; “Generalized Selective Modal Analysis,” IEEE Power Engineering Society Winter Meeting, vol. 2, pp. 1194-1199, 2002

[4] Huang, Y.; Xu, Z.; Pan, W.; “A Practical Analysis Method of Low Frequency Oscillation for Large Power Systems,” IEEE Power Engineering Society General Meeting, vol. 2, pp. 1623-1629, June 2005

[5] Huang, Z.; Bao, L.; Xu, W.; “Generator Ranking Using Modal Analysis,” IEEE Generation, Transmission and Distribution, vol. 150, pp. 709-716, November 2003

[6] Tong, S.; Miu, K.N.; “Participation Factor Studies for Distributed Slack Bus Models in Three-Phase Distribution Power Flow Analysis,” IEEE Transmission and Distribution Conference and Exhibition, pp. 92-96, 2006

[7] Kopcak, I.; da Silva, L.C.P.; da Costa, V.F.; Naturesa, J.S.; “Transmission Systems Congestion Management by Using Modal Participation Factors,” IEEE Power Tech Conference, vol. 2, 2003

[8] da Silva, L.C.P.; Wang, Y.; da Costa, V.F.; Xu, W.; “Assessment of Generator Impact on System Power Transfer Capability using Modal Participation Factors,” IEEE Generation, Transmission and Distribution, vol. 149, pp. 564-570, 2002

[9] Abed, E.H.; Hassouneh, M.A.; Hashlamoun, W.A.; “Modal Participation Factors Revisited: One Definition Replaced by Two,” American Control Conference, pp. 1140-1145, 2009

[10] Bedoya, D.; Bedrinana, B.F.; Castro, C.A.; da Silva, L.C.P.; “Power System Critical Areas by Using Sensitivities and Participation Factors for Online Applications,” IEEE Transmission and Distribution Conference and Exposition, Latin America, pp. 1-6, 2008

[11] Zhang, J.; Sun, Y.; “Variational Approach in Modal Analysis,” IEEE Power Engineering Society General Meeting, vol. 1, pp. 259-265, 2005

[12] Sharma, C.; Ganness, M.G.; “Determination of the Applicability of Using Modal Analysis for the Prediction of Voltage Stability,” IEEE Transmission and Distribution Conference and Exposition, pp. 1-7, 2008

[13] Kundur, P., Wang, L., “Small Signal Stability Analysis: Experiences, Achievements, and Challenges,” IEEE and Power Tech Labs Inc., pp. 6-12, 2002

[14] Hausknecht, A. O.; Kowalczyk, “Linear Systems of Differential Equations,” http://www.faculty.umassd.edu/adam.hausknecht/temath/TEMATH2/Examples/LinearSystemsOfDiffEqs.html

[15] Shimada, “Visualization of Power System Swing Phenomena Using Animation,” http://www.google.com/imgres?imgurl=http://www.syl.t.u-tokyo.ac.jp/E-Web/img/NewEngland38_2.gif&imgrefurl=http://www.syl.t.u-tokyo.ac.jp/E-Web/museum/list_e.html&usg=__LPiL1GMdrLLbMjj3M7Em6bW-VFY=&h=244&w=320&sz=8&hl=en&start=2&zoom=1&tbnid=9uhE8afGfjVq6M:&tbnh=90&tbnw=118&ei=bY7KTtiJAcK7tgfrmMWuDA&prev=/search%3Fq%3Dieee%2B39%2Bbus%2Btest%2Bsystem%26um%3D1%26hl%3Den%26sa%3DN%26gbv%3D2%26tbm%3Disch&um=1&itbs=1

[16] Pablo, L. E., “New England test system, IEEE 39 Bus System, 10 generators, in PSS/E format,” http://electrica.uc3m.es/pablole/varios_e.html

[17] Pannhorst, H., “NEVA, PSS NETOMAC Eigenvalue Analysis Getting Started,” Siemens Power Transmission and Distribution, 2006

Appendix

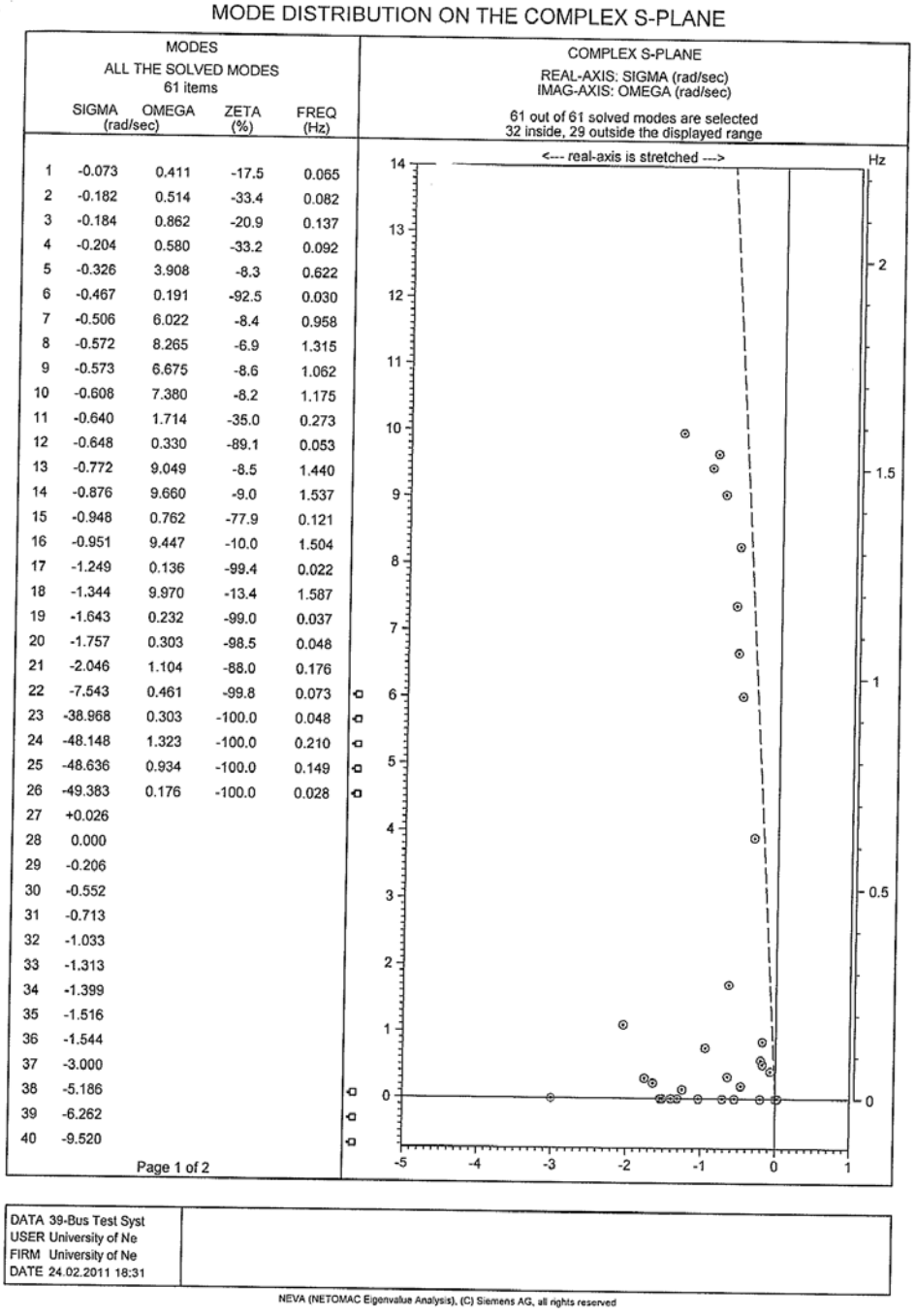

Fig 19: Modal analysis (eigenvalues) of 39 bus test system with shunt capacitor B = 1000 at load bus 3

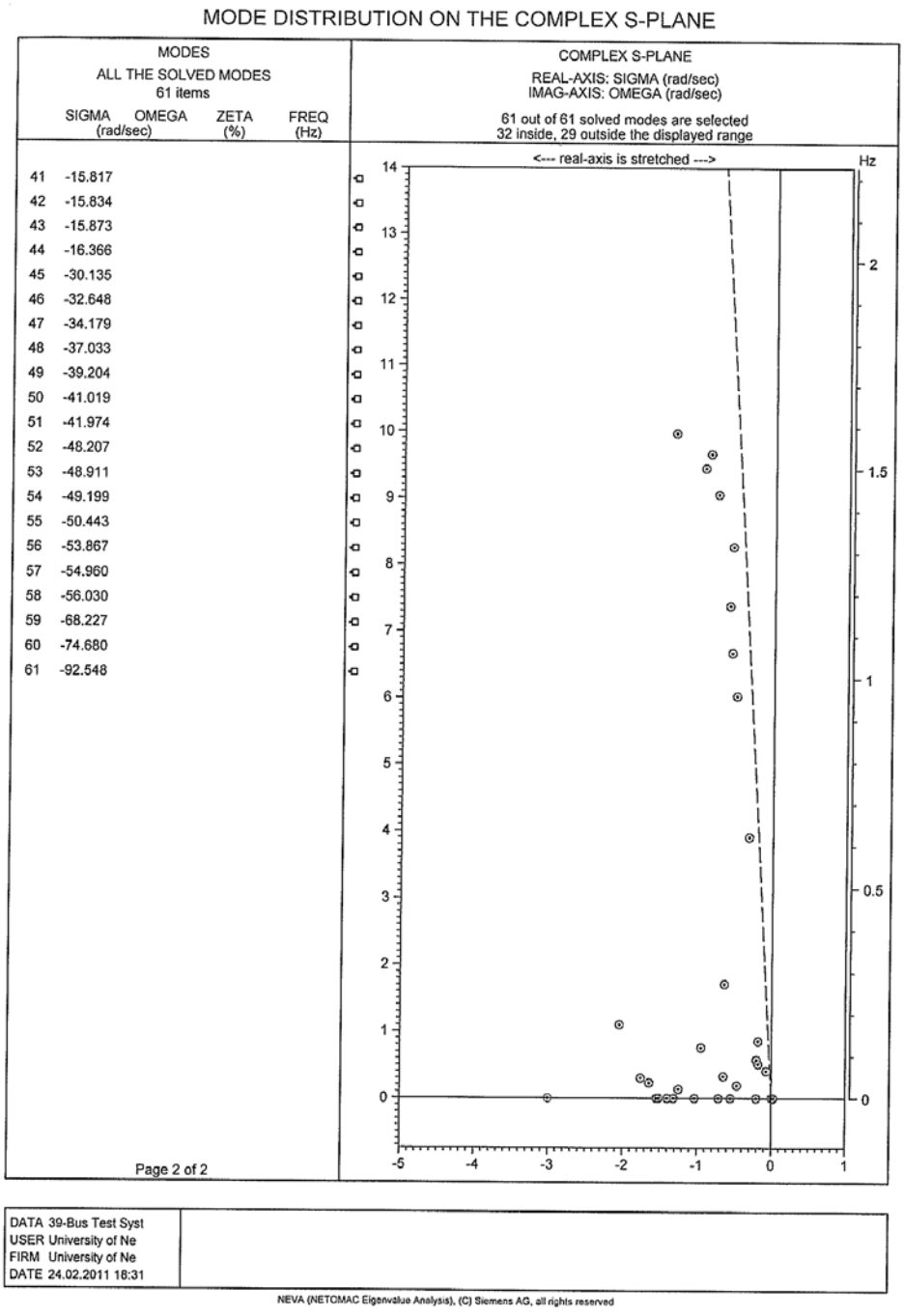

Fig 20: Modal analysis (eigenvalues) of 39 bus test system with shunt capacitor B = 1000 at load bus 3

MODE DISTRIBUTION ON THE COMPLEX S-PLANE

MODES
ALL THE SOLVED MODES
61 items

	SIGMA (rad/sec)	OMEGA (rad/sec)	ZETA (%)	FREQ (Hz)
1	-0.103	0.443	-22.7	0.070
2	-0.156	0.531	-28.1	0.085
3	-0.208	0.581	-33.7	0.092
4	-0.321	3.919	-8.2	0.624
5	-0.471	0.195	-92.4	0.031
6	-0.493	6.018	-8.2	0.958
7	-0.571	6.632	-8.6	1.055
8	-0.585	8.269	-7.1	1.316
9	-0.626	7.329	-8.5	1.167
10	-0.650	0.332	-89.0	0.053
11	-0.682	1.707	-37.1	0.272
12	-0.776	0.010	-100.0	0.002
13	-0.809	8.852	-9.1	1.409
14	-0.945	9.730	-9.7	1.549
15	-0.954	9.456	-10.0	1.505
16	-0.968	0.768	-78.3	0.122
17	-1.233	0.133	-99.4	0.021
18	-1.347	9.978	-13.4	1.588
19	-1.666	0.223	-99.1	0.035
20	-1.789	0.284	-98.8	0.045
21	-2.038	1.107	-87.9	0.176
22	-7.558	0.471	-99.8	0.075
23	-39.083	0.222	-100.0	0.035
24	-48.138	1.314	-100.0	0.209
25	-48.731	0.972	-100.0	0.155
26	-49.318	0.122	-100.0	0.019
27	+0.024			
28	+0.000			
29	-0.206			
30	-0.402			
31	-0.513			
32	-1.023			
33	-1.275			
34	-1.378			
35	-1.511			
36	-2.998			
37	-5.161			
38	-5.957			
39	-7.458			
40	-8.715			

Page 1 of 2

COMPLEX S-PLANE
REAL-AXIS: SIGMA (rad/sec)
IMAG-AXIS: OMEGA (rad/sec)
61 out of 61 solved modes are selected
31 inside, 30 outside the displayed range

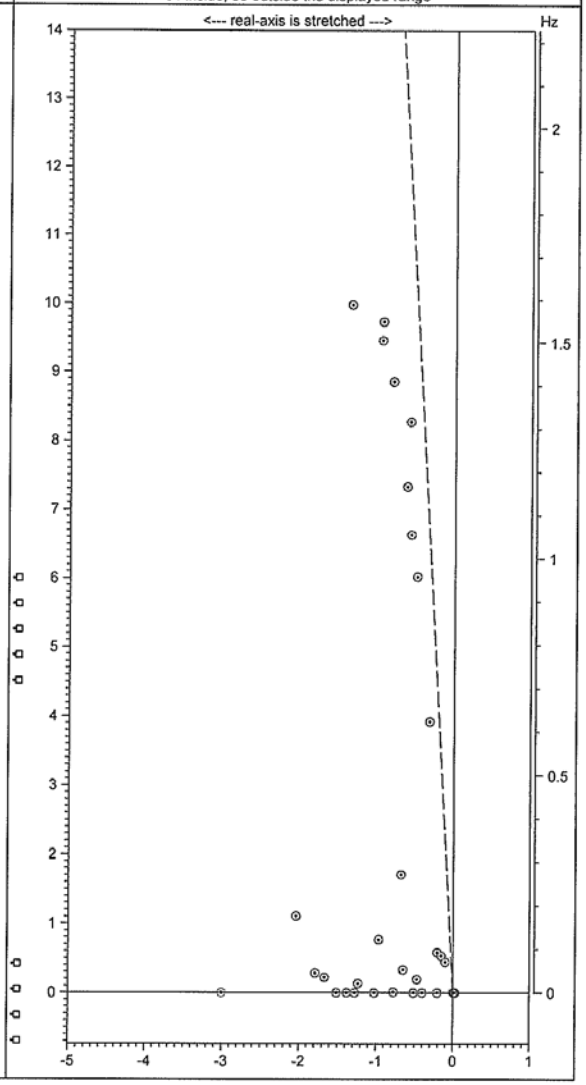

DATA 39-Bus Test Syst
USER University of Ne
FIRM University of Ne
DATE 24.02.2011 18:36

Fig 21: Modal analysis (eigenvalues) of 39 bus test system with shunt capacitor B = 1000 at load bus 4

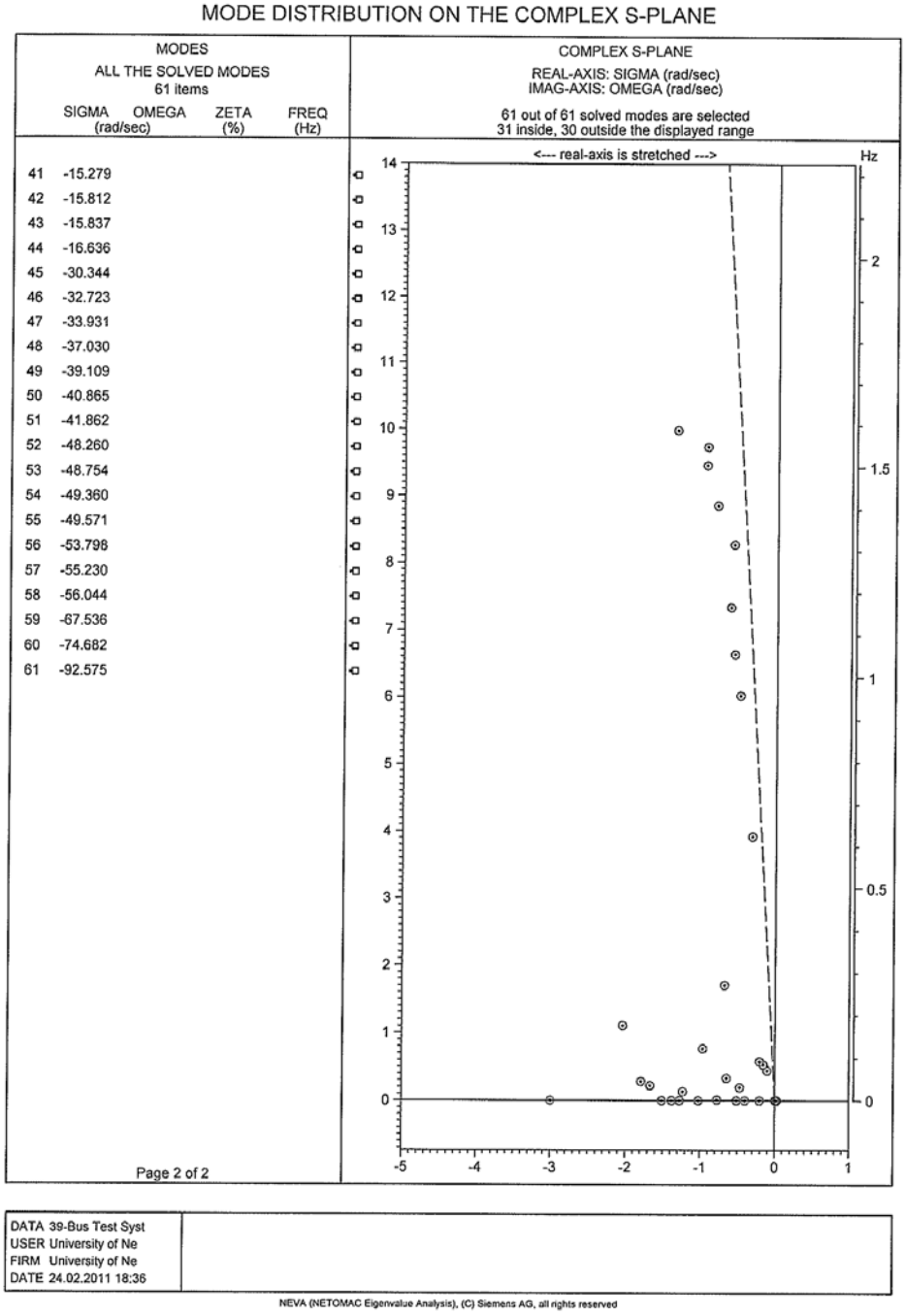

Fig 22: Modal analysis (eigenvalues) of 39 bus test system with shunt capacitor B = 1000 at load bus 4

MODE DISTRIBUTION ON THE COMPLEX S-PLANE

MODES
ALL THE SOLVED MODES
61 items

	SIGMA (rad/sec)	OMEGA (rad/sec)	ZETA (%)	FREQ (Hz)
1	-0.116	0.449	-25.0	0.071
2	-0.153	0.543	-27.1	0.086
3	-0.217	0.578	-35.1	0.092
4	-0.320	3.945	-8.1	0.628
5	-0.480	0.202	-92.2	0.032
6	-0.482	6.015	-8.0	0.957
7	-0.570	6.616	-8.6	1.053
8	-0.586	8.262	-7.1	1.315
9	-0.630	7.297	-8.6	1.161
10	-0.659	0.325	-89.7	0.052
11	-0.693	1.705	-37.6	0.271
12	-0.832	8.680	-9.5	1.381
13	-0.960	9.479	-10.1	1.509
14	-0.981	9.761	-10.0	1.554
15	-0.983	0.758	-79.2	0.121
16	-1.222	0.131	-99.4	0.021
17	-1.358	10.004	-13.4	1.592
18	-1.685	0.230	-99.1	0.037
19	-1.783	0.273	-98.8	0.043
20	-2.019	1.125	-87.4	0.179
21	-7.607	0.491	-99.8	0.078
22	-39.280	0.179	-100.0	0.028
23	-48.159	1.319	-100.0	0.210
24	-48.763	1.000	-100.0	0.159
25	-49.284	0.138	-100.0	0.022
26	-49.466	0.047	-100.0	0.007
27	+0.023			
28	+0.001			
29	-0.205			
30	-0.386			
31	-0.461			
32	-0.780			
33	-0.804			
34	-1.019			
35	-1.228			
36	-1.366			
37	-1.510			
38	-2.991			
39	-5.132			
40	-5.837			

Page 1 of 2

COMPLEX S-PLANE
REAL-AXIS: SIGMA (rad/sec)
IMAG-AXIS: OMEGA (rad/sec)

61 out of 61 solved modes are selected
32 inside, 29 outside the displayed range

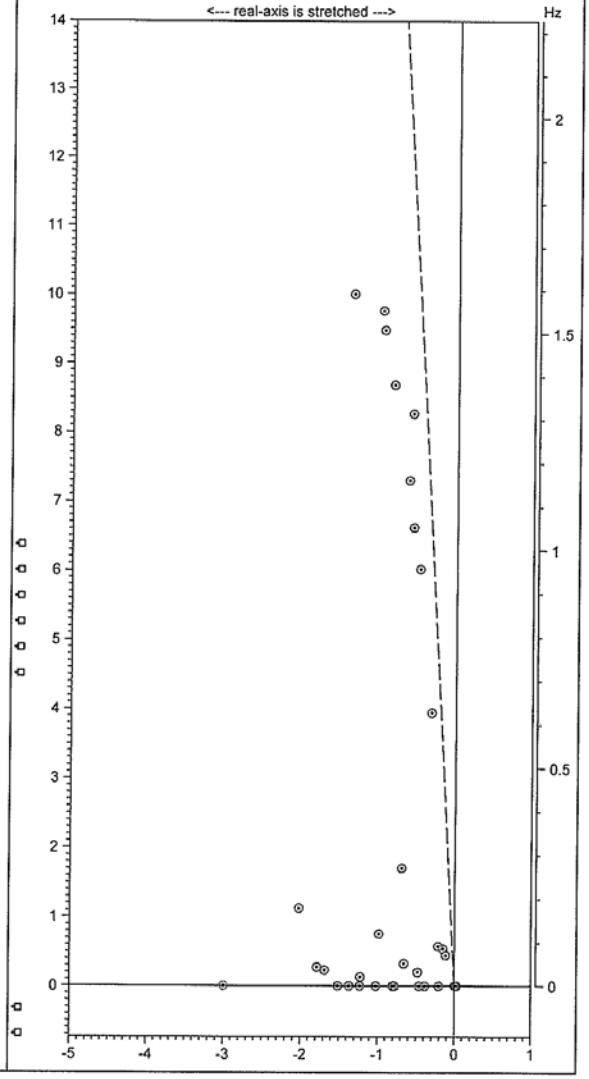

DATA 39-Bus Test Syst
USER University of Ne
FIRM University of Ne
DATE 24.02.2011 18:40

Fig 23: Modal analysis (eigenvalues) of 39 bus test system with shunt capacitor B = 1000 at load bus 7

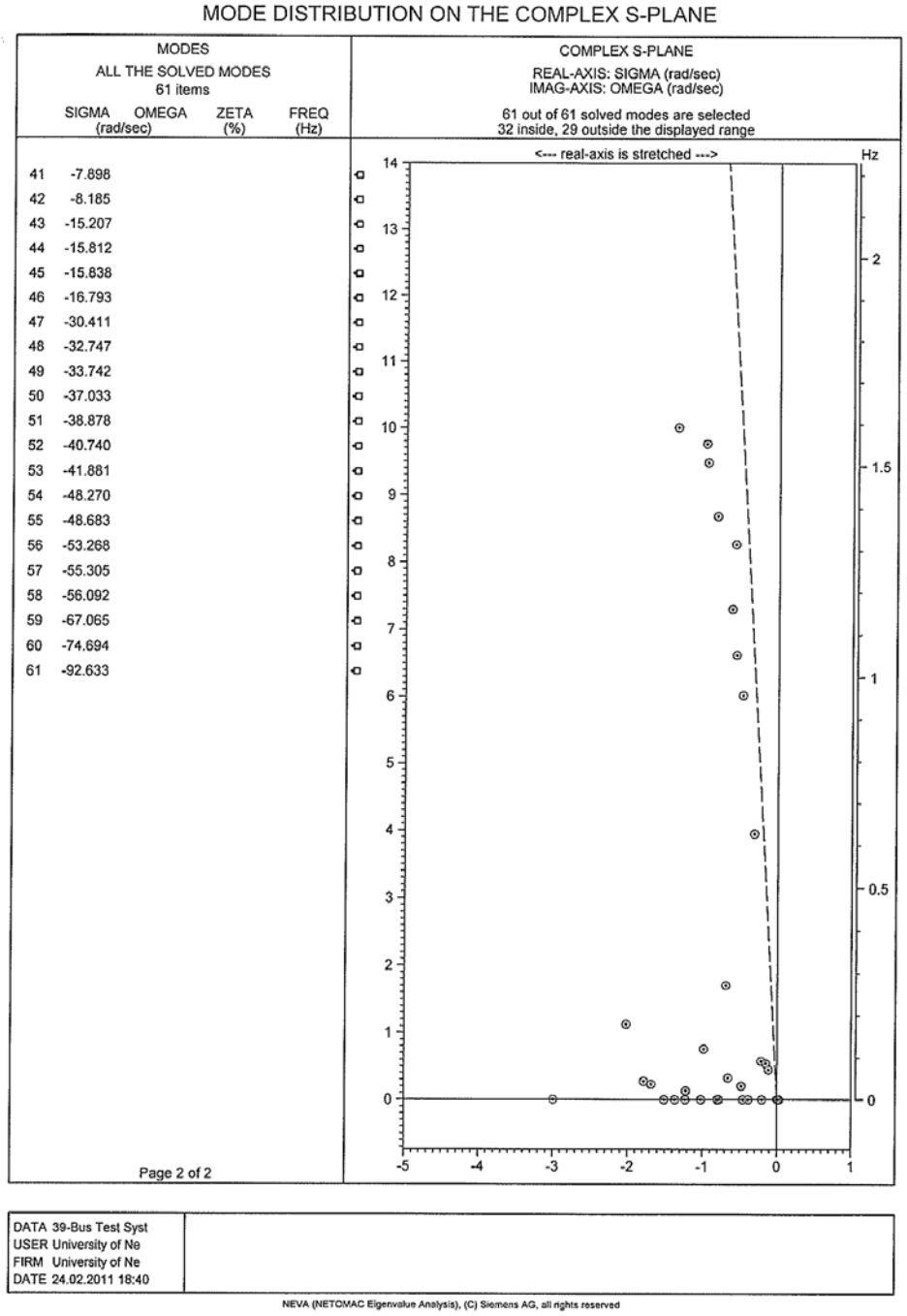

Fig 24: Modal analysis (eigenvalues) of 39 bus test system with shunt capacitor B = 1000 at load bus 7

MODE DISTRIBUTION ON THE COMPLEX S-PLANE

MODES
ALL THE SOLVED MODES
62 items

	SIGMA (rad/sec)	OMEGA (rad/sec)	ZETA (%)	FREQ (Hz)
1	-0.116	0.449	-25.1	0.071
2	-0.156	0.541	-27.8	0.086
3	-0.218	0.580	-35.1	0.092
4	-0.320	3.954	-8.1	0.629
5	-0.480	0.202	-92.2	0.032
6	-0.481	6.015	-8.0	0.957
7	-0.571	6.625	-8.6	1.054
8	-0.585	8.263	-7.1	1.315
9	-0.629	7.302	-8.6	1.162
10	-0.659	0.324	-89.7	0.052
11	-0.694	1.705	-37.7	0.271
12	-0.830	8.711	-9.5	1.386
13	-0.960	9.480	-10.1	1.509
14	-0.982	9.762	-10.0	1.554
15	-0.984	0.756	-79.3	0.120
16	-1.222	0.131	-99.4	0.021
17	-1.358	10.005	-13.5	1.592
18	-1.678	0.230	-99.1	0.037
19	-1.781	0.279	-98.8	0.044
20	-2.017	1.126	-87.3	0.179
21	-7.609	0.492	-99.8	0.078
22	-39.287	0.174	-100.0	0.028
23	-48.165	1.322	-100.0	0.210
24	-48.756	0.996	-100.0	0.158
25	-49.299	0.134	-100.0	0.021
26	+0.023			
27	+0.001			
28	-0.205			
29	-0.386			
30	-0.470			
31	-0.780			
32	-0.805			
33	-1.021			
34	-1.235			
35	-1.366			
36	-1.507			
37	-2.991			
38	-5.132			
39	-5.834			
40	-7.908			

Page 1 of 2

COMPLEX S-PLANE
REAL-AXIS: SIGMA (rad/sec)
IMAG-AXIS: OMEGA (rad/sec)
62 out of 62 solved modes are selected
32 inside, 30 outside the displayed range

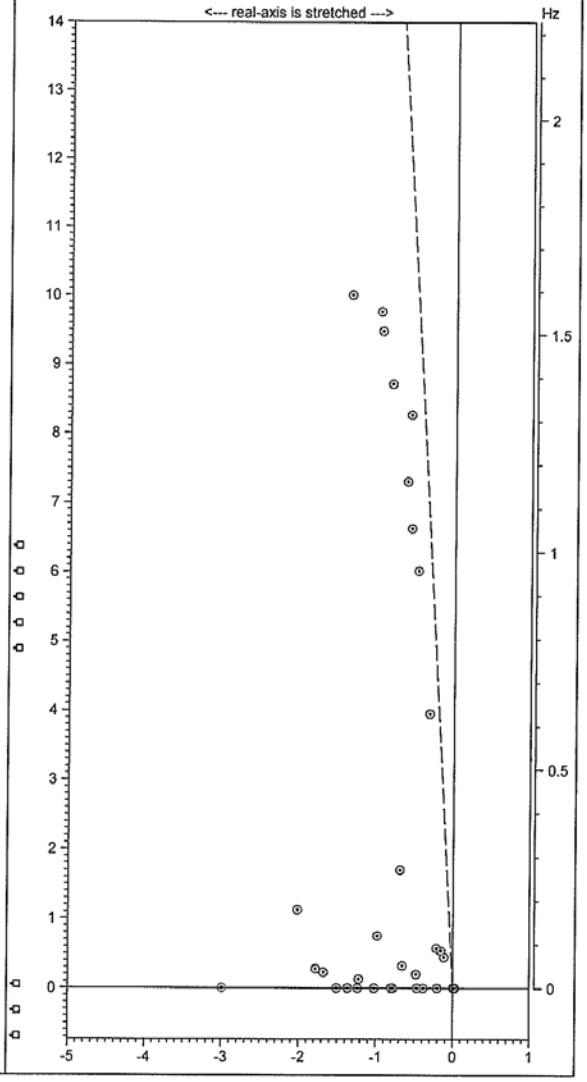

DATA 39-Bus Test Syst
USER University of Ne
FIRM University of Ne
DATE 24.02.2011 18:44

Fig 25: Modal analysis (eigenvalues) of 39 bus test system with shunt capacitor B = 1000 at load bus 8

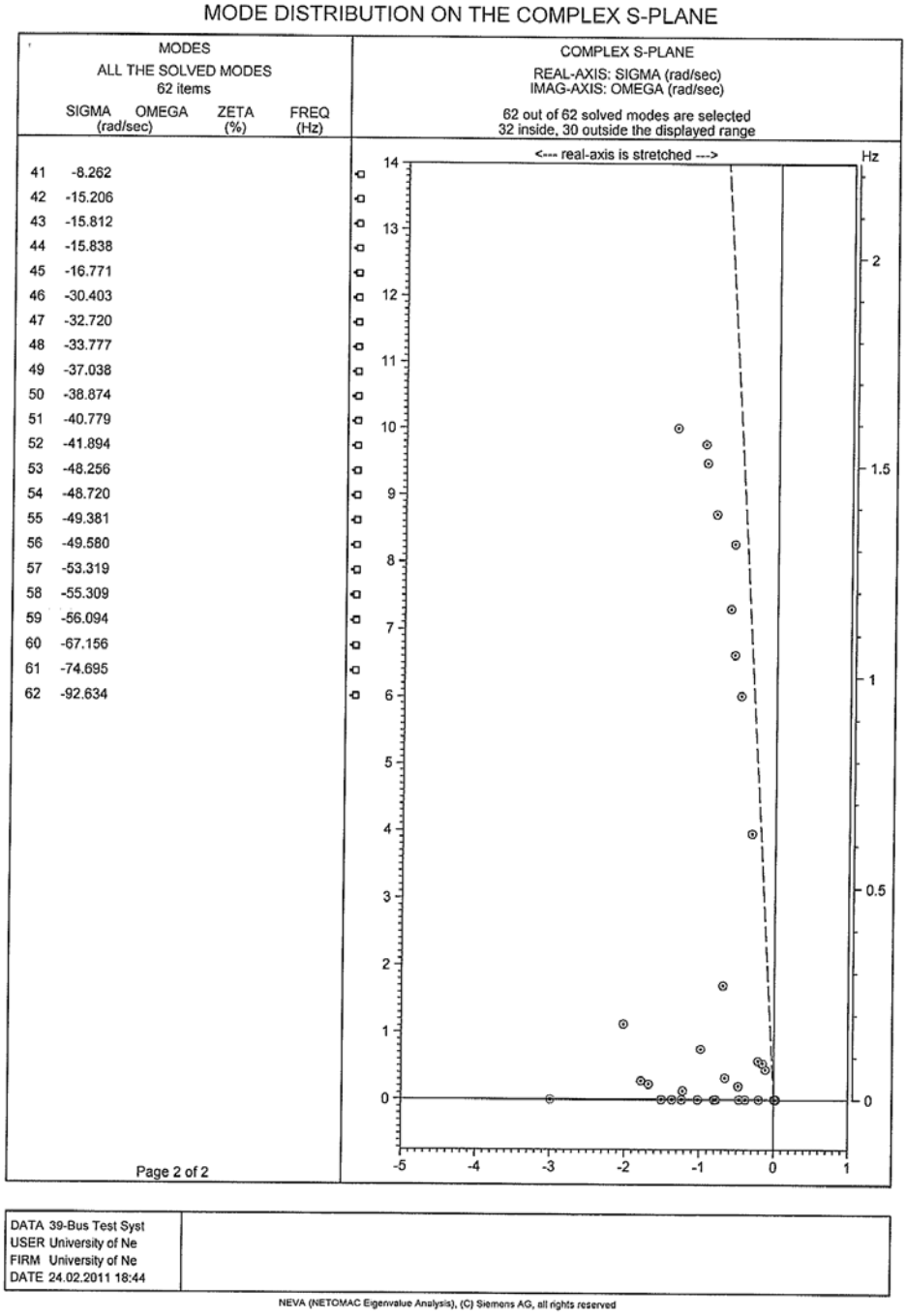

Fig 26: Modal analysis (eigenvalues) of 39 bus test system with shunt capacitor B = 1000 at load bus 8

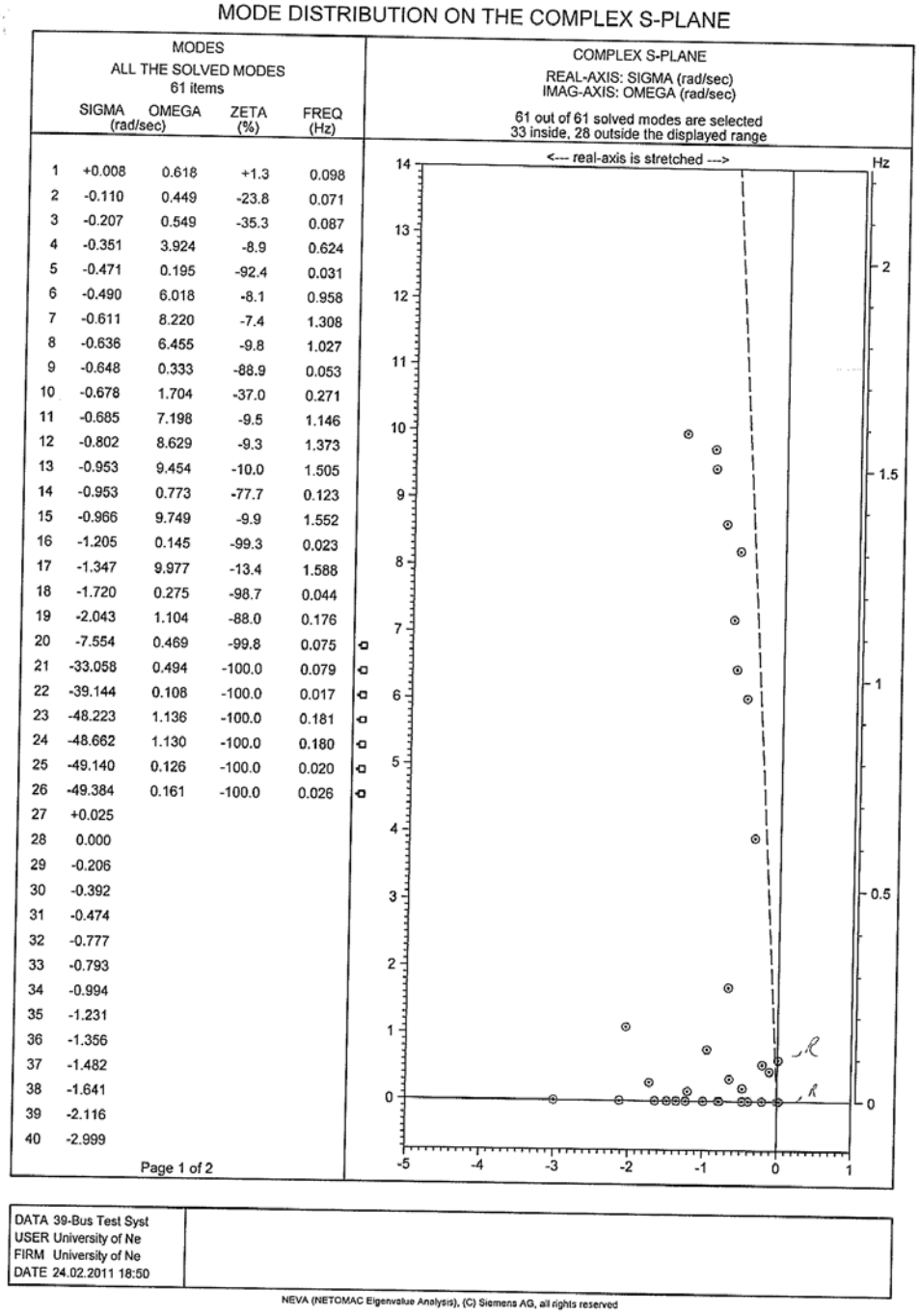

Fig 27: Modal analysis (eigenvalues) of 39 bus test system with shunt capacitor B = 1000 at load bus 12

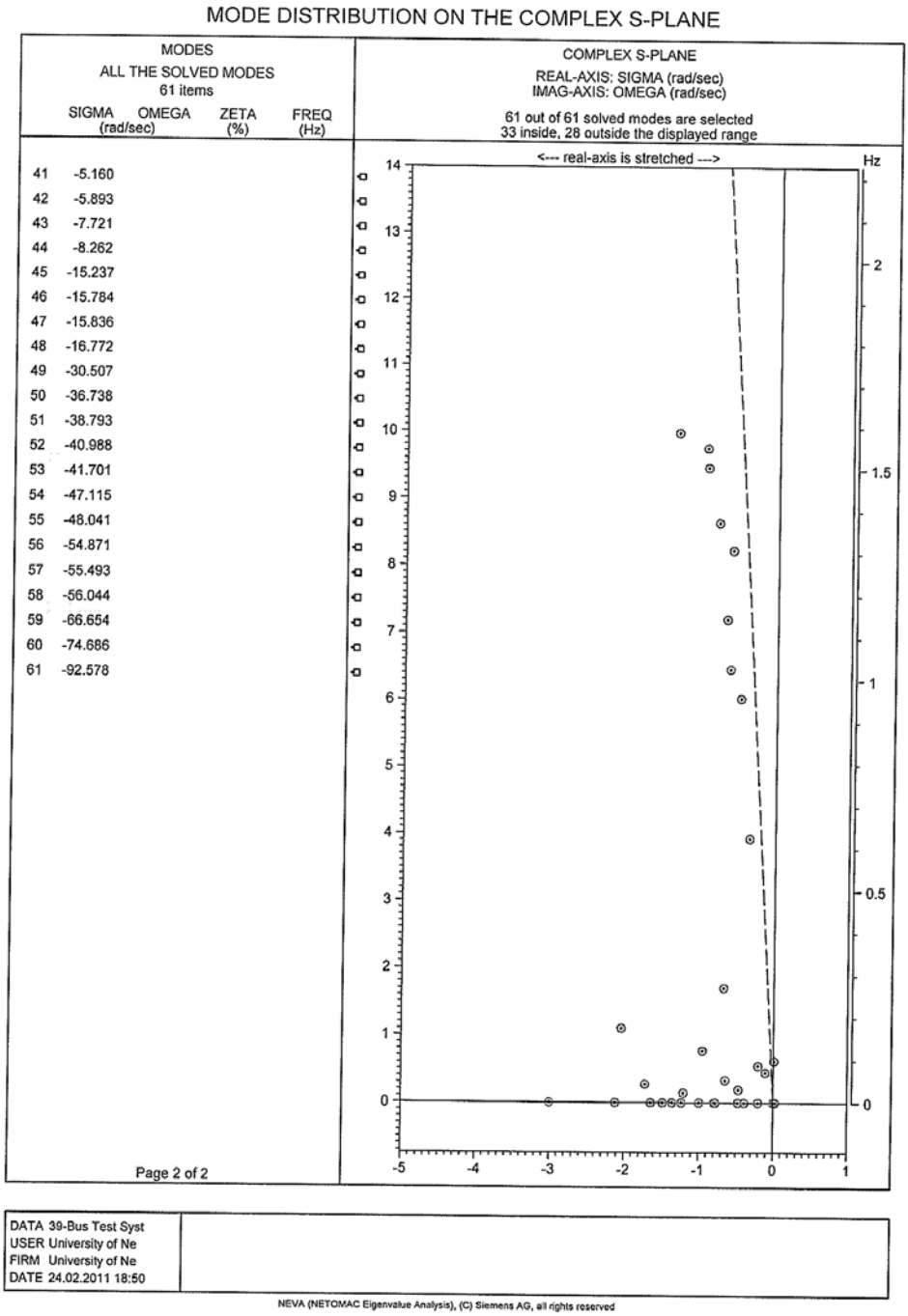

Fig 28: Modal analysis (eigenvalues) of 39 bus test system with shunt capacitor B = 1000 at load bus 12

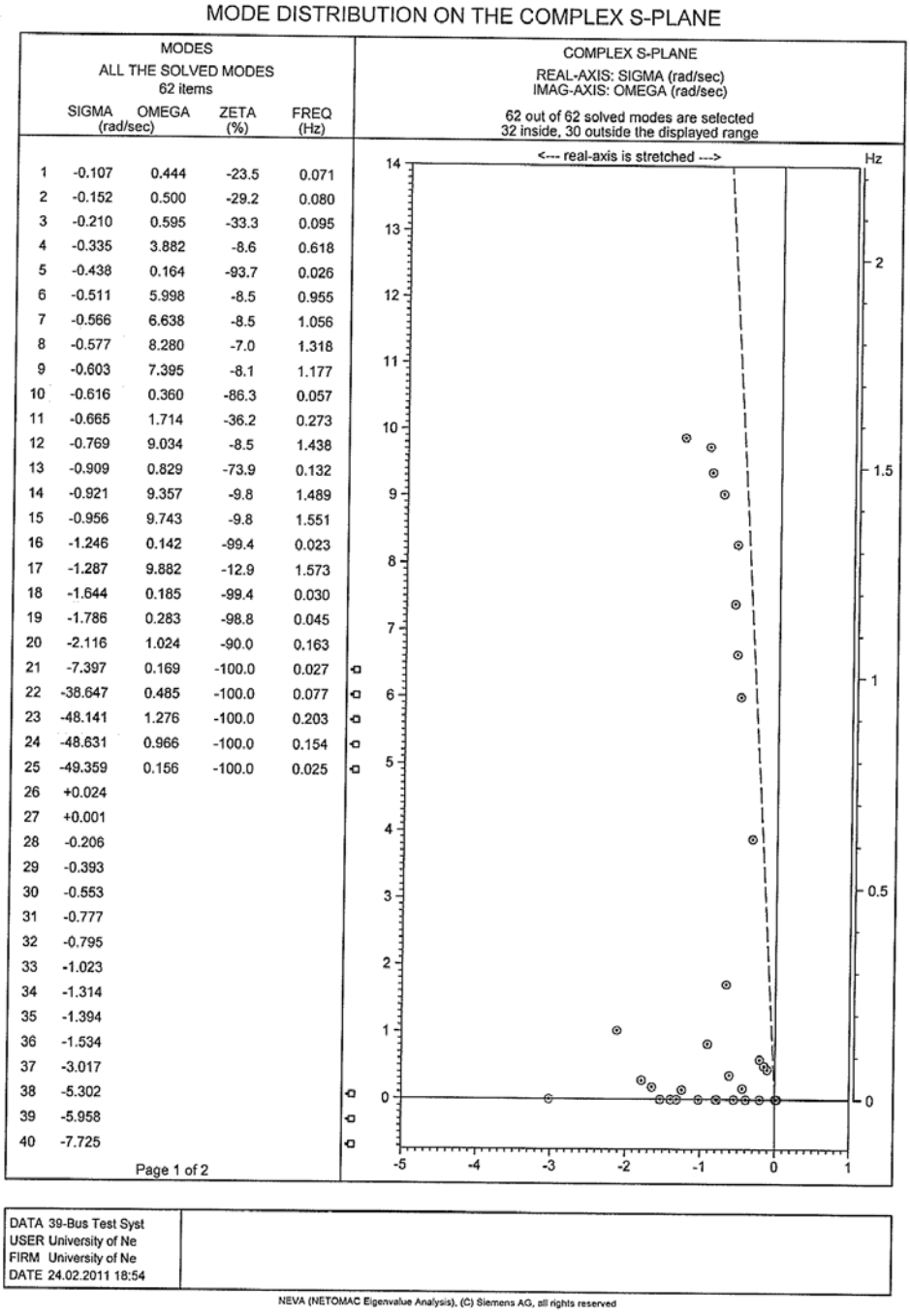

Fig 29: Modal analysis (eigenvalues) of 39 bus test system with shunt capacitor B = 1000 at load bus 15

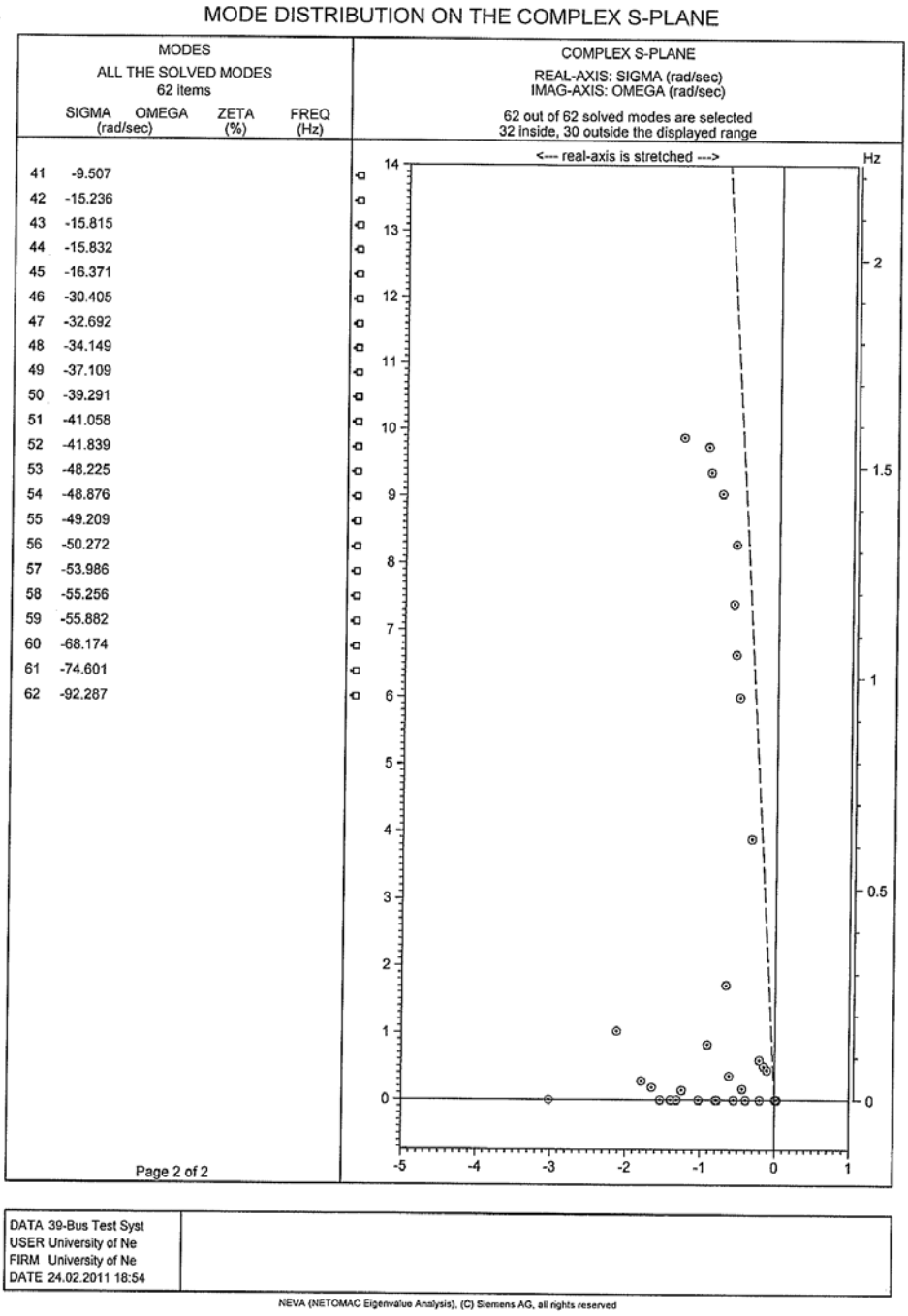

Fig 30: Modal analysis (eigenvalues) of 39 bus test system with shunt capacitor B = 1000 at load bus 15

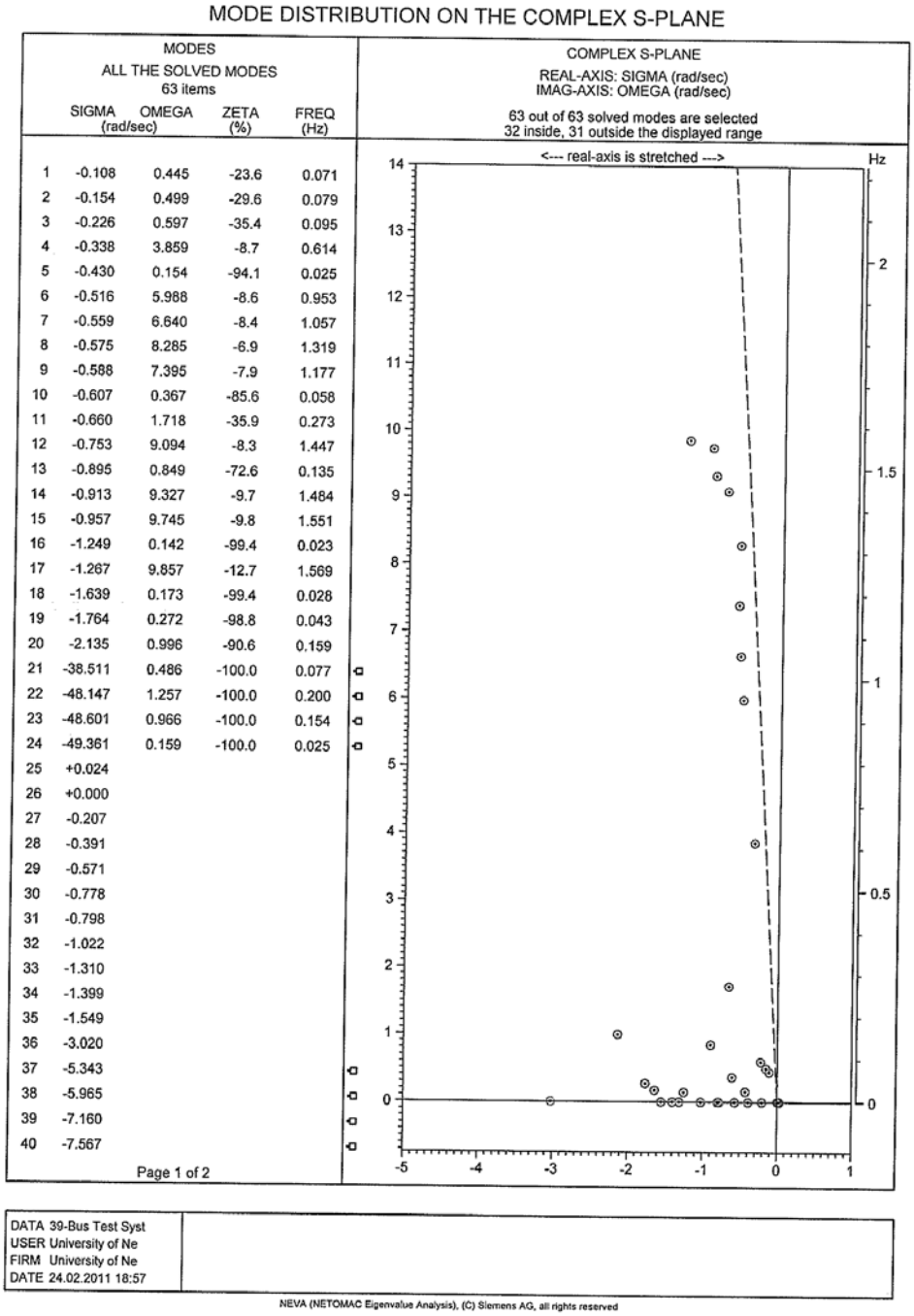

Fig 31: Modal analysis (eigenvalues) of 39 bus test system with shunt capacitor B = 1000 at load bus 16

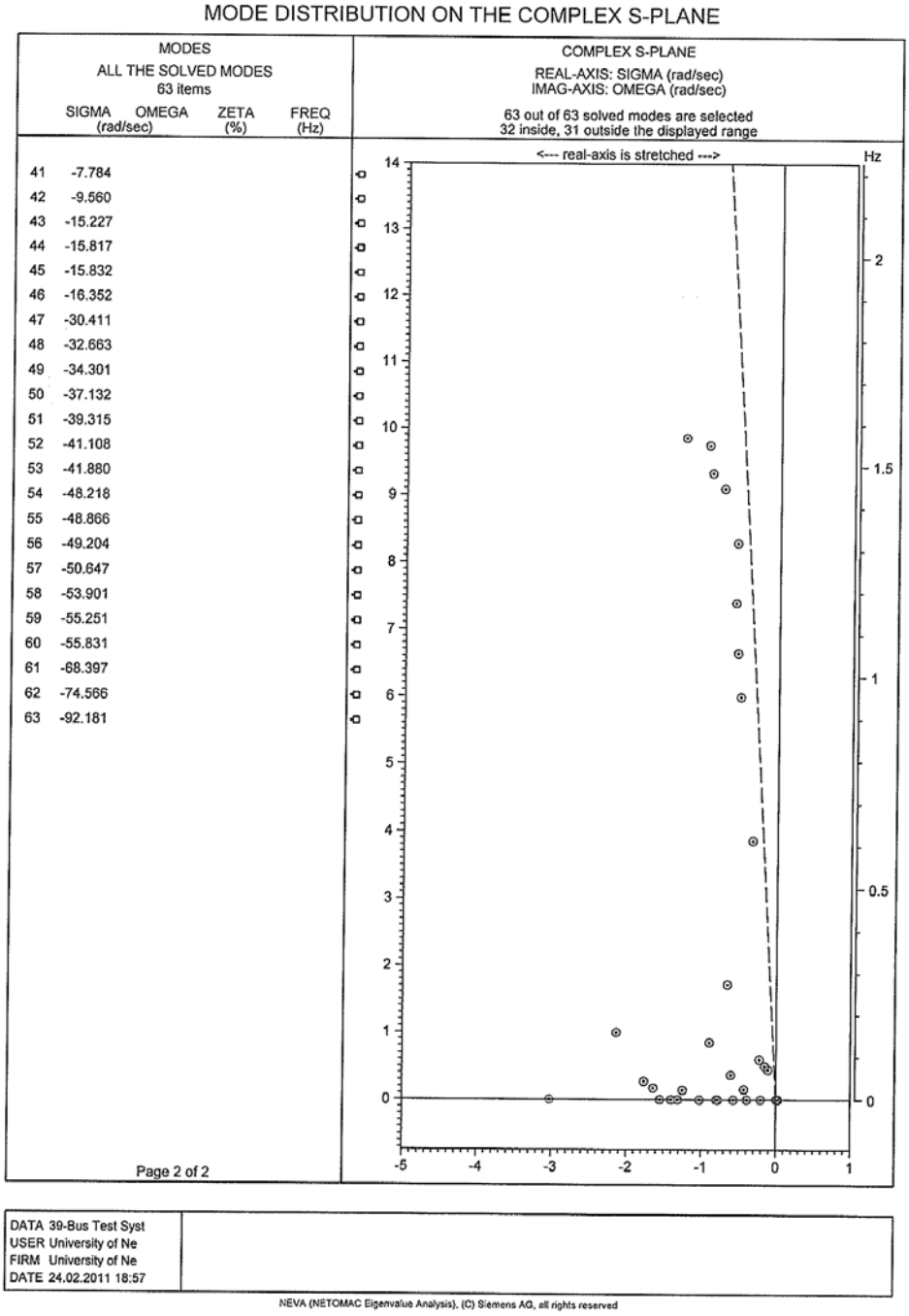

Fig 32: Modal analysis (eigenvalues) of 39 bus test system with shunt capacitor B = 1000 at load bus 16

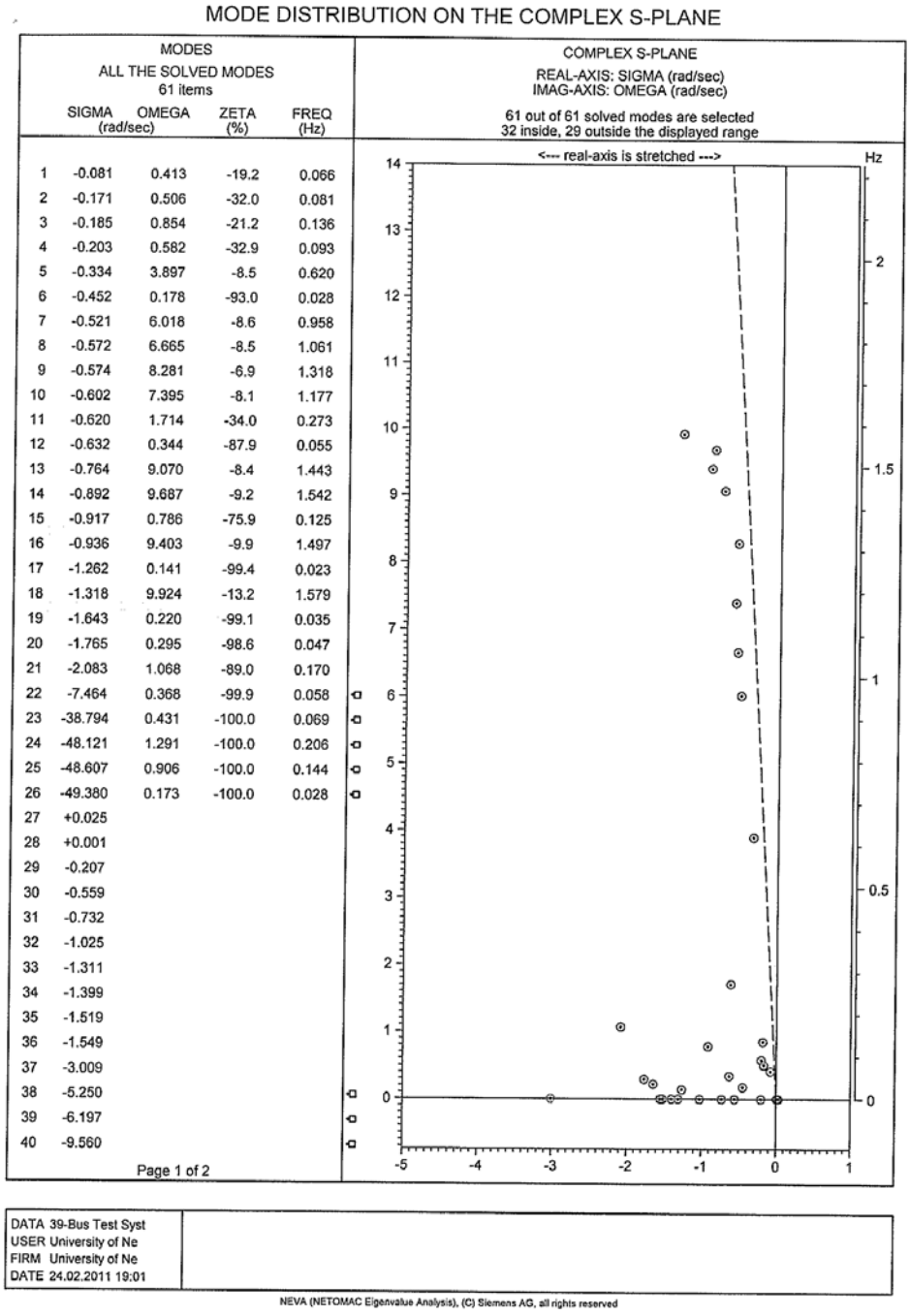

Fig 33: Modal analysis (eigenvalues) of 39 bus test system with shunt capacitor B = 1000 at load bus 18

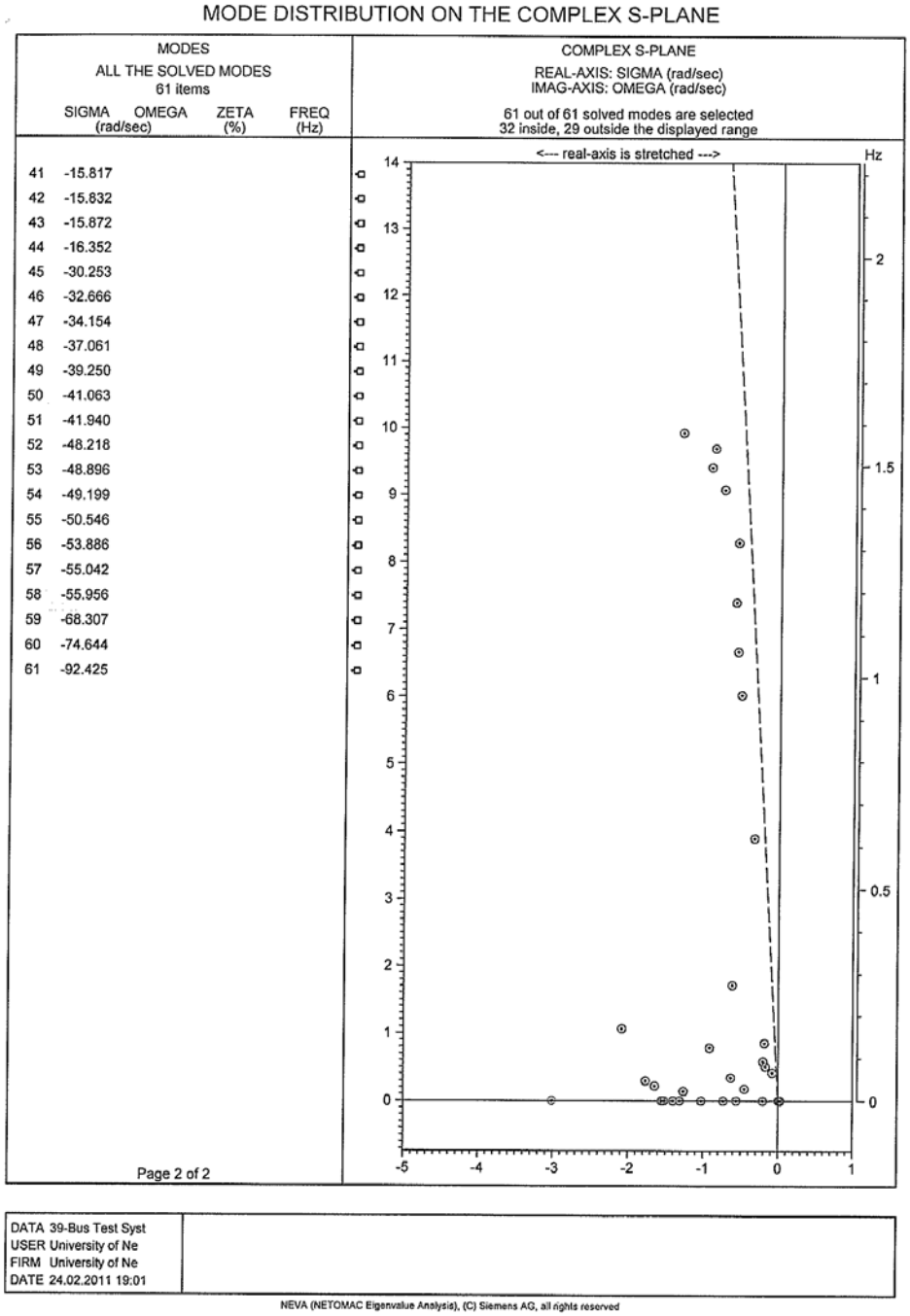

Fig 34: Modal analysis (eigenvalues) of 39 bus test system with shunt capacitor B = 1000 at load bus 18

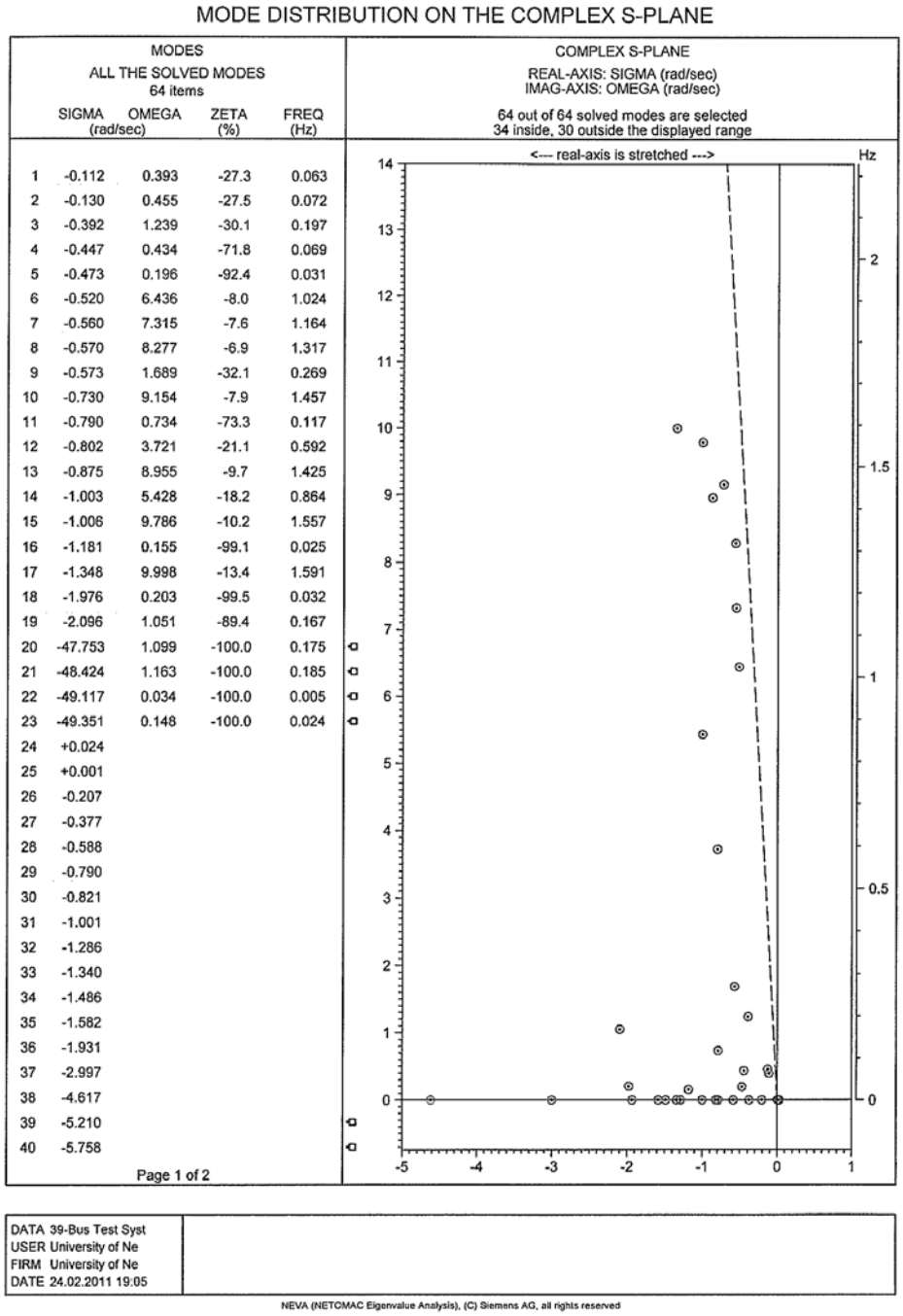

Fig 35: Modal analysis (eigenvalues) of 39 bus test system with shunt capacitor B = 1000 at load bus 20

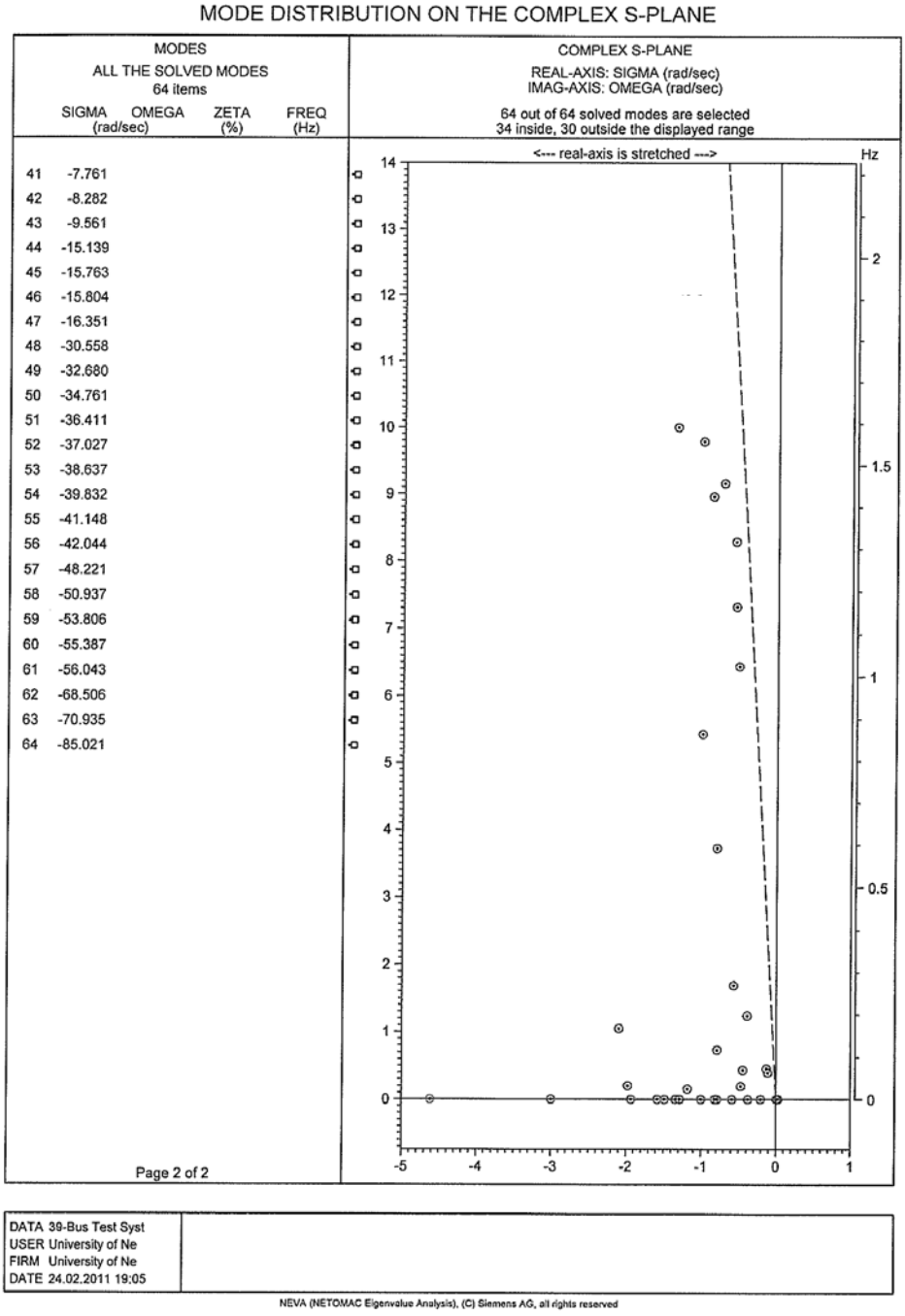

Fig 36: Modal analysis (eigenvalues) of 39 bus test system with shunt capacitor B = 1000 at load bus 20

MODE DISTRIBUTION ON THE COMPLEX S-PLANE

MODES
ALL THE SOLVED MODES
62 items

	SIGMA (rad/sec)	OMEGA (rad/sec)	ZETA (%)	FREQ (Hz)
1	-0.116	0.448	-25.0	0.071
2	-0.174	0.505	-32.6	0.080
3	-0.238	0.596	-37.1	0.095
4	-0.349	3.838	-9.1	0.611
5	-0.392	0.029	-99.7	0.005
6	-0.501	5.999	-8.3	0.955
7	-0.550	7.363	-7.4	1.172
8	-0.555	6.650	-8.3	1.058
9	-0.569	8.275	-6.9	1.317
10	-0.622	0.349	-87.2	0.056
11	-0.660	1.731	-35.6	0.275
12	-0.745	9.116	-8.1	1.451
13	-0.852	0.932	-67.4	0.148
14	-0.933	9.362	-9.9	1.490
15	-0.976	9.760	-10.0	1.553
16	-1.074	9.719	-11.0	1.547
17	-1.238	0.151	-99.3	0.024
18	-1.620	0.147	-99.6	0.023
19	-1.734	0.288	-98.6	0.046
20	-2.183	0.885	-92.7	0.141
21	-7.459	0.308	-99.9	0.049
22	-38.381	0.411	-100.0	0.065
23	-48.155	1.179	-100.0	0.188
24	-48.613	0.978	-100.0	0.156
25	-49.353	0.152	-100.0	0.024
26	+0.025			
27	0.000			
28	-0.206			
29	-0.345			
30	-0.578			
31	-0.781			
32	-0.808			
33	-1.016			
34	-1.306			
35	-1.393			
36	-1.555			
37	-3.026			
38	-5.603			
39	-6.165			
40	-7.970			

Page 1 of 2

COMPLEX S-PLANE
REAL-AXIS: SIGMA (rad/sec)
IMAG-AXIS: OMEGA (rad/sec)
62 out of 62 solved modes are selected
32 inside, 30 outside the displayed range

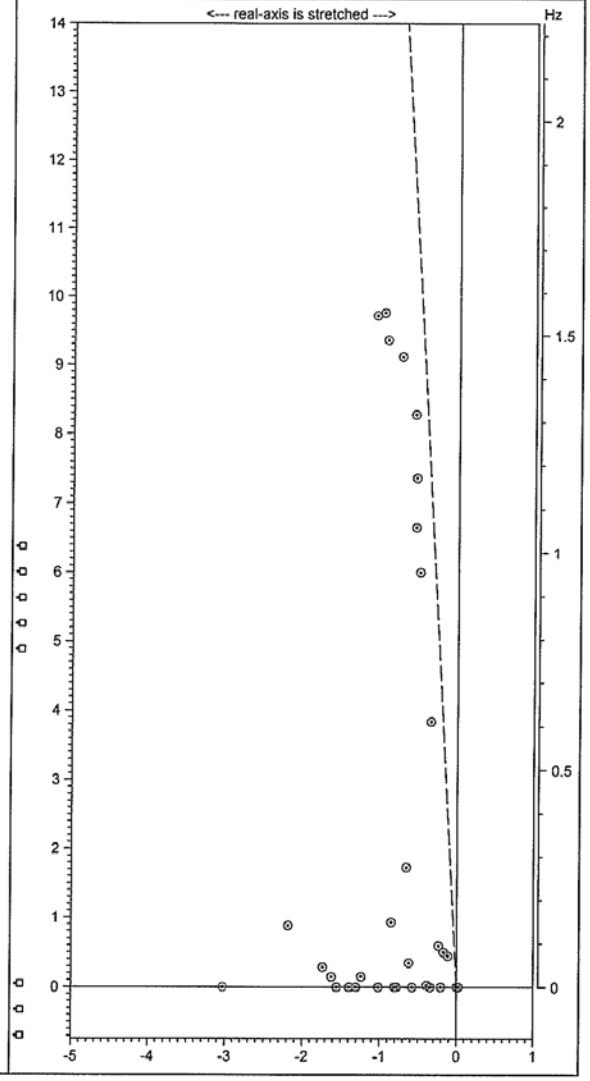

DATA 39-Bus Test Syst
USER University of Ne
FIRM University of Ne
DATE 24.02.2011 19:09

Fig 37: Modal analysis (eigenvalues) of 39 bus test system with shunt capacitor B = 1000 at load bus 21

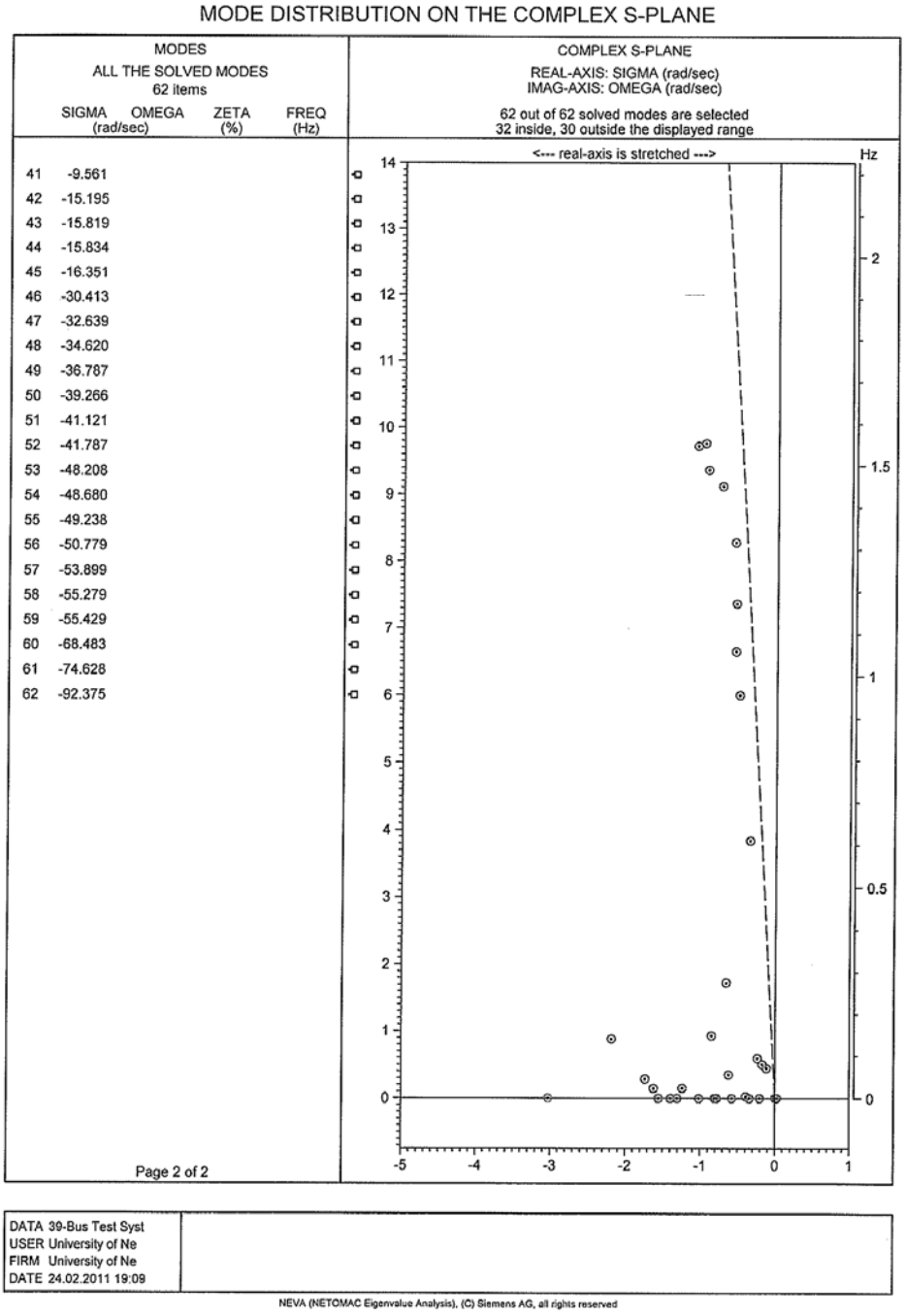

Fig 38: Modal analysis (eigenvalues) of 39 bus test system with shunt capacitor B = 1000 at load bus 21

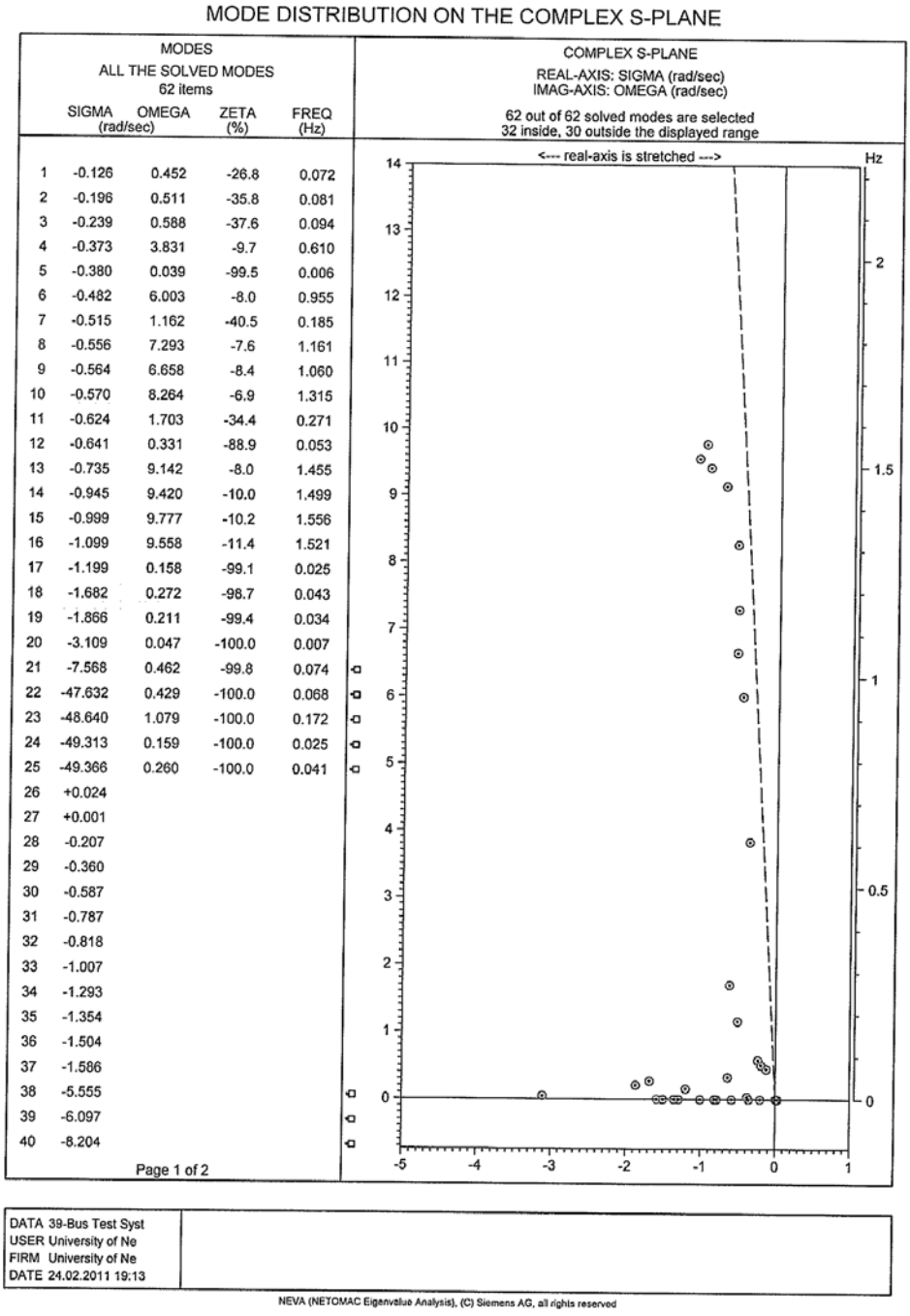

Fig 39: Modal analysis (eigenvalues) of 39 bus test system with shunt capacitor B = 1000 at load bus 23

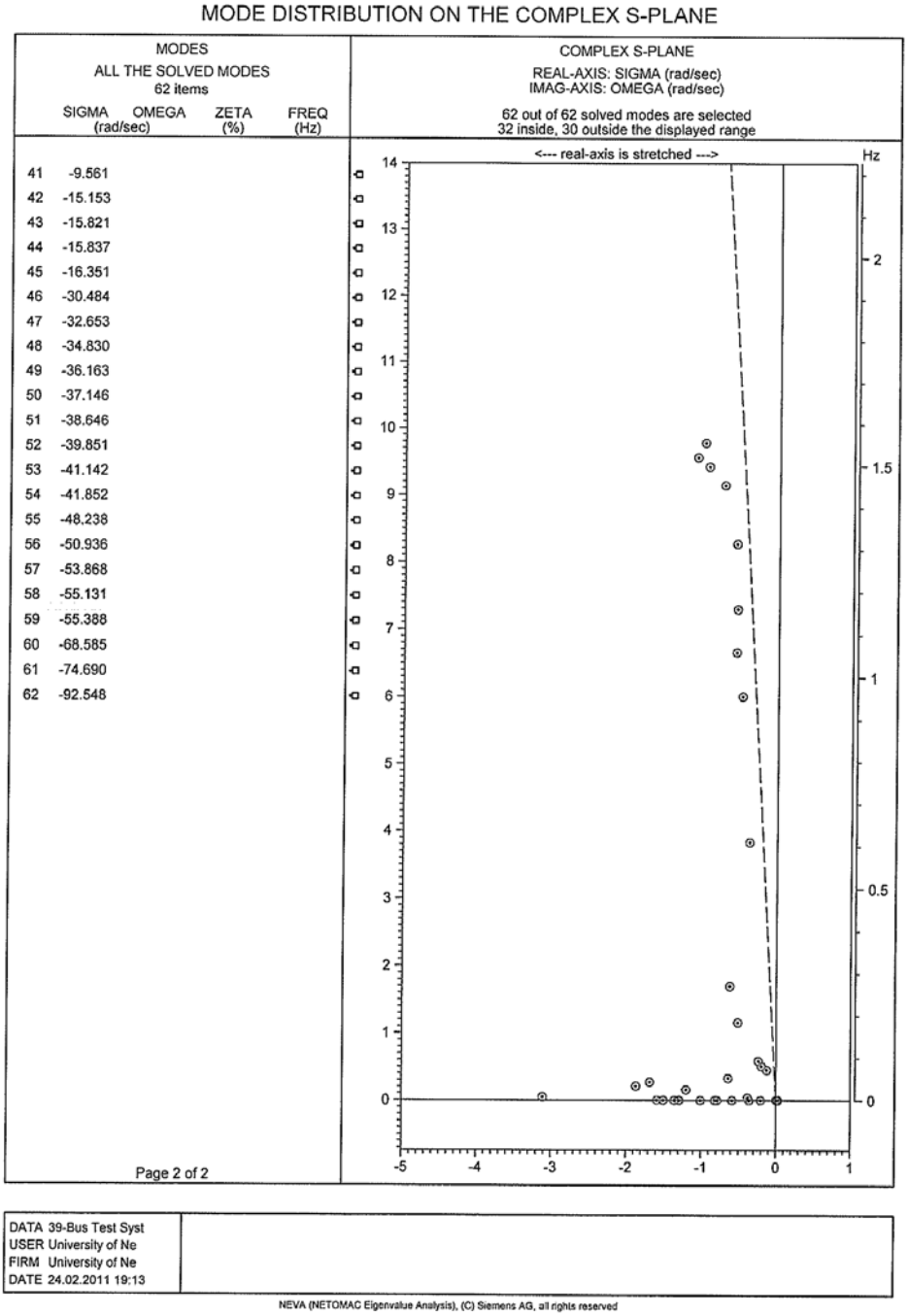

Fig 40: Modal analysis (eigenvalues) of 39 bus test system with shunt capacitor B = 1000 at load bus 23

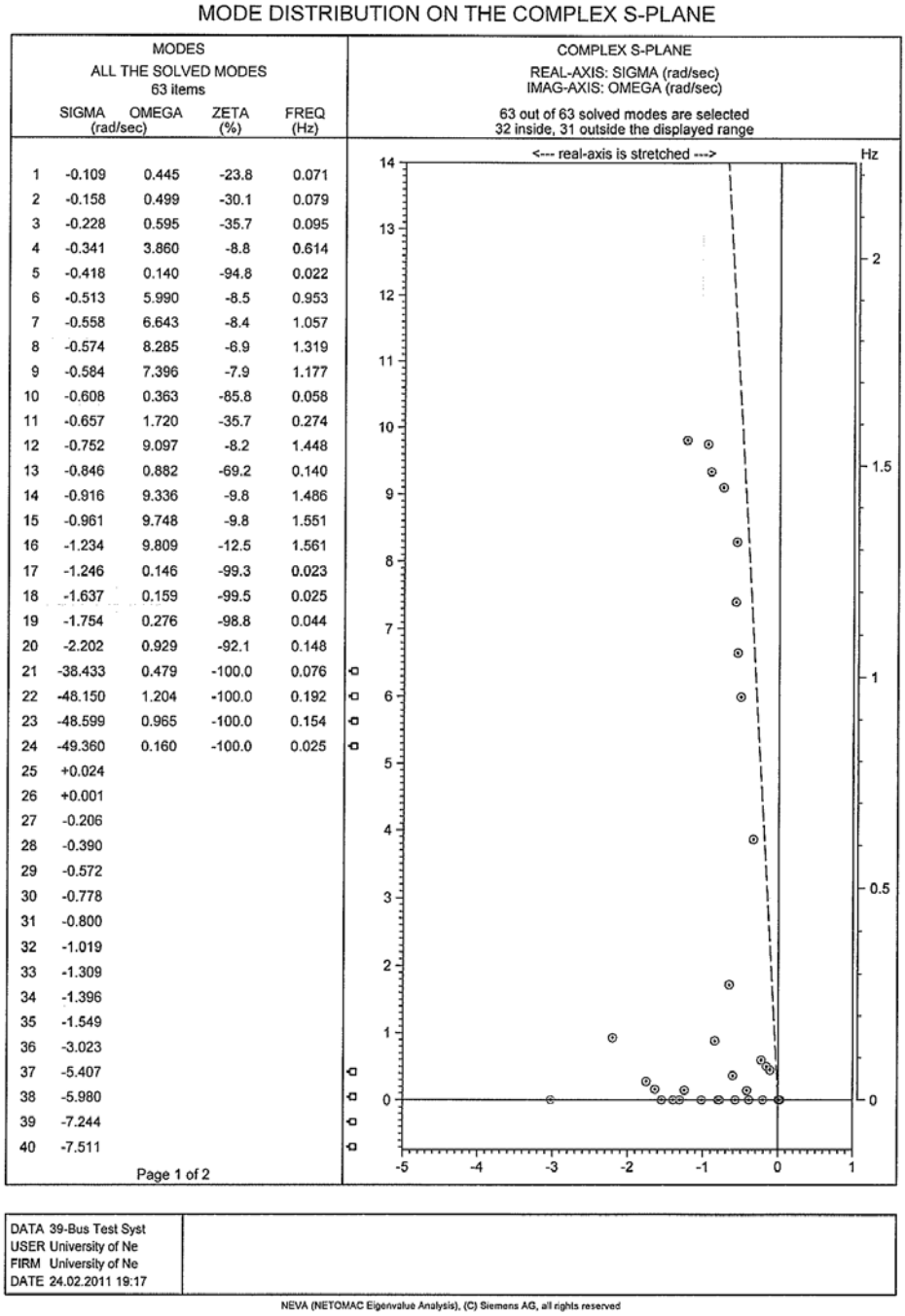

Fig 41: Modal analysis (eigenvalues) of 39 bus test system with shunt capacitor B = 1000 at load bus 24

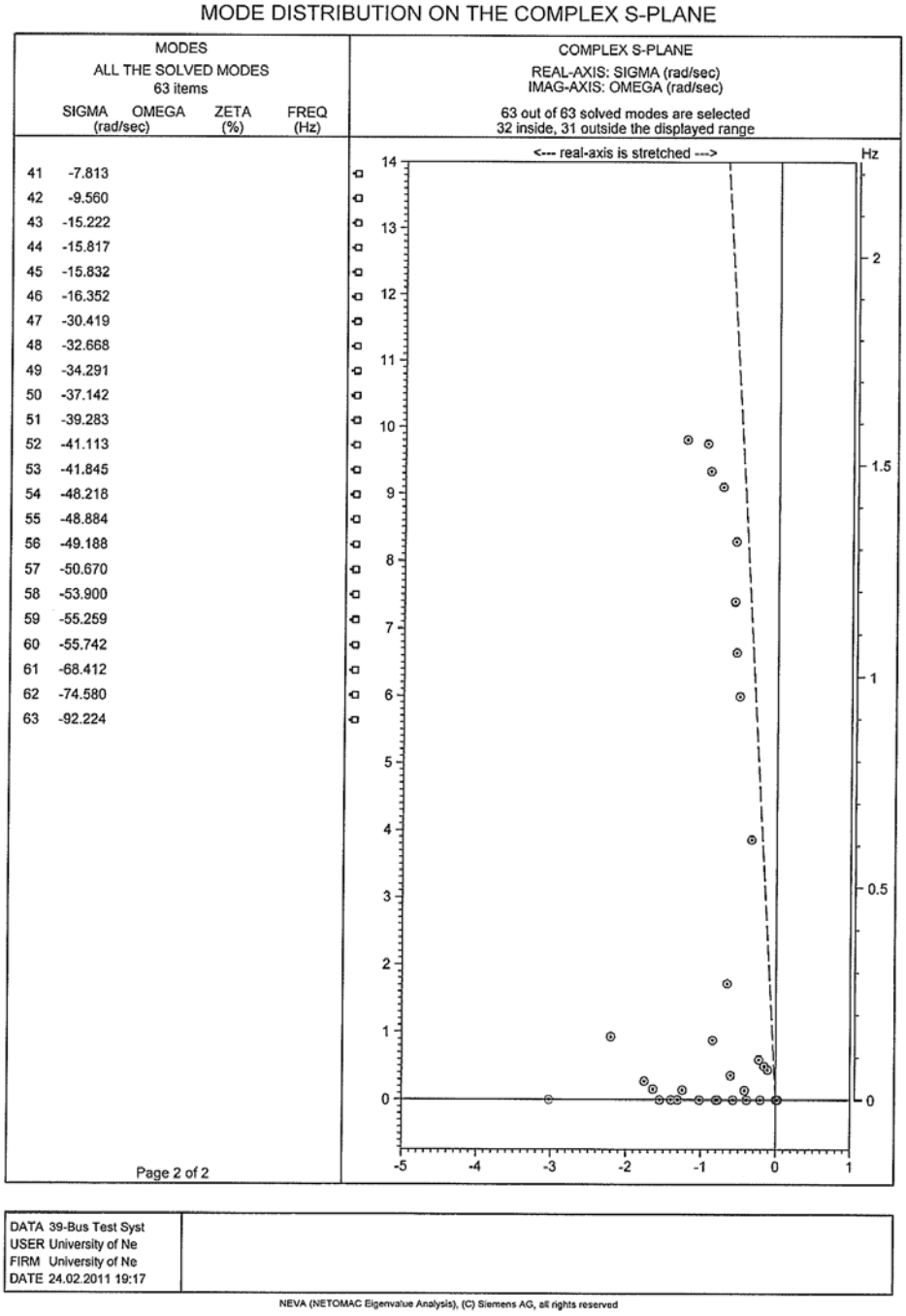

Fig 42: Modal analysis (eigenvalues) of 39 bus test system with shunt capacitor B = 1000 at load bus 24

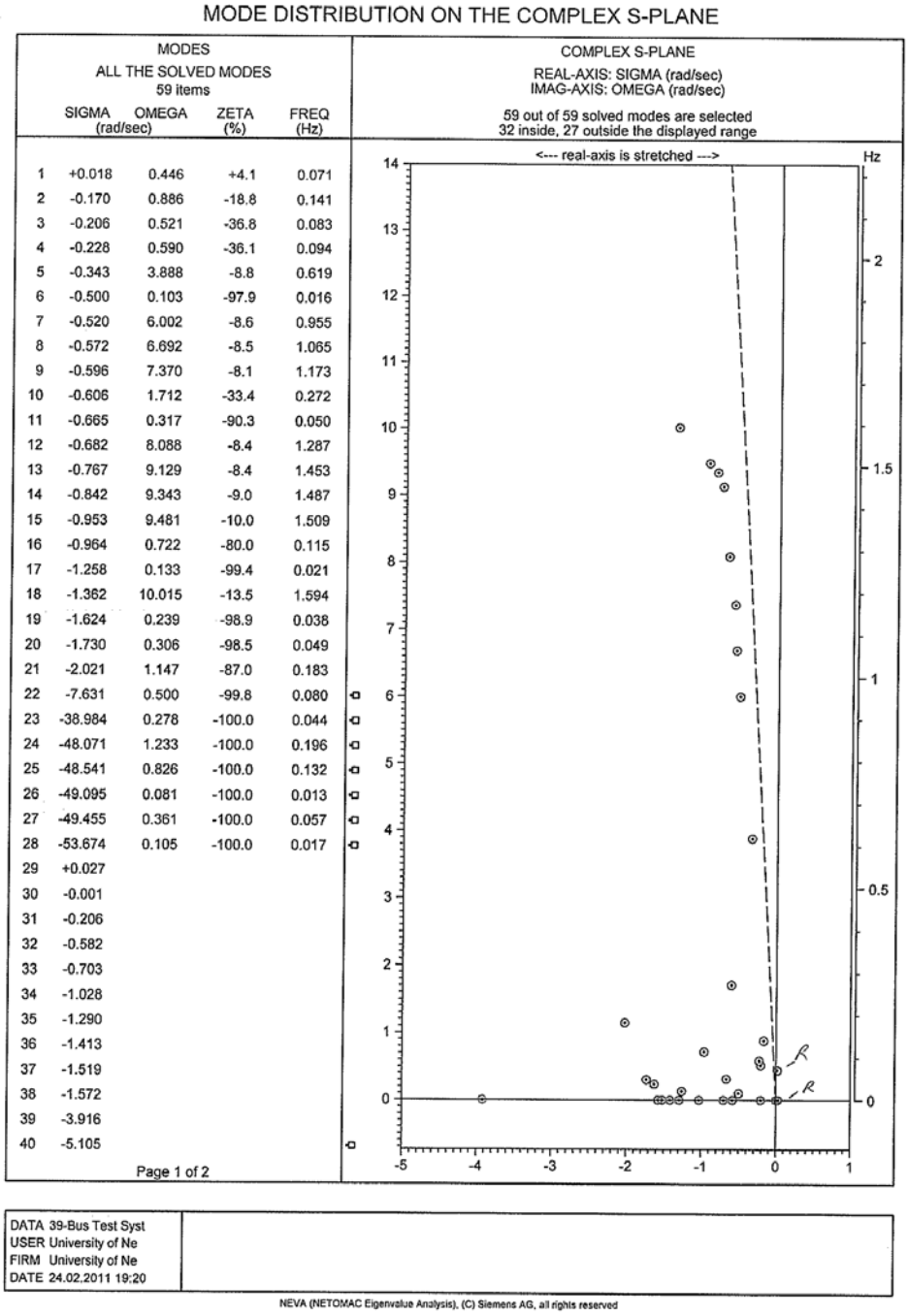

Fig 43: Modal analysis (eigenvalues) of 39 bus test system with shunt capacitor B = 1000 at load bus 25

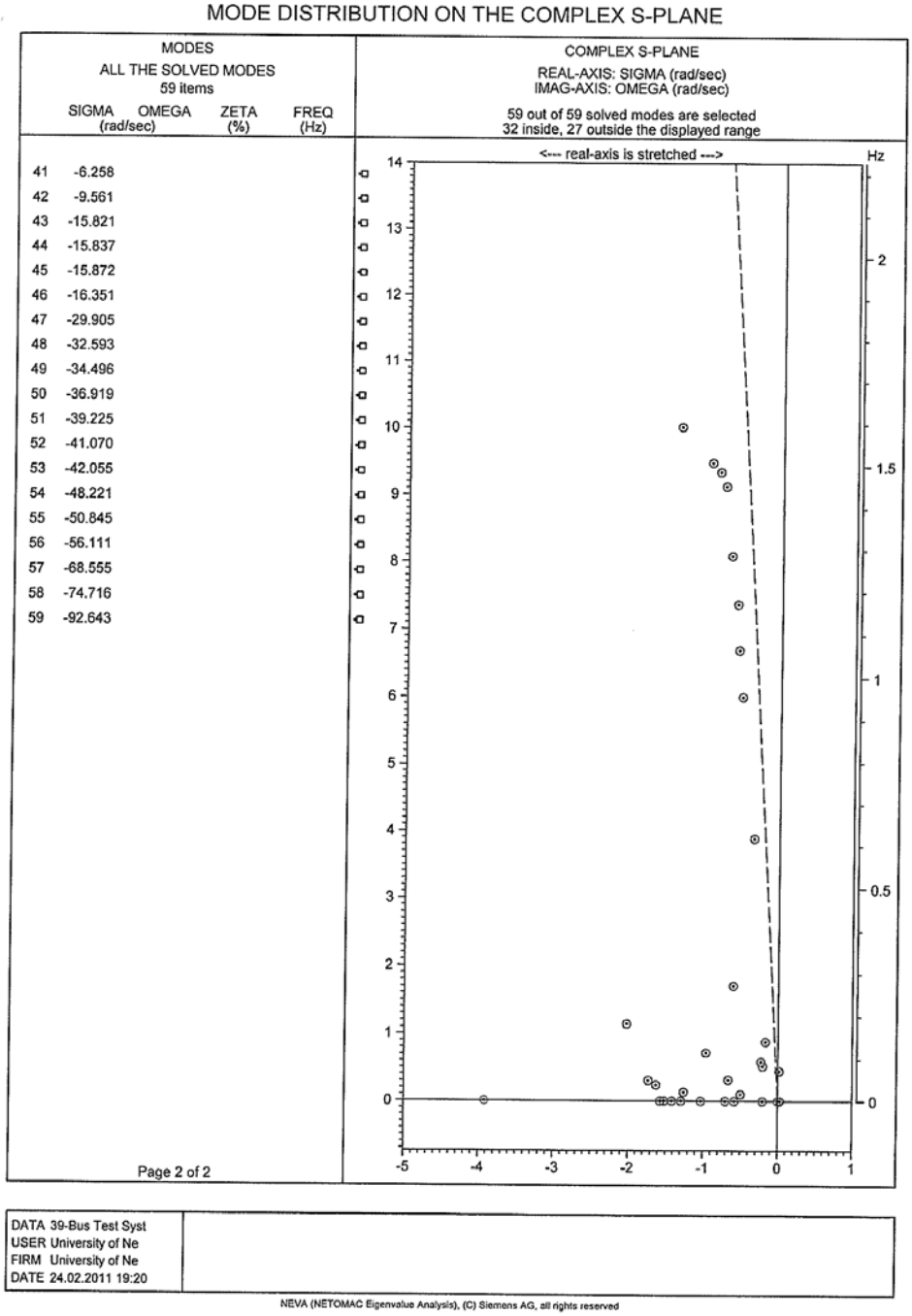

Fig 44: Modal analysis (eigenvalues) of 39 bus test system with shunt capacitor B = 1000 at load bus 25

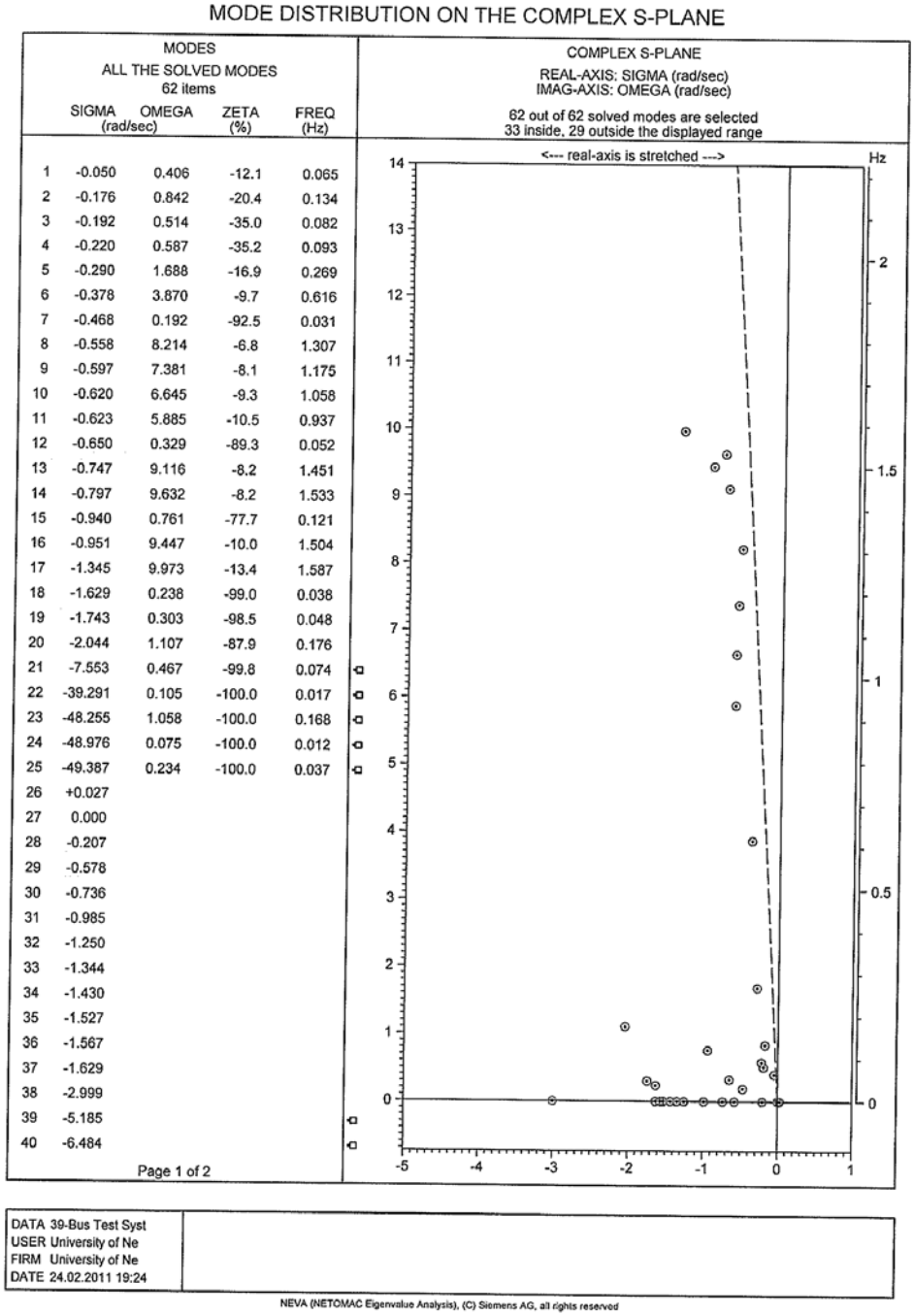

Fig 45: Modal analysis (eigenvalues) of 39 bus test system with shunt capacitor B = 1000 at load bus 26

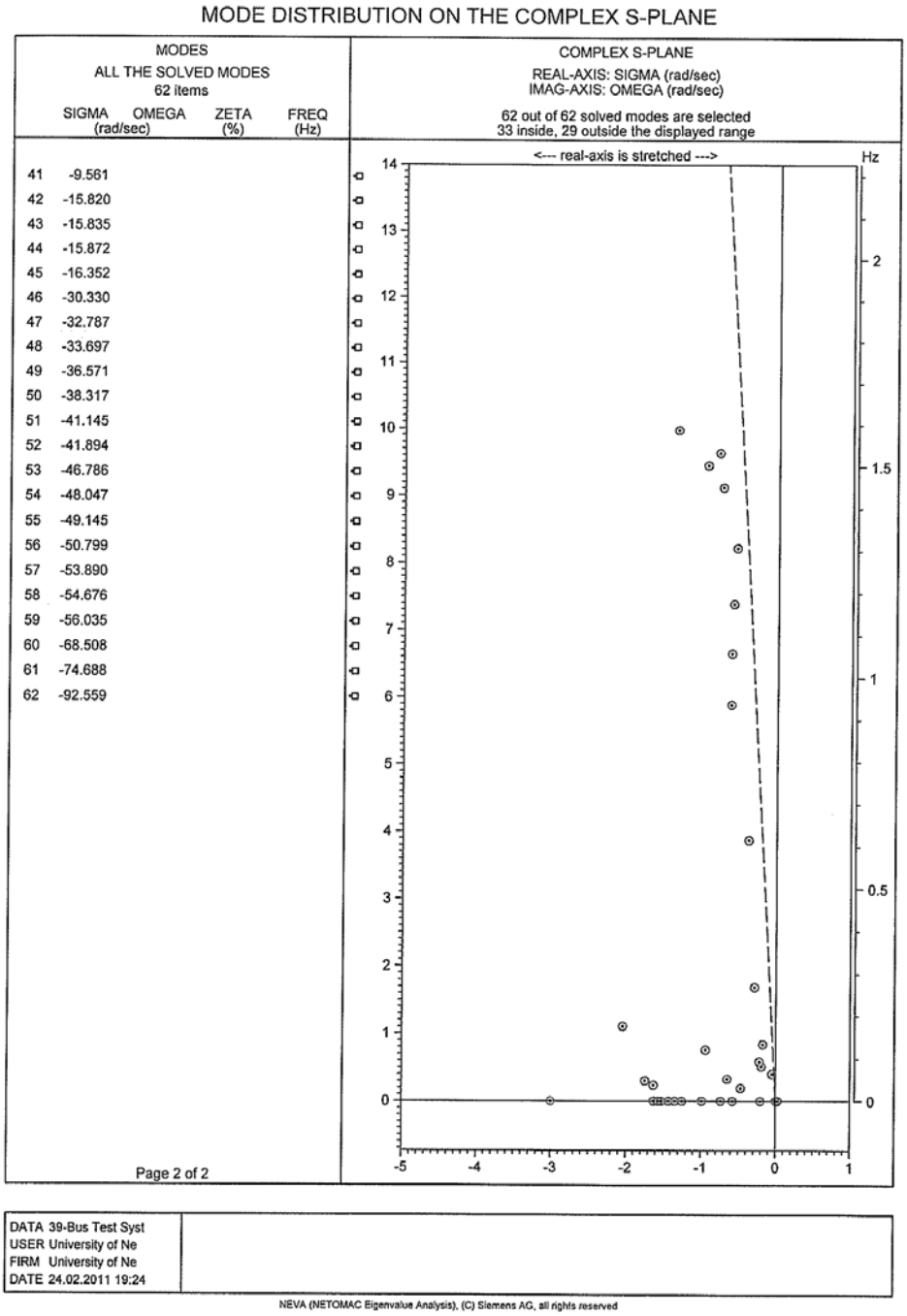

Fig 46: Modal analysis (eigenvalues) of 39 bus test system with shunt capacitor B = 1000 at load bus 26

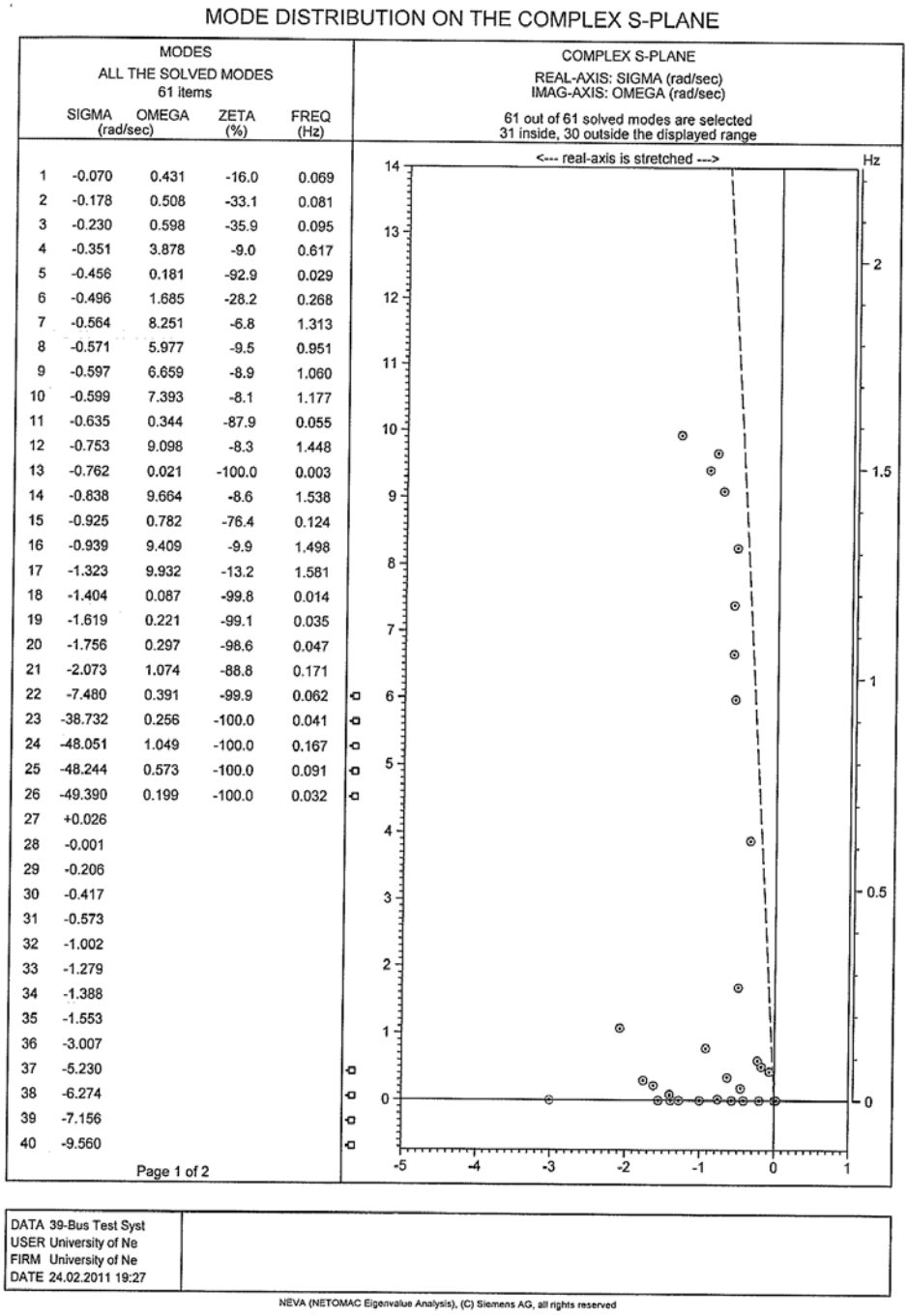

Fig 47: Modal analysis (eigenvalues) of 39 bus test system with shunt capacitor B = 1000 at load bus 27

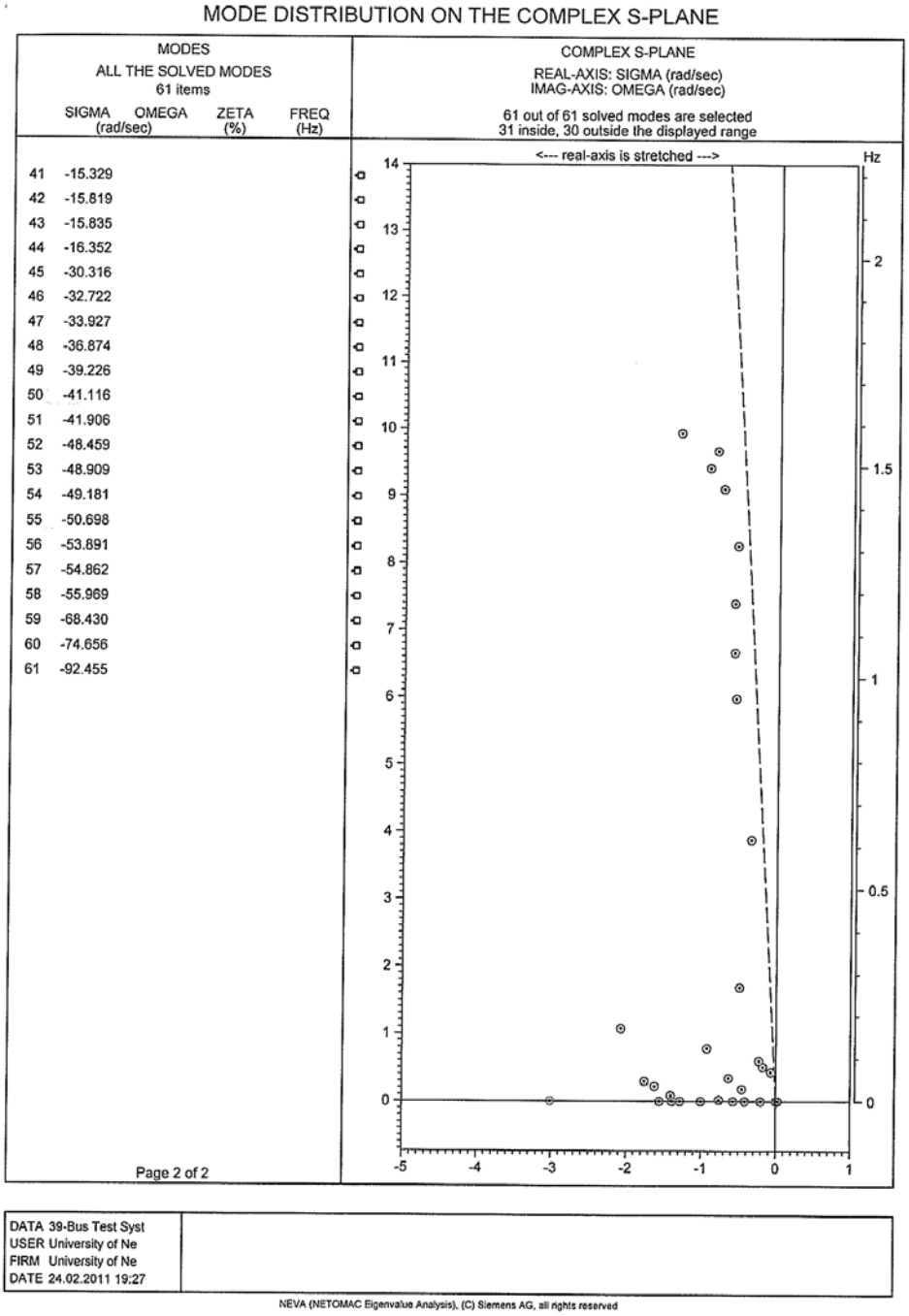

Fig 48: Modal analysis (eigenvalues) of 39 bus test system with shunt capacitor B = 1000 at load bus 27

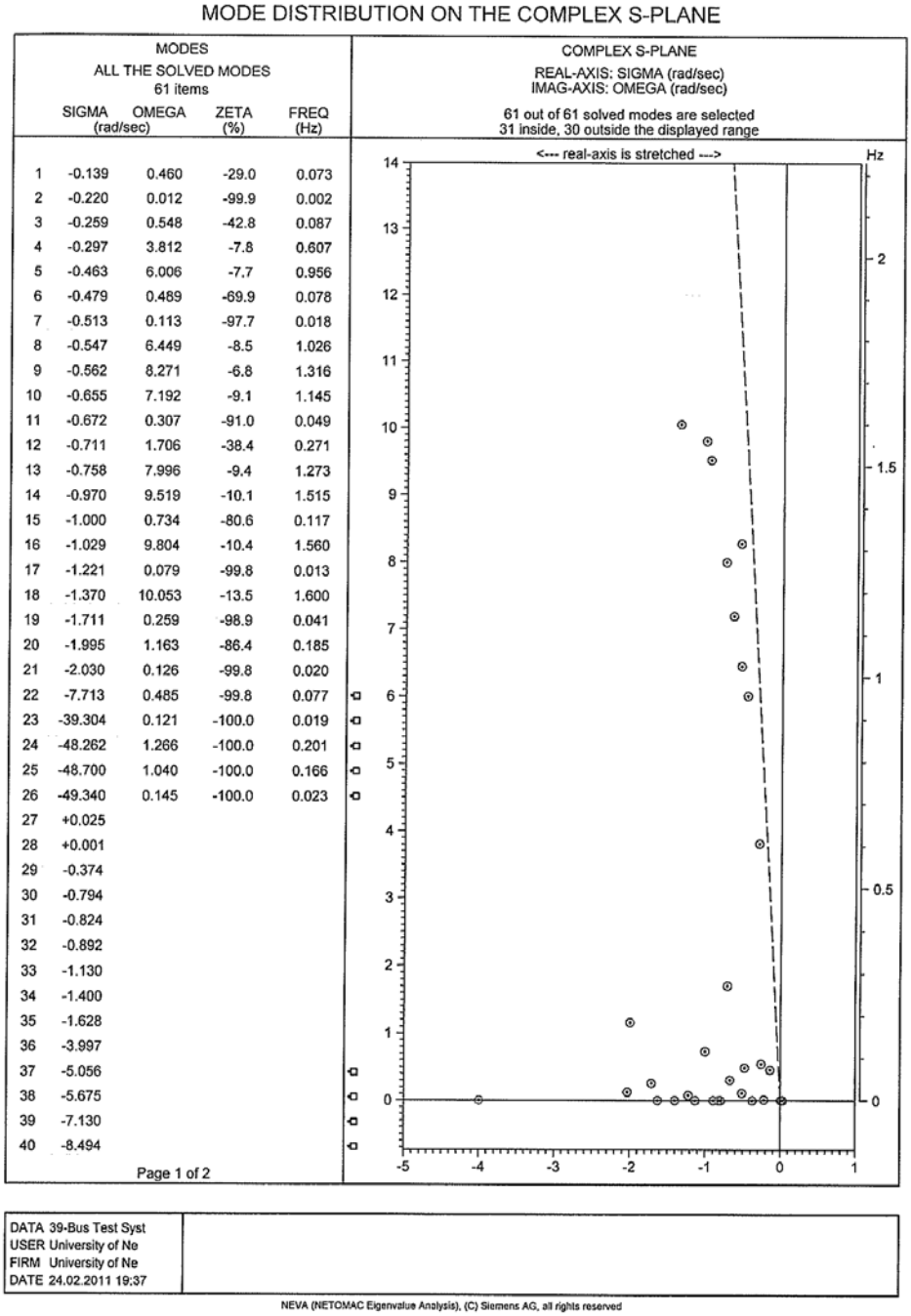

Fig 49: Modal analysis (eigenvalues) of 39 bus test system with shunt capacitor B = 1000 at load bus 31

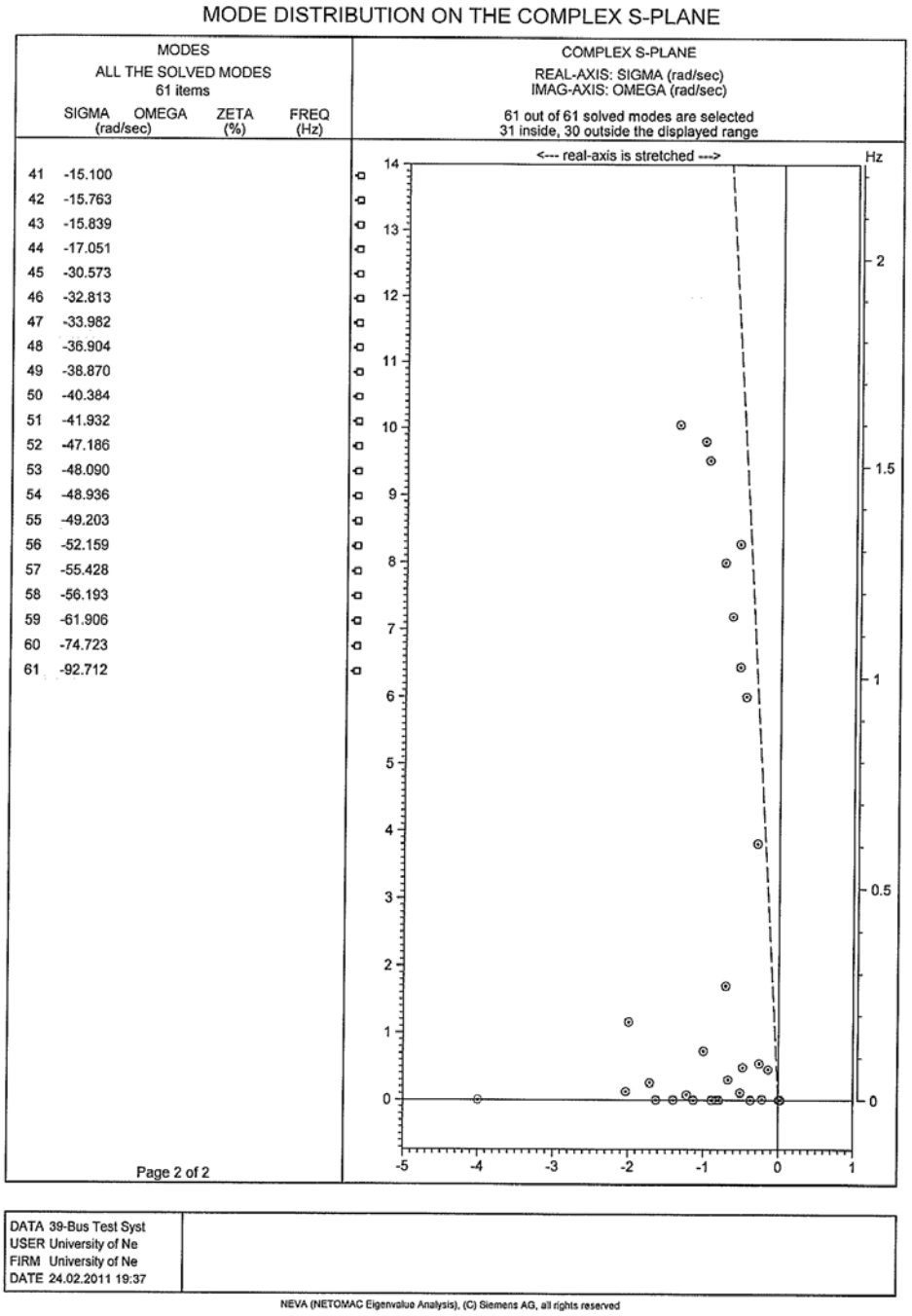

Fig 50: Modal analysis (eigenvalues) of 39 bus test system with shunt capacitor B = 1000 at load bus 31

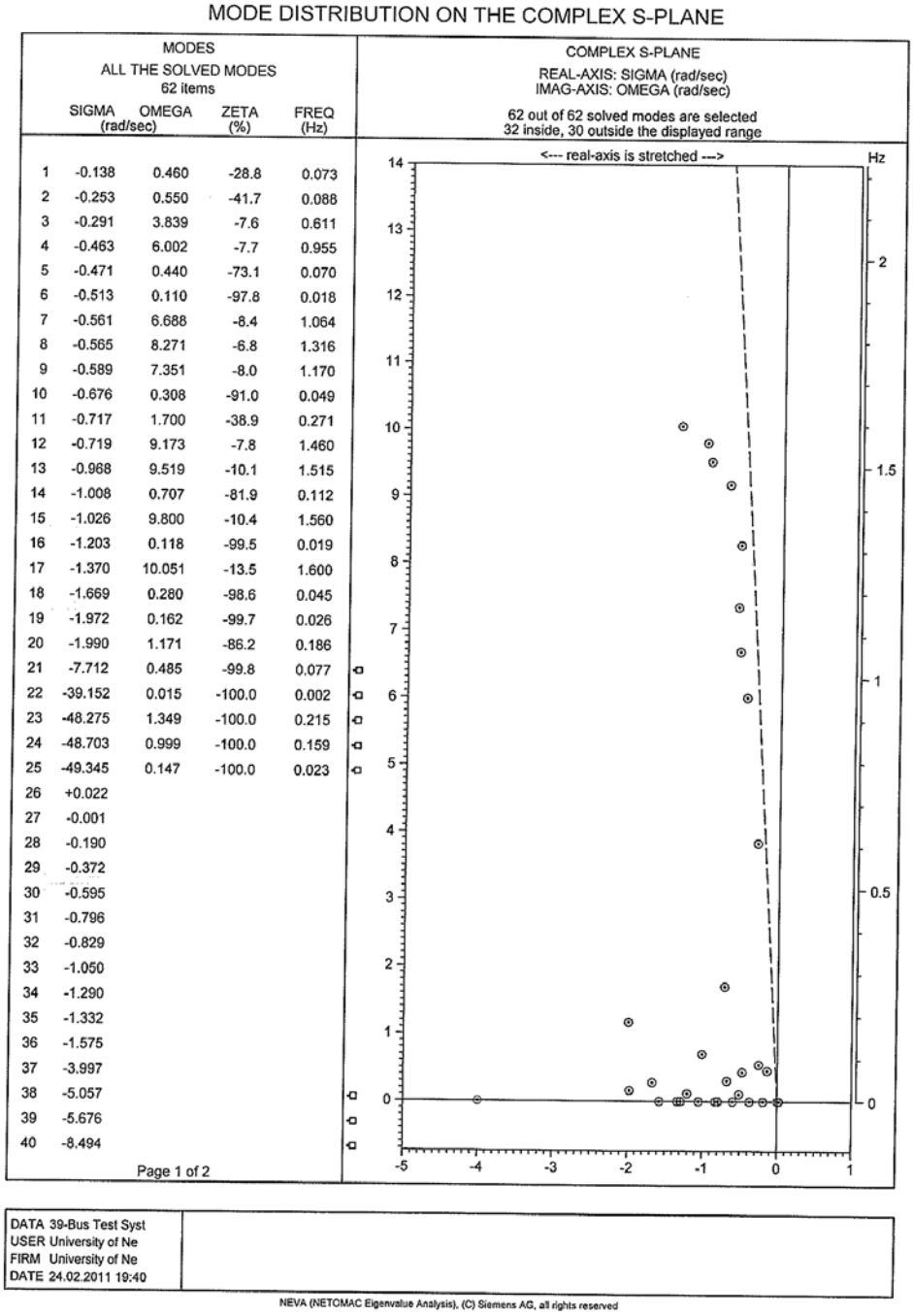

Fig 51: Modal analysis (eigenvalues) of 39 bus test system with shunt capacitor B = 1000 at load bus 39

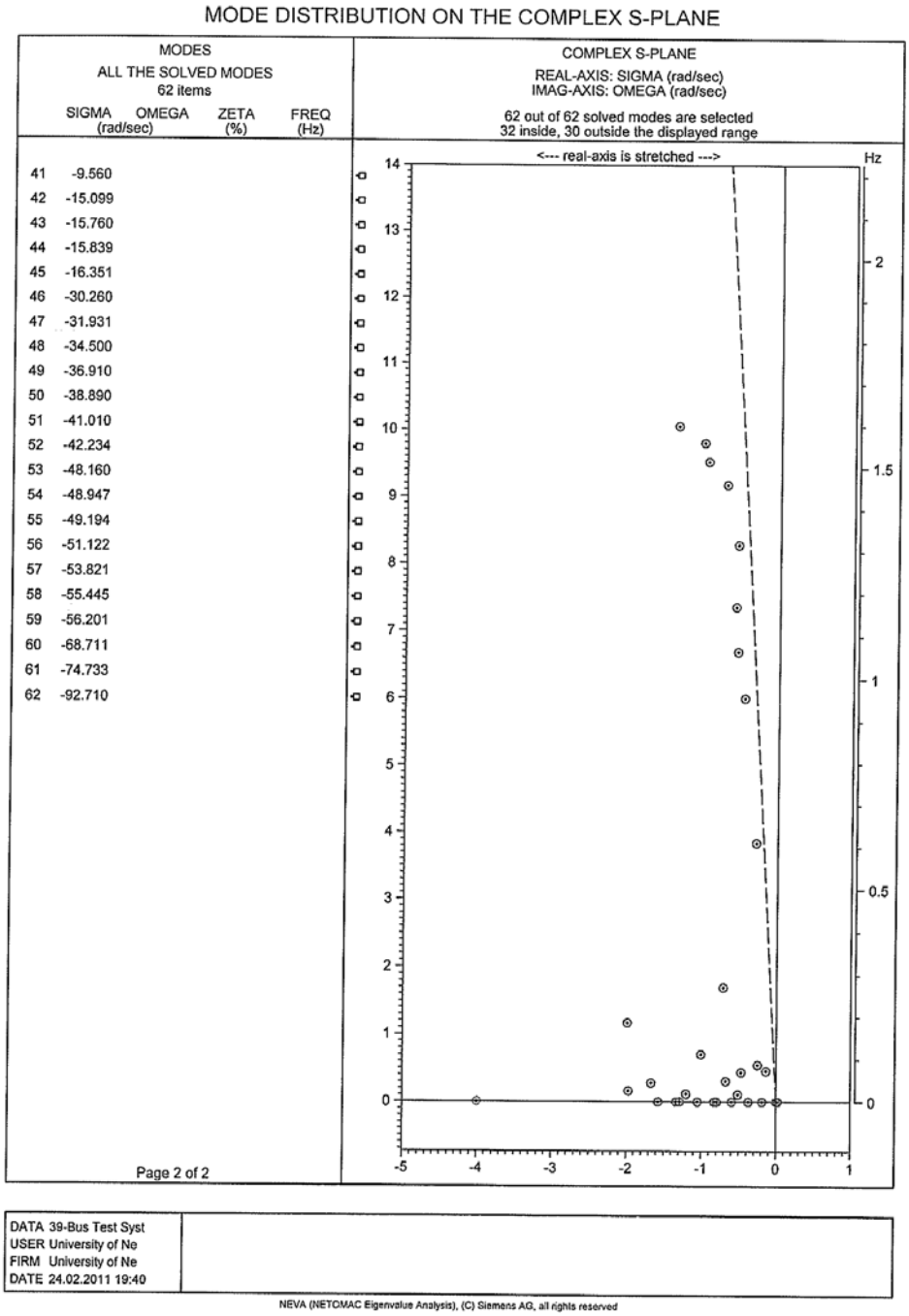

Fig 52: Modal analysis (eigenvalues) of 39 bus test system with shunt capacitor B = 1000 at load bus 39

MODE DISTRIBUTION ON THE COMPLEX S-PLANE

MODES
ALL THE SOLVED MODES
64 items

	SIGMA (rad/sec)	OMEGA (rad/sec)	ZETA (%)	FREQ (Hz)
1	-0.185	0.478	-36.0	0.076
2	-0.243	3.764	-6.4	0.599
3	-0.276	0.567	-43.8	0.090
4	-0.425	5.959	-7.1	0.948
5	-0.526	6.663	-7.9	1.060
6	-0.526	8.224	-6.4	1.309
7	-0.535	0.117	-97.7	0.019
8	-0.550	0.408	-80.3	0.065
9	-0.571	7.278	-7.8	1.158
10	-0.679	8.980	-7.5	1.429
11	-0.700	0.285	-92.6	0.045
12	-0.748	1.695	-40.4	0.270
13	-0.978	9.567	-10.2	1.523
14	-1.049	0.672	-84.2	0.107
15	-1.105	9.908	-11.1	1.577
16	-1.177	0.066	-99.8	0.011
17	-1.370	10.119	-13.4	1.611
18	-1.662	0.281	-98.6	0.045
19	-1.948	1.208	-85.0	0.192
20	-7.895	0.320	-99.9	0.051
21	-48.384	1.345	-100.0	0.214
22	-48.748	1.049	-100.0	0.167
23	-49.345	0.132	-100.0	0.021
24	+0.024			
25	-0.001			
26	-0.207			
27	-0.345			
28	-0.593			
29	-0.846			
30	-0.865			
31	-1.130			
32	-1.287			
33	-1.473			
34	-1.617			
35	-1.779			
36	-2.364			
37	-4.162			
38	-5.042			
39	-5.402			
40	-9.560			

Page 1 of 2

COMPLEX S-PLANE
REAL-AXIS: SIGMA (rad/sec)
IMAG-AXIS: OMEGA (rad/sec)
64 out of 64 solved modes are selected
33 inside, 31 outside the displayed range

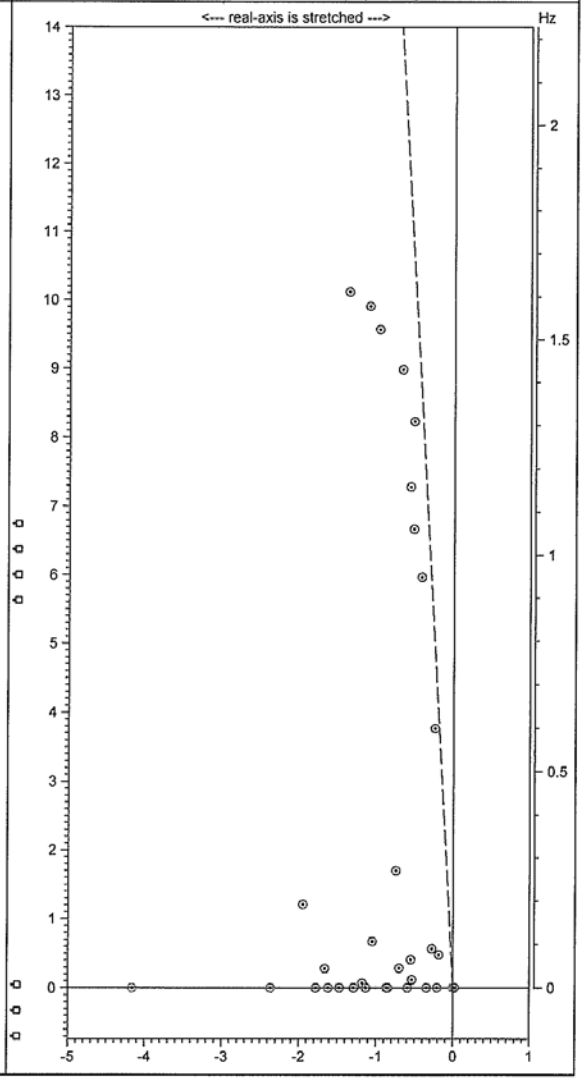

DATA 39-Bus Test Syst
USER University of Ne
FIRM University of Ne
DATE 24.02.2011 18:34

Fig 53: Modal analysis (eigenvalues) of 39 bus test system with shunt capacitor B = -1000 at load bus 3

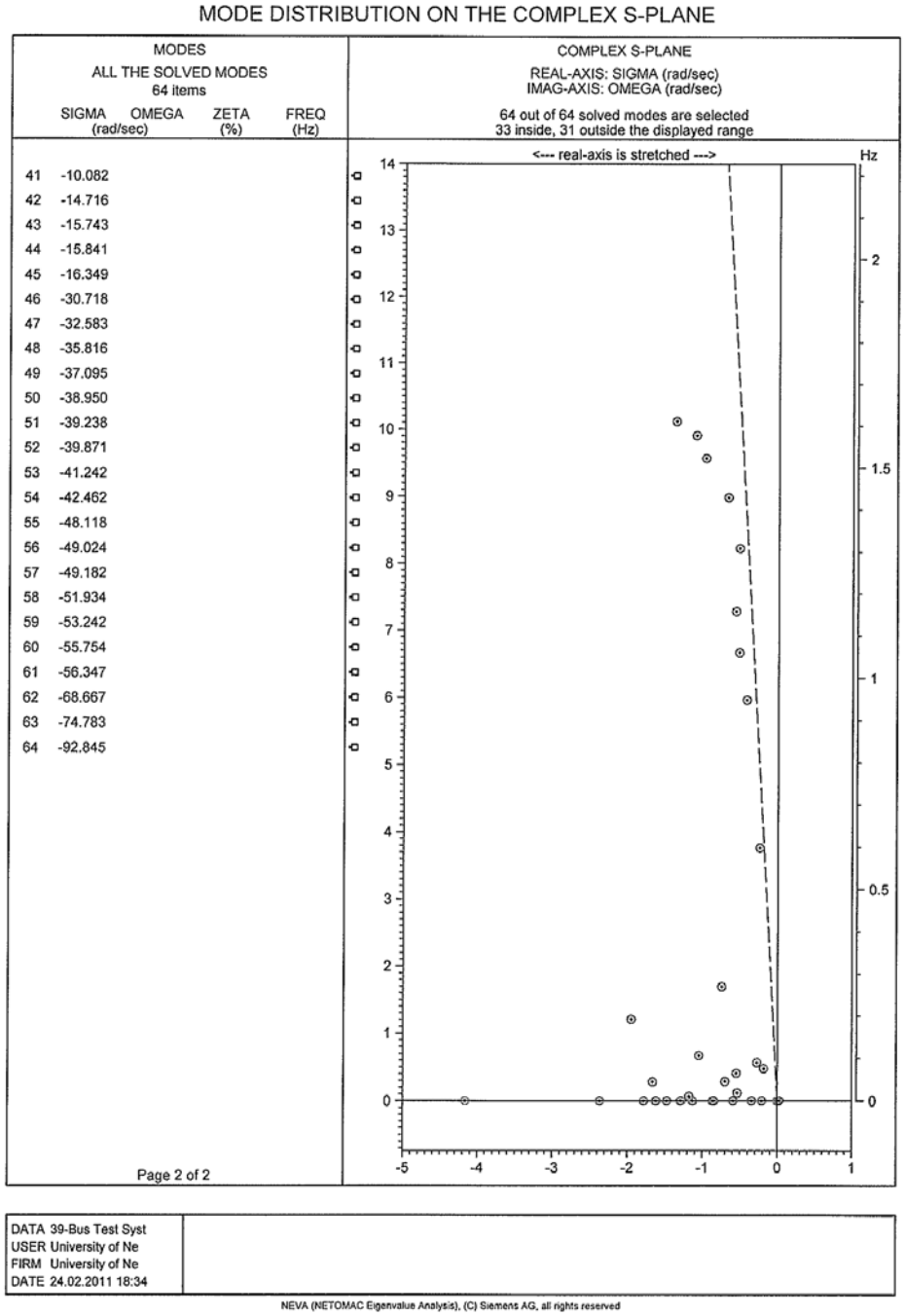

Fig 54: Modal analysis (eigenvalues) of 39 bus test system with shunt capacitor B = -1000 at load bus 3

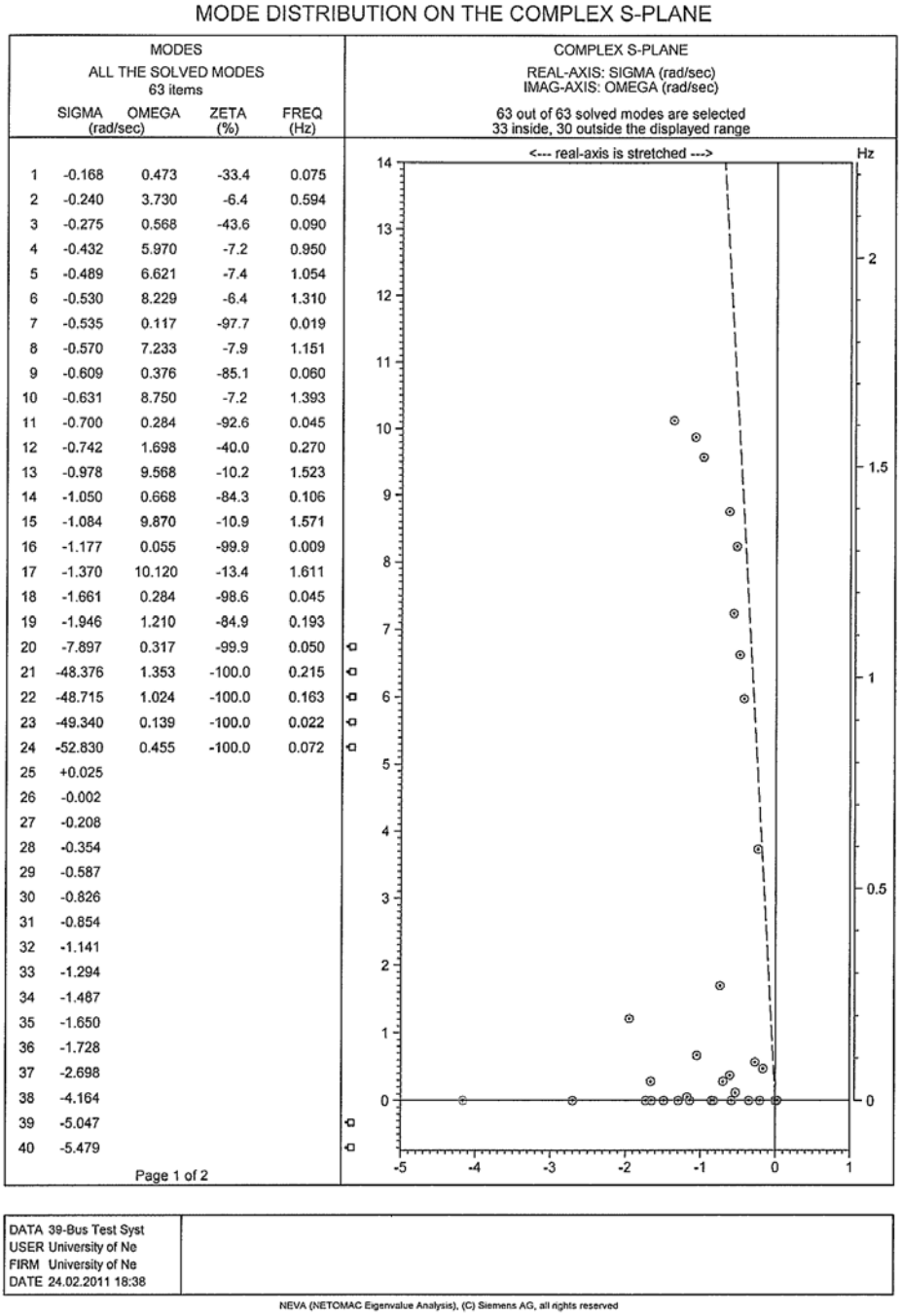

Fig 55: Modal analysis (eigenvalues) of 39 bus test system with shunt capacitor B = -1000 at load bus 4

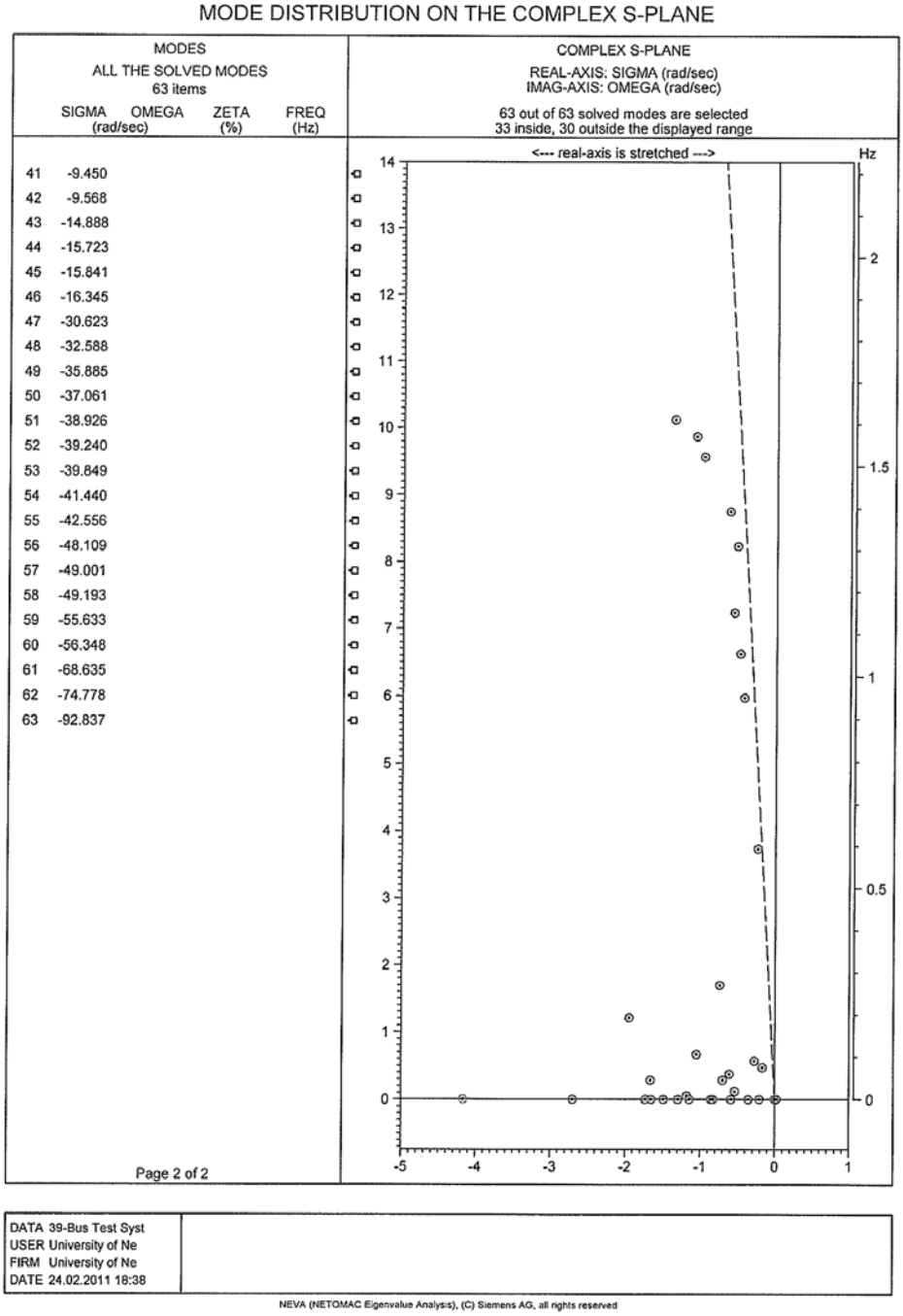

Fig 56: Modal analysis (eigenvalues) of 39 bus test system with shunt capacitor B = -1000 at load bus 4

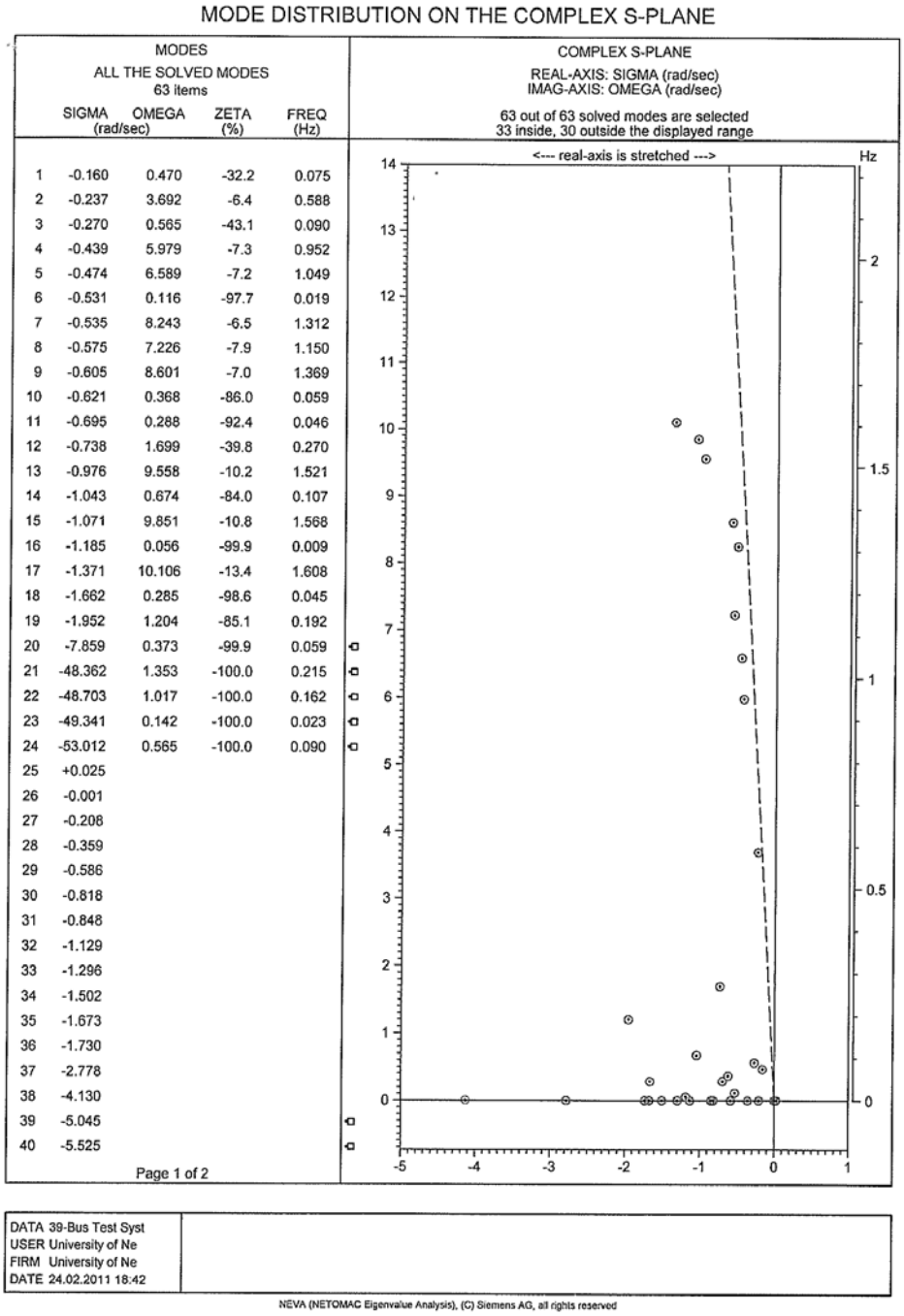

Fig 57: Modal analysis (eigenvalues) of 39 bus test system with shunt capacitor B = -1000 at load bus 7

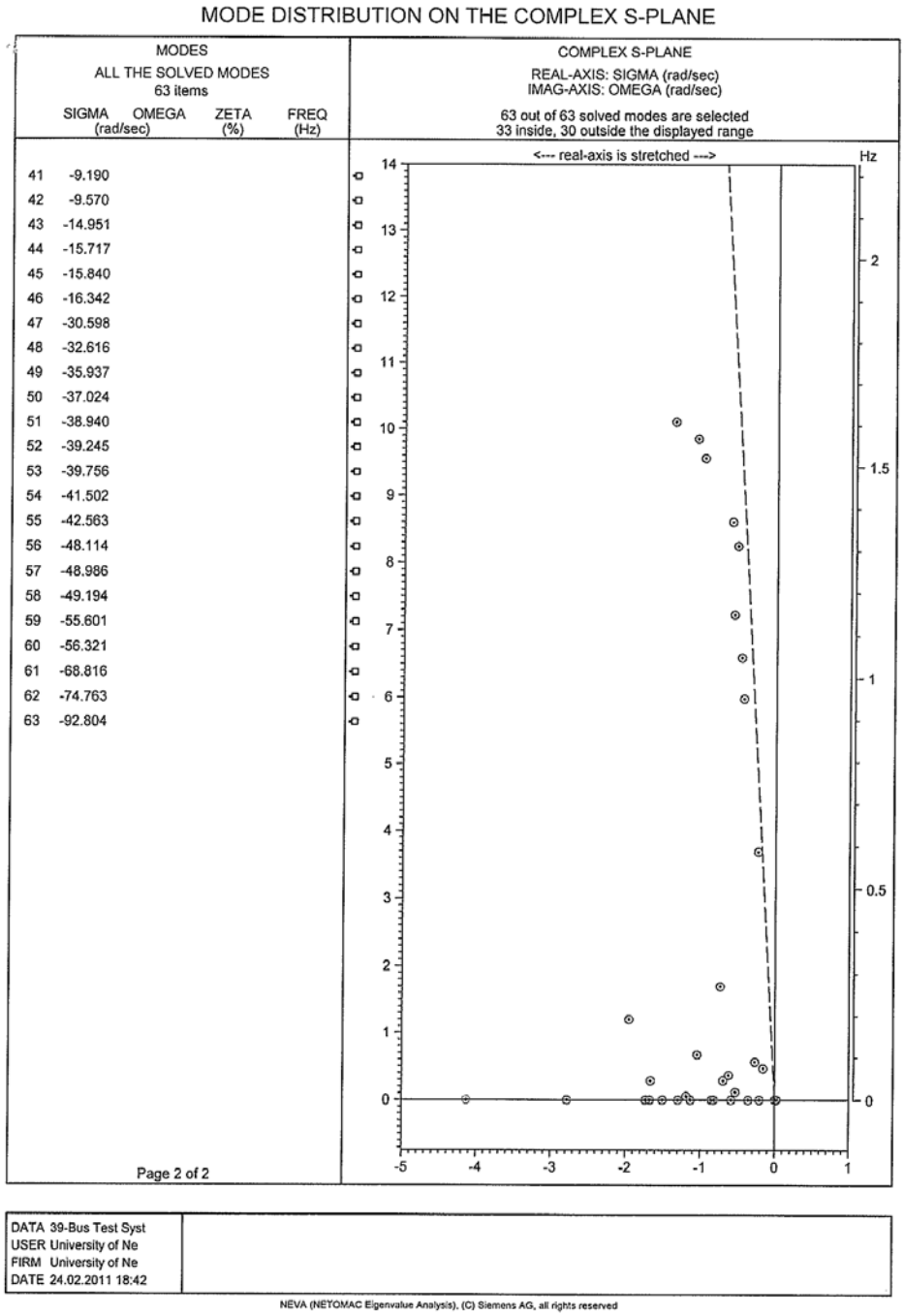

Fig 58: Modal analysis (eigenvalues) of 39 bus test system with shunt capacitor B = -1000 at load bus 7

MODE DISTRIBUTION ON THE COMPLEX S-PLANE

MODES
ALL THE SOLVED MODES
63 items

	SIGMA (rad/sec)	OMEGA (rad/sec)	ZETA (%)	FREQ (Hz)
1	-0.160	0.470	-32.2	0.075
2	-0.236	3.687	-6.4	0.587
3	-0.270	0.565	-43.1	0.090
4	-0.440	5.980	-7.3	0.952
5	-0.477	6.591	-7.2	1.049
6	-0.531	0.116	-97.7	0.019
7	-0.535	8.245	-6.5	1.312
8	-0.575	7.230	-7.9	1.151
9	-0.609	8.620	-7.0	1.372
10	-0.617	0.371	-85.7	0.059
11	-0.694	0.288	-92.3	0.046
12	-0.737	1.699	-39.8	0.270
13	-0.976	9.557	-10.2	1.521
14	-1.042	0.675	-84.0	0.107
15	-1.070	9.850	-10.8	1.568
16	-1.186	0.057	-99.9	0.009
17	-1.371	10.105	-13.4	1.608
18	-1.662	0.285	-98.6	0.045
19	-1.953	1.203	-85.1	0.191
20	-7.856	0.377	-99.9	0.060
21	-48.360	1.353	-100.0	0.215
22	-48.703	1.017	-100.0	0.162
23	-49.341	0.142	-100.0	0.023
24	-52.974	0.559	-100.0	0.089
25	+0.023			
26	+0.001			
27	-0.209			
28	-0.359			
29	-0.586			
30	-0.818			
31	-0.848			
32	-1.128			
33	-1.297			
34	-1.505			
35	-1.670			
36	-1.730			
37	-2.755			
38	-4.127			
39	-5.044			
40	-5.527			

Page 1 of 2

COMPLEX S-PLANE
REAL-AXIS: SIGMA (rad/sec)
IMAG-AXIS: OMEGA (rad/sec)
63 out of 63 solved modes are selected
33 inside, 30 outside the displayed range

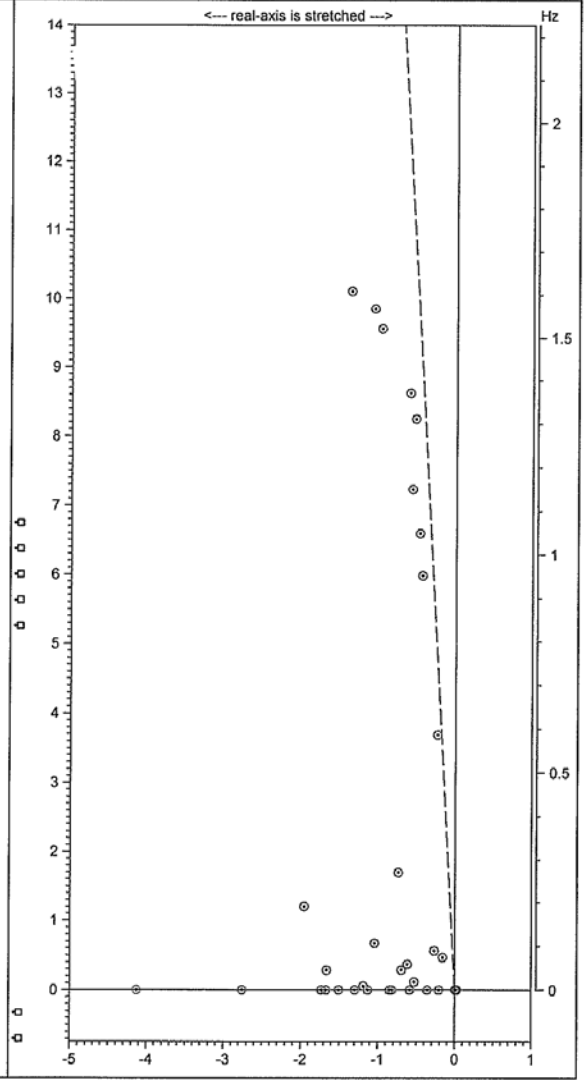

DATA 39-Bus Test Syst
USER University of Ne
FIRM University of Ne
DATE 24.02.2011 18:46

Fig 59: Modal analysis (eigenvalues) of 39 bus test system with shunt capacitor B = -1000 at load bus 8

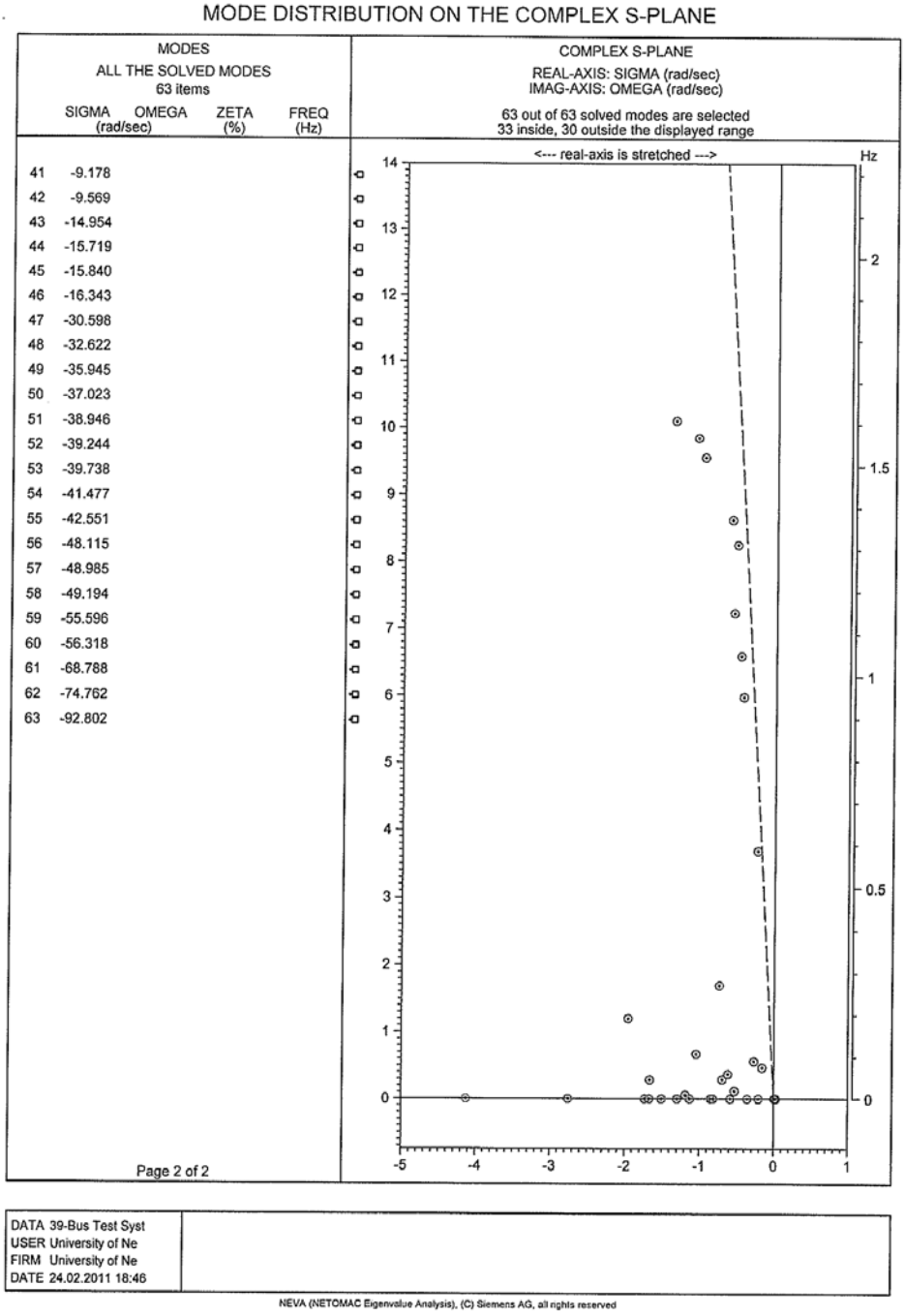

Fig 60: Modal analysis (eigenvalues) of 39 bus test system with shunt capacitor B = -1000 at load bus 8

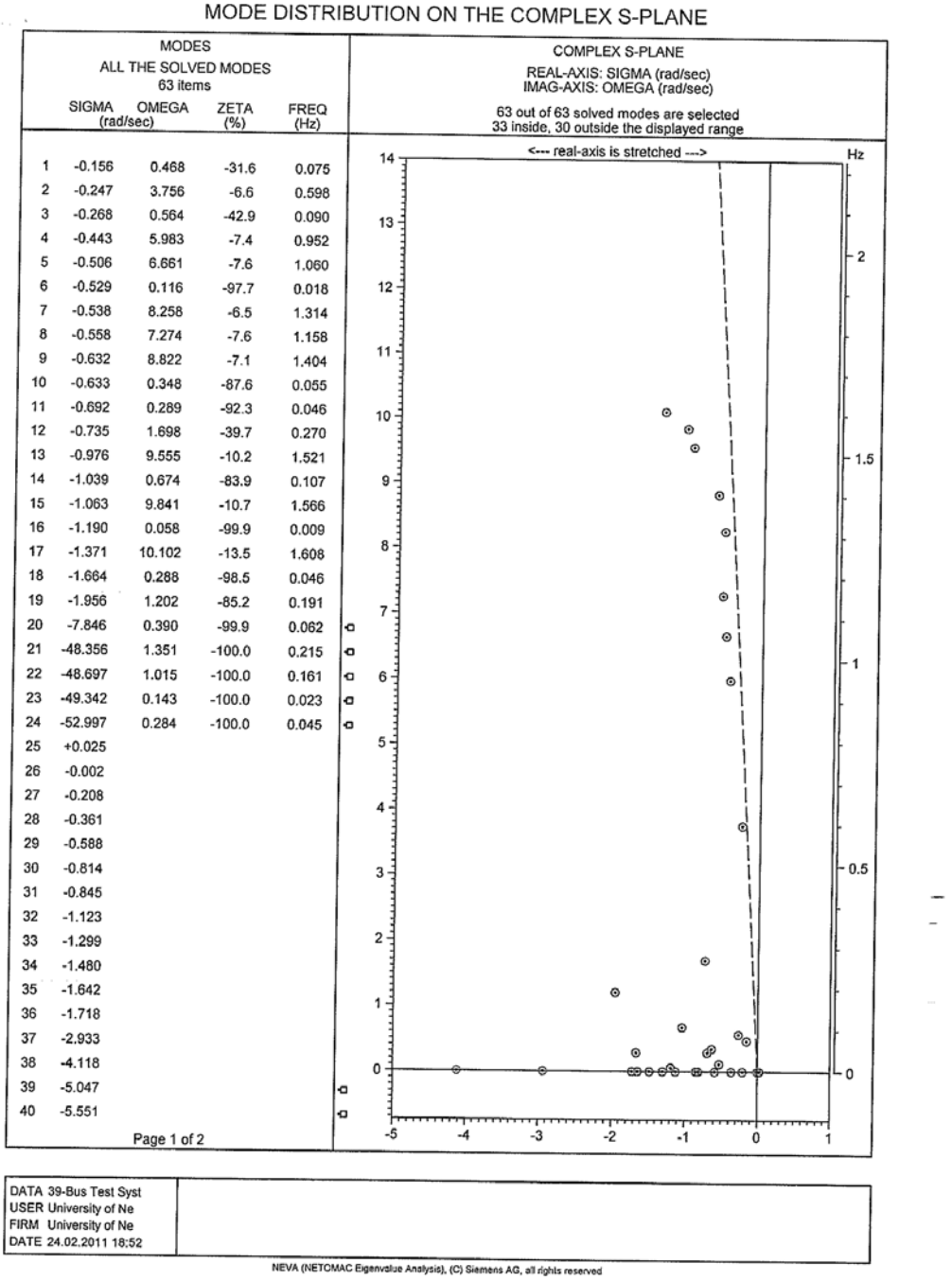

Fig 61: Modal analysis (eigenvalues) of 39 bus test system with shunt capacitor B = -1000 at load bus 12

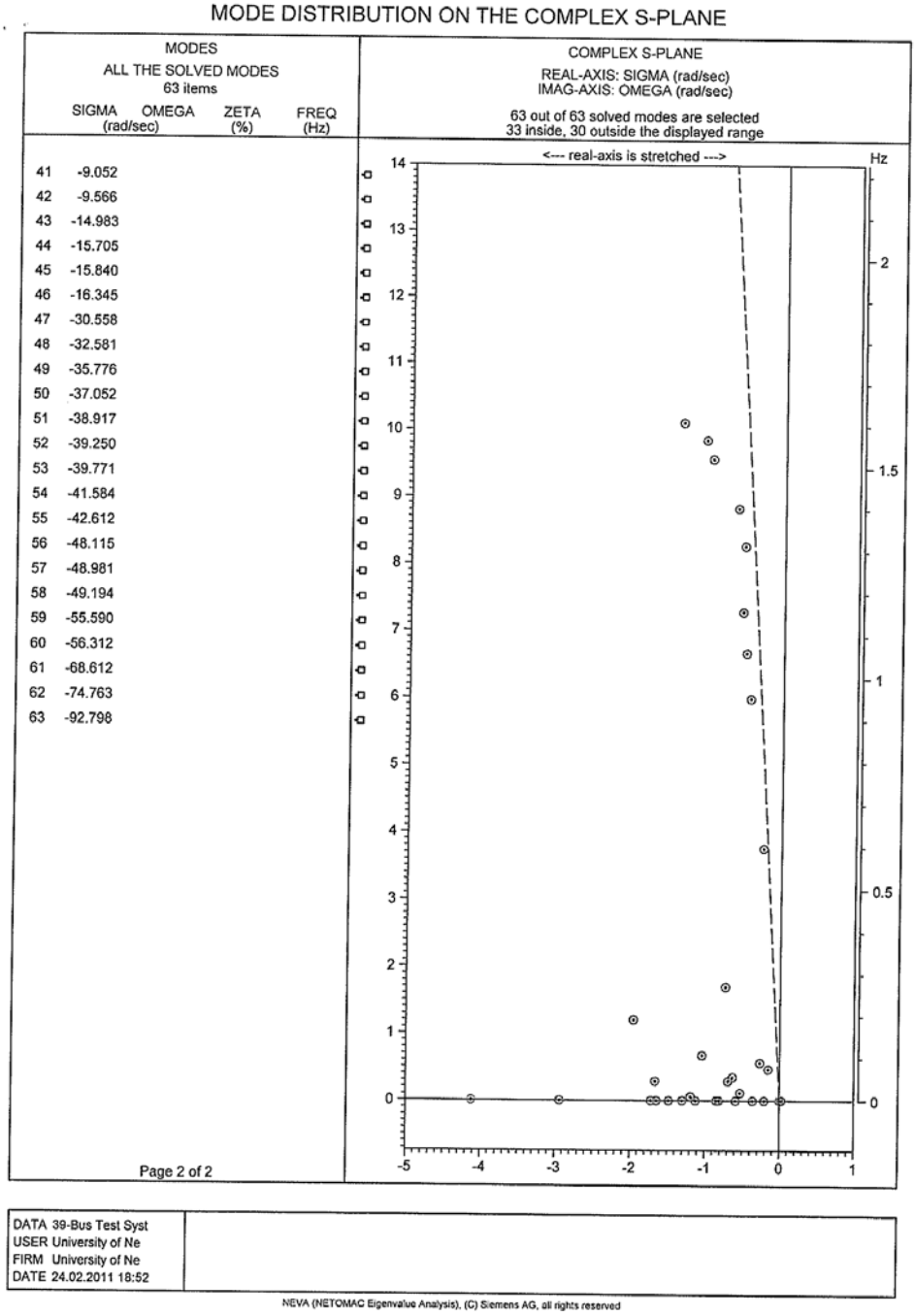

Fig 62: Modal analysis (eigenvalues) of 39 bus test system with shunt capacitor B = -1000 at load bus 12

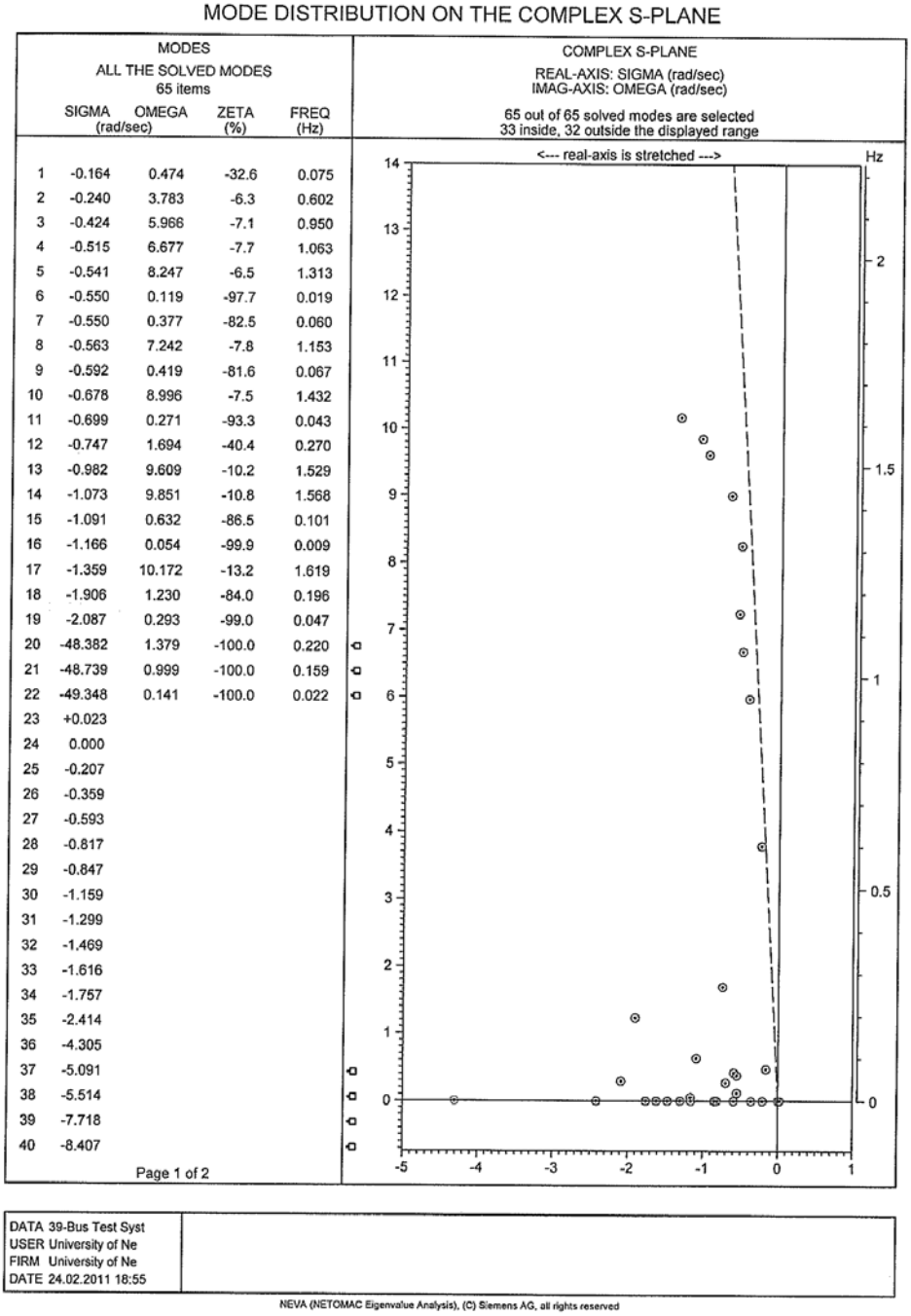

Fig 63: Modal analysis (eigenvalues) of 39 bus test system with shunt capacitor B = -1000 at load bus 15

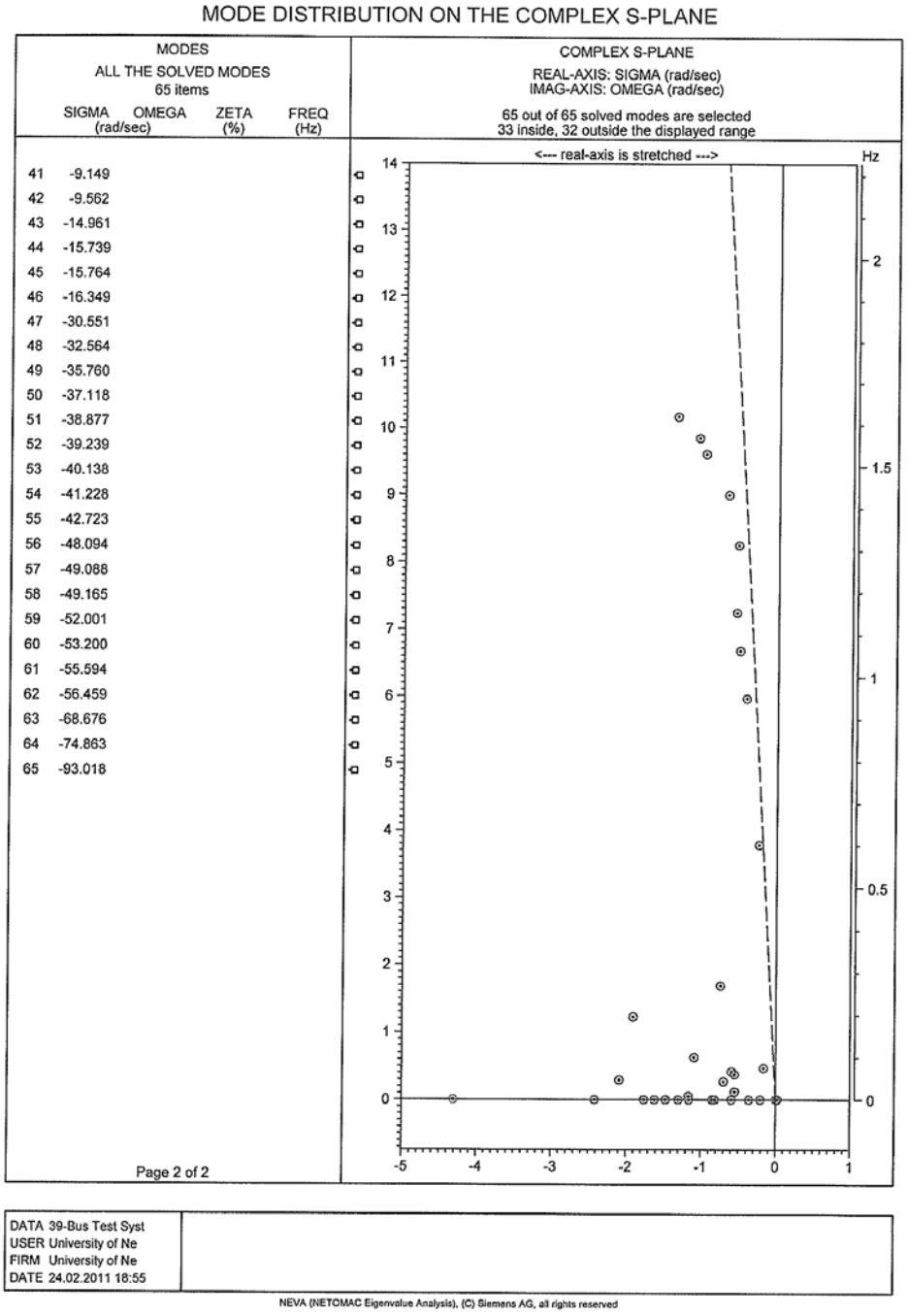

Fig 64: Modal analysis (eigenvalues) of 39 bus test system with shunt capacitor B = -1000 at load bus 15

MODE DISTRIBUTION ON THE COMPLEX S-PLANE

MODES
ALL THE SOLVED MODES
64 items

	SIGMA (rad/sec)	OMEGA (rad/sec)	ZETA (%)	FREQ (Hz)
1	-0.164	0.474	-32.7	0.075
2	-0.240	3.798	-6.3	0.604
3	-0.418	5.963	-7.0	0.949
4	-0.529	6.693	-7.9	1.065
5	-0.539	0.398	-80.4	0.063
6	-0.543	8.245	-6.6	1.312
7	-0.557	0.119	-97.8	0.019
8	-0.559	7.258	-7.7	1.155
9	-0.592	0.406	-82.5	0.065
10	-0.692	9.063	-7.6	1.442
11	-0.708	0.262	-93.8	0.042
12	-0.749	1.693	-40.5	0.270
13	-0.983	9.628	-10.2	1.532
14	-1.075	9.851	-10.8	1.568
15	-1.102	0.624	-87.0	0.099
16	-1.160	0.057	-99.9	0.009
17	-1.350	10.196	-13.1	1.623
18	-1.898	1.238	-83.8	0.197
19	-2.121	0.252	-99.3	0.040
20	-48.387	1.390	-100.0	0.221
21	-48.756	0.993	-100.0	0.158
22	-49.141	0.034	-100.0	0.005
23	-49.352	0.141	-100.0	0.022
24	+0.022			
25	+0.001			
26	-0.207			
27	-0.360			
28	-0.595			
29	-0.816			
30	-0.847			
31	-1.167			
32	-1.299			
33	-1.465			
34	-1.607			
35	-1.796			
36	-2.272			
37	-4.375			
38	-5.119			
39	-5.512			
40	-7.634			

Page 1 of 2

COMPLEX S-PLANE
REAL-AXIS: SIGMA (rad/sec)
IMAG-AXIS: OMEGA (rad/sec)

64 out of 64 solved modes are selected
33 inside, 31 outside the displayed range

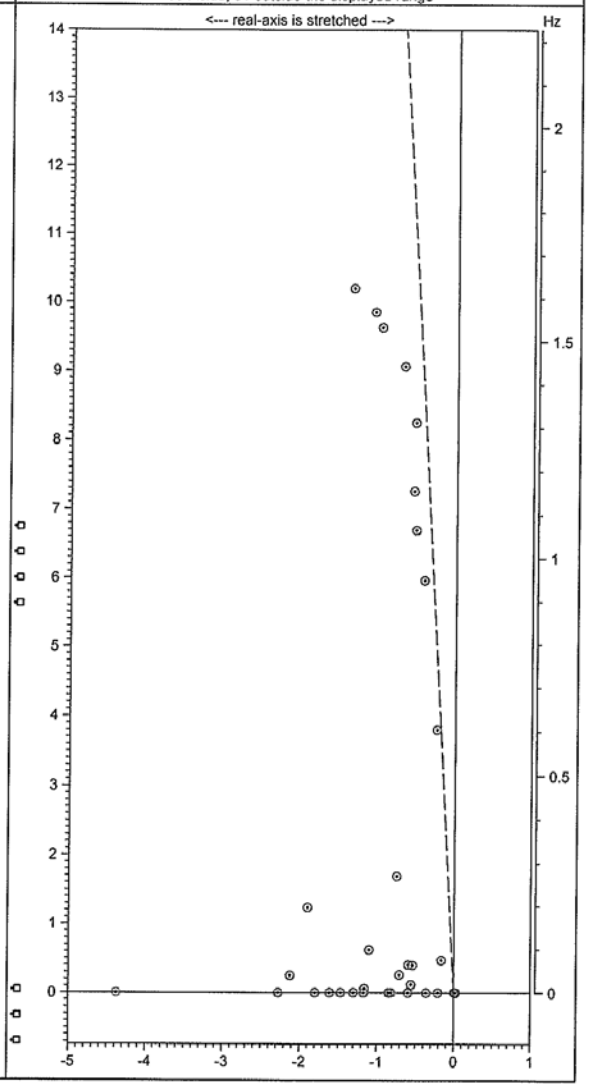

DATA 39-Bus Test Syst
USER University of Ne
FIRM University of Ne
DATE 24.02.2011 18:59

Fig 65: Modal analysis (eigenvalues) of 39 bus test system with shunt capacitor B = -1000 at load bus 16

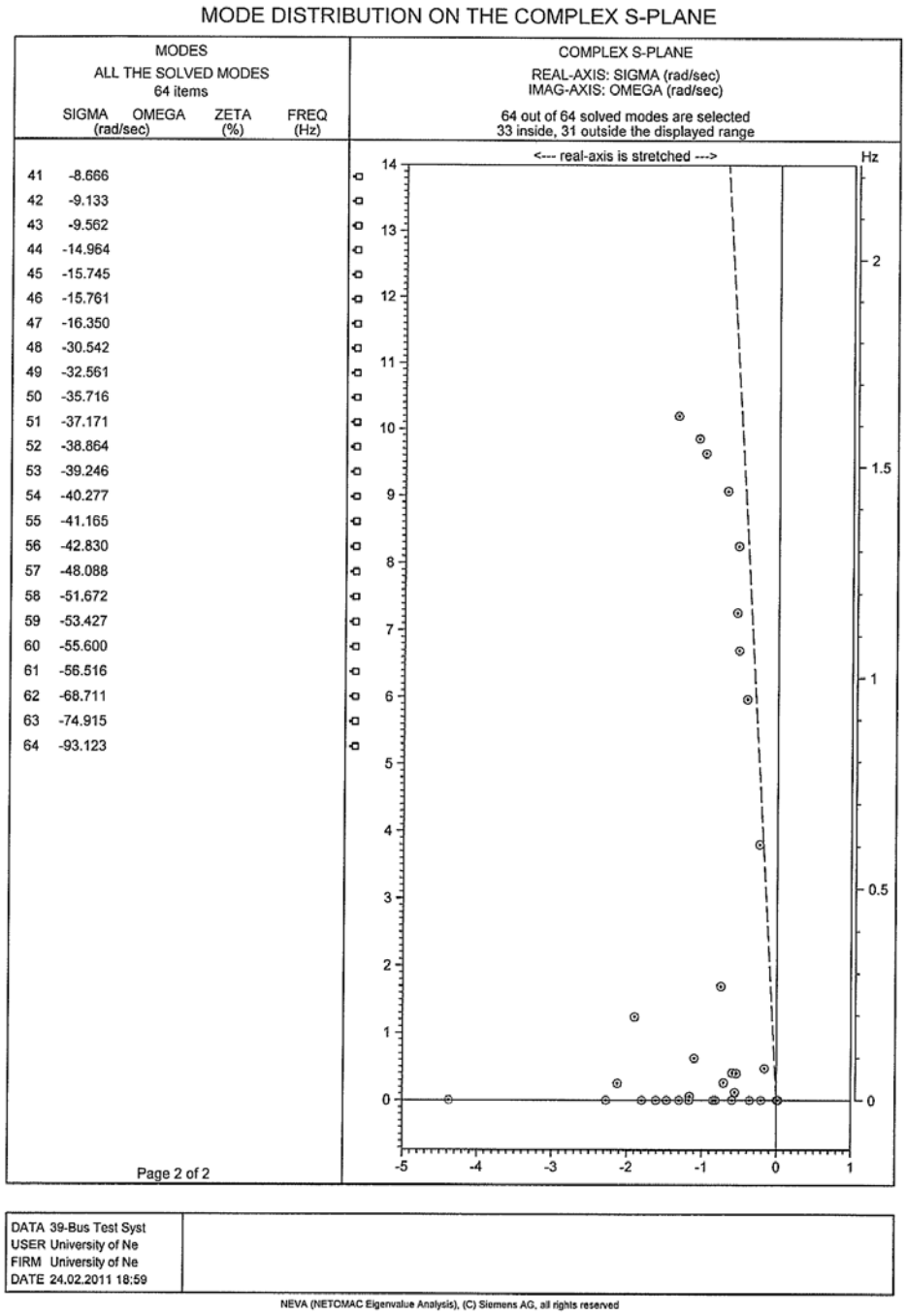

Fig 66: Modal analysis (eigenvalues) of 39 bus test system with shunt capacitor B = -1000 at load bus 16

MODE DISTRIBUTION ON THE COMPLEX S-PLANE

MODES
ALL THE SOLVED MODES
64 items

	SIGMA (rad/sec)	OMEGA	ZETA (%)	FREQ (Hz)
1	-0.180	0.479	-35.1	0.076
2	-0.240	3.778	-6.3	0.601
3	-0.414	5.947	-6.9	0.946
4	-0.530	0.384	-81.0	0.061
5	-0.530	6.675	-7.9	1.062
6	-0.532	8.229	-6.5	1.310
7	-0.542	0.118	-97.7	0.019
8	-0.569	7.271	-7.8	1.157
9	-0.573	0.426	-80.3	0.068
10	-0.687	9.029	-7.6	1.437
11	-0.689	0.281	-92.6	0.045
12	-0.757	1.695	-40.8	0.270
13	-0.980	9.586	-10.2	1.526
14	-1.083	0.646	-85.9	0.103
15	-1.097	9.889	-11.0	1.574
16	-1.163	0.060	-99.9	0.010
17	-1.366	10.145	-13.3	1.615
18	-1.917	1.218	-84.4	0.194
19	-2.057	0.325	-98.8	0.052
20	-7.972	0.106	-100.0	0.017
21	-48.408	1.357	-100.0	0.216
22	-48.750	1.058	-100.0	0.168
23	-49.340	0.134	-100.0	0.021
24	+0.023			
25	+0.000			
26	-0.207			
27	-0.351			
28	-0.594			
29	-0.833			
30	-0.858			
31	-1.154			
32	-1.292			
33	-1.468			
34	-1.611			
35	-1.785			
36	-2.302			
37	-4.229			
38	-5.060			
39	-5.432			
40	-9.556			

Page 1 of 2

COMPLEX S-PLANE
REAL-AXIS: SIGMA (rad/sec)
IMAG-AXIS: OMEGA (rad/sec)

64 out of 64 solved modes are selected
33 inside, 31 outside the displayed range

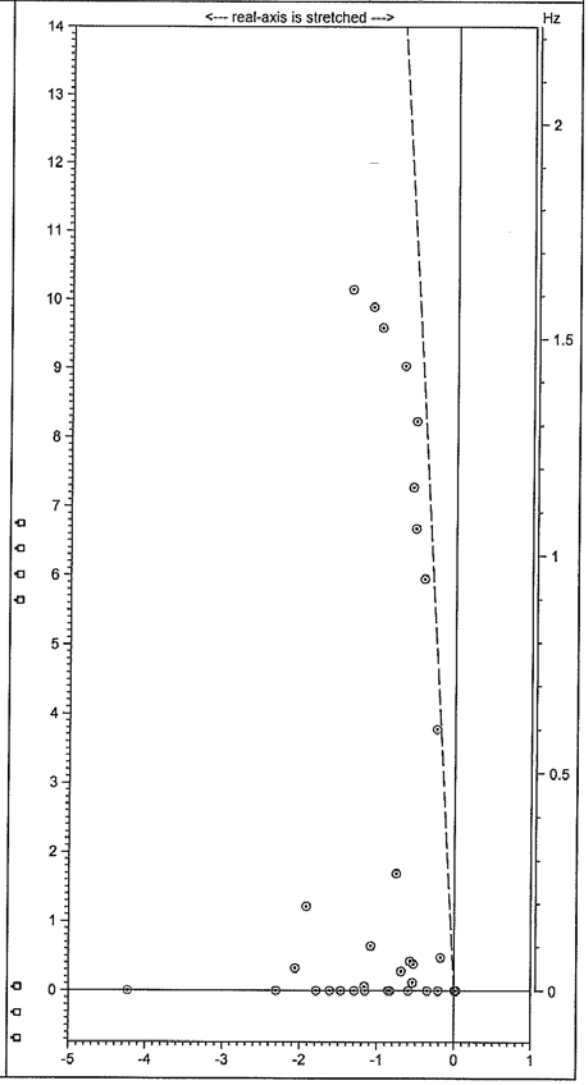

DATA 39-Bus Test Syst
USER University of Ne
FIRM University of Ne
DATE 24.02.2011 19:03

Fig 67: Modal analysis (eigenvalues) of 39 bus test system with shunt capacitor B = -1000 at load bus 18

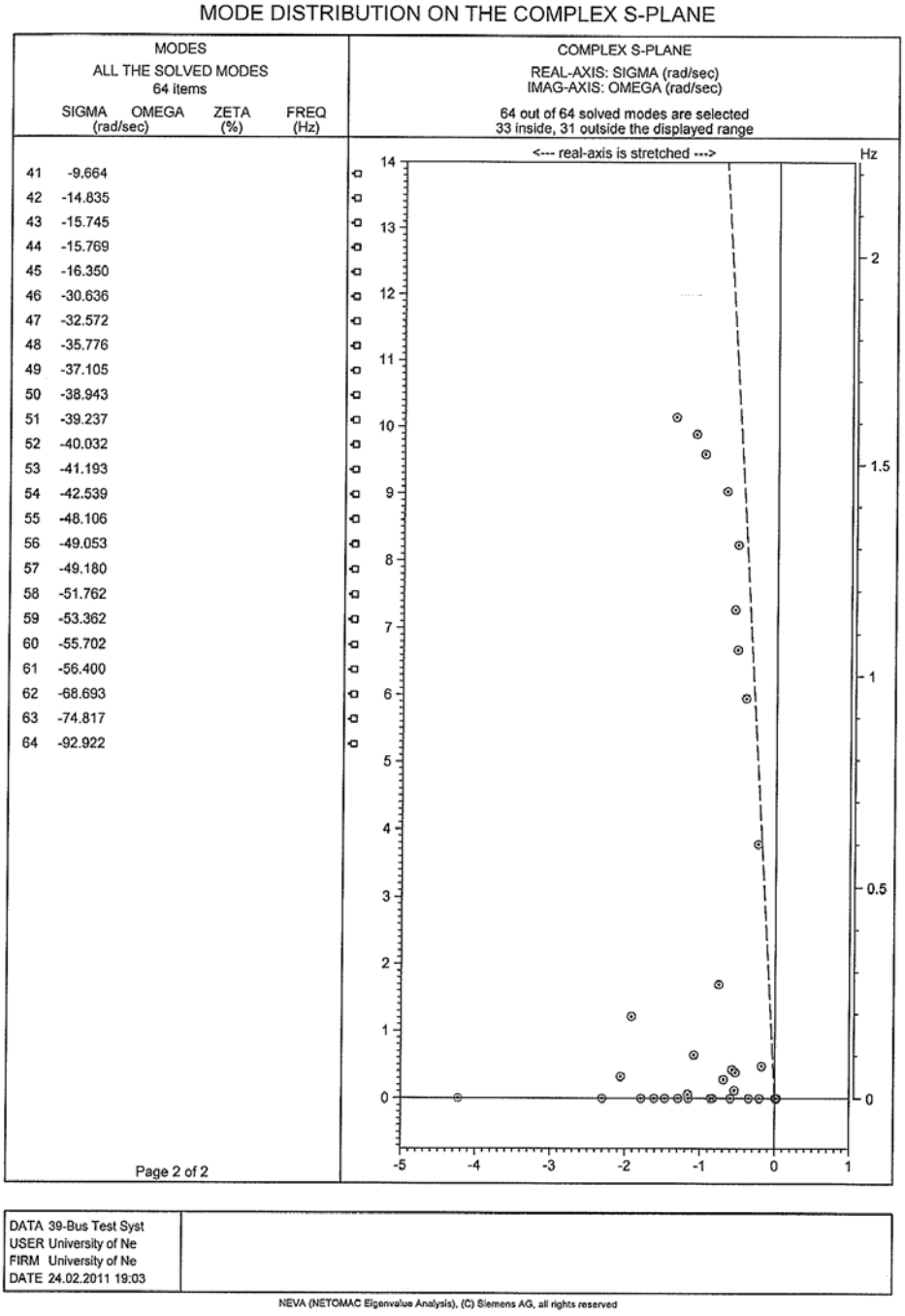

Fig 68: Modal analysis (eigenvalues) of 39 bus test system with shunt capacitor B = -1000 at load bus 18

MODE DISTRIBUTION ON THE COMPLEX S-PLANE

MODES
ALL THE SOLVED MODES
64 items

	SIGMA (rad/sec)	OMEGA (rad/sec)	ZETA (%)	FREQ (Hz)
1	-0.157	0.471	-31.6	0.075
2	-0.248	3.818	-6.5	0.608
3	-0.431	5.979	-7.2	0.952
4	-0.518	0.399	-79.2	0.064
5	-0.542	6.693	-8.1	1.065
6	-0.547	7.277	-7.5	1.158
7	-0.548	8.253	-6.6	1.313
8	-0.566	0.419	-80.4	0.067
9	-0.578	0.116	-98.0	0.018
10	-0.693	0.279	-92.8	0.044
11	-0.700	9.112	-7.7	1.450
12	-0.742	1.692	-40.2	0.269
13	-0.978	9.588	-10.1	1.526
14	-1.060	9.834	-10.7	1.565
15	-1.116	0.618	-87.5	0.098
16	-1.175	0.059	-99.9	0.009
17	-1.312	10.266	-12.7	1.634
18	-1.896	1.229	-83.9	0.196
19	-2.077	0.317	-98.9	0.051
20	-48.388	1.432	-100.0	0.228
21	-48.757	1.008	-100.0	0.160
22	-49.203	0.100	-100.0	0.016
23	-49.410	0.127	-100.0	0.020
24	+0.023			
25	+0.001			
26	-0.207			
27	-0.363			
28	-0.597			
29	-0.810			
30	-0.842			
31	-1.141			
32	-1.303			
33	-1.461			
34	-1.601			
35	-1.841			
36	-2.169			
37	-4.648			
38	-5.260			
39	-5.574			
40	-7.839			

Page 1 of 2

COMPLEX S-PLANE
REAL-AXIS: SIGMA (rad/sec)
IMAG-AXIS: OMEGA (rad/sec)

64 out of 64 solved modes are selected
33 inside, 31 outside the displayed range

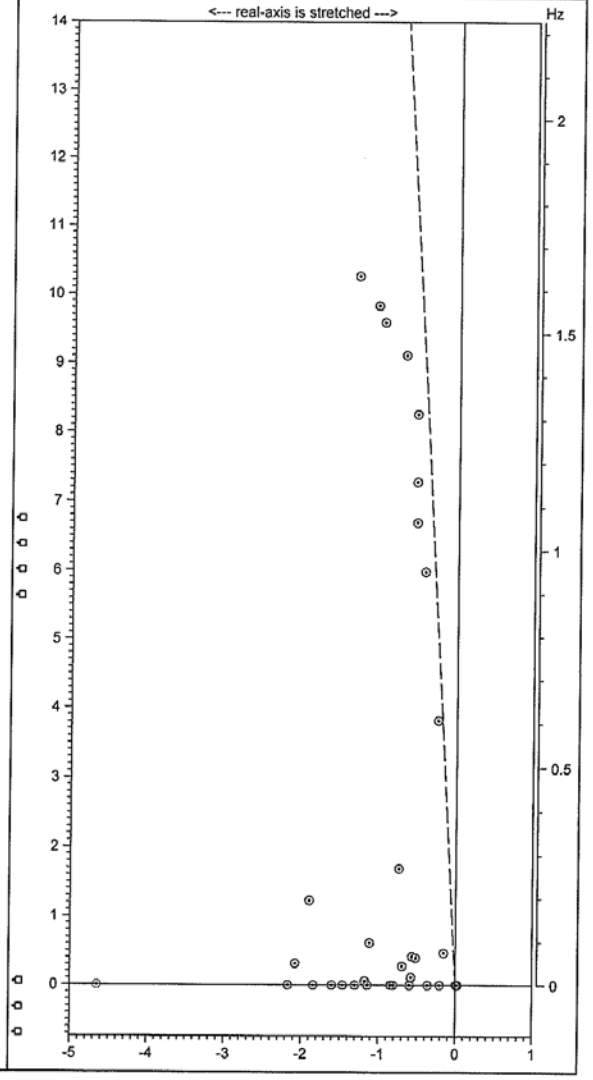

DATA 39-Bus Test Syst
USER University of Ne
FIRM University of Ne
DATE 24.02.2011 19:11

Fig 69: Modal analysis (eigenvalues) of 39 bus test system with shunt capacitor B = -1000 at load bus 21

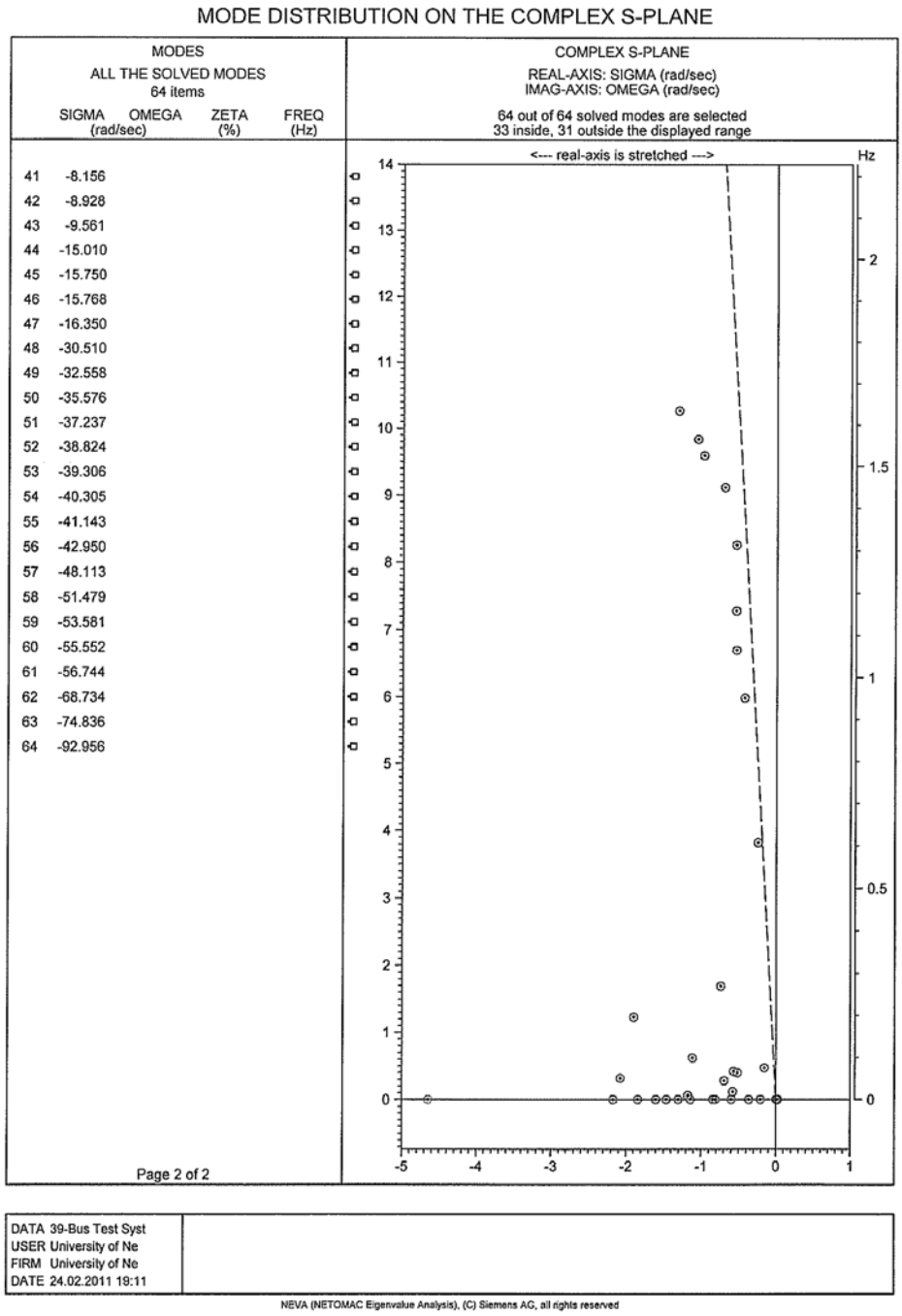

Fig 70: Modal analysis (eigenvalues) of 39 bus test system with shunt capacitor B = -1000 at load bus 21

MODE DISTRIBUTION ON THE COMPLEX S-PLANE

MODES
ALL THE SOLVED MODES
63 items

	SIGMA (rad/sec)	OMEGA (rad/sec)	ZETA (%)	FREQ (Hz)
1	-0.148	0.465	-30.4	0.074
2	-0.256	3.850	-6.6	0.613
3	-0.276	0.573	-43.5	0.091
4	-0.445	5.992	-7.4	0.954
5	-0.495	0.432	-75.3	0.069
6	-0.546	6.696	-8.1	1.066
7	-0.552	8.265	-6.7	1.315
8	-0.553	7.344	-7.5	1.169
9	-0.581	0.116	-98.1	0.019
10	-0.704	0.288	-92.6	0.046
11	-0.707	9.158	-7.7	1.458
12	-0.725	1.684	-39.5	0.268
13	-0.891	0.397	-91.3	0.063
14	-0.970	9.566	-10.1	1.522
15	-1.046	9.819	-10.6	1.563
16	-1.183	0.063	-99.9	0.010
17	-1.266	10.297	-12.2	1.639
18	-1.680	0.270	-98.7	0.043
19	-2.020	0.031	-100.0	0.005
20	-7.875	0.352	-99.9	0.056
21	-48.515	1.542	-99.9	0.245
22	-48.769	1.021	-100.0	0.163
23	-49.172	0.063	-100.0	0.010
24	-49.390	0.125	-100.0	0.020
25	+0.022			
26	+0.001			
27	-0.207			
28	-0.367			
29	-0.598			
30	-0.804			
31	-0.837			
32	-1.130			
33	-1.306			
34	-1.456			
35	-1.595			
36	-1.944			
37	-4.643			
38	-5.197			
39	-5.617			
40	-6.207			

Page 1 of 2

COMPLEX S-PLANE
REAL-AXIS: SIGMA (rad/sec)
IMAG-AXIS: OMEGA (rad/sec)

63 out of 63 solved modes are selected
32 inside, 31 outside the displayed range

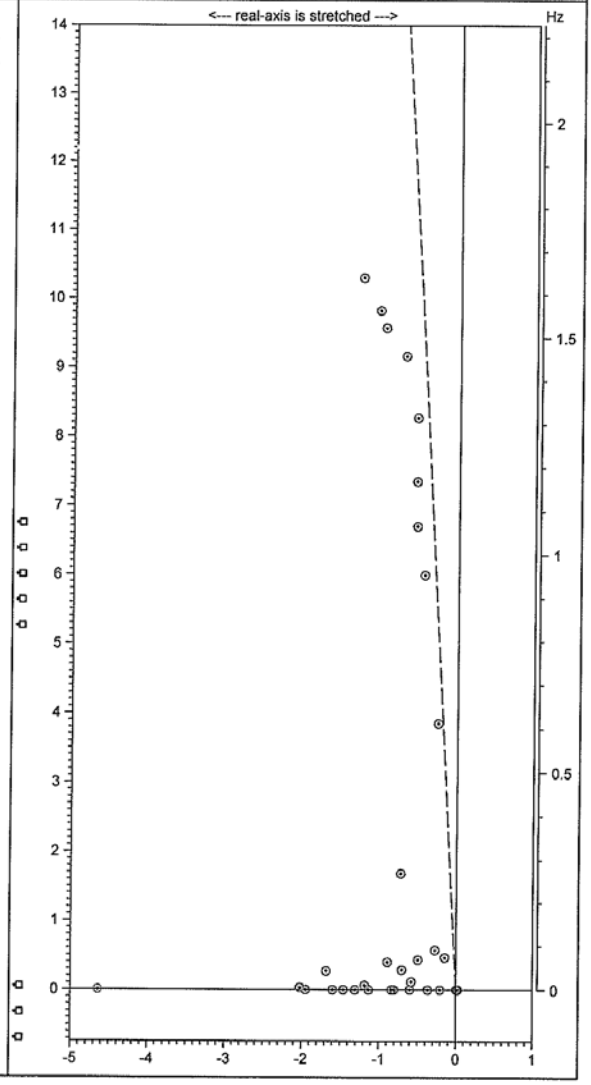

DATA 39-Bus Test Syst
USER University of Ne
FIRM University of Ne
DATE 24.02.2011 19:15

Fig 71: Modal analysis (eigenvalues) of 39 bus test system with shunt capacitor B = -1000 at load bus 23

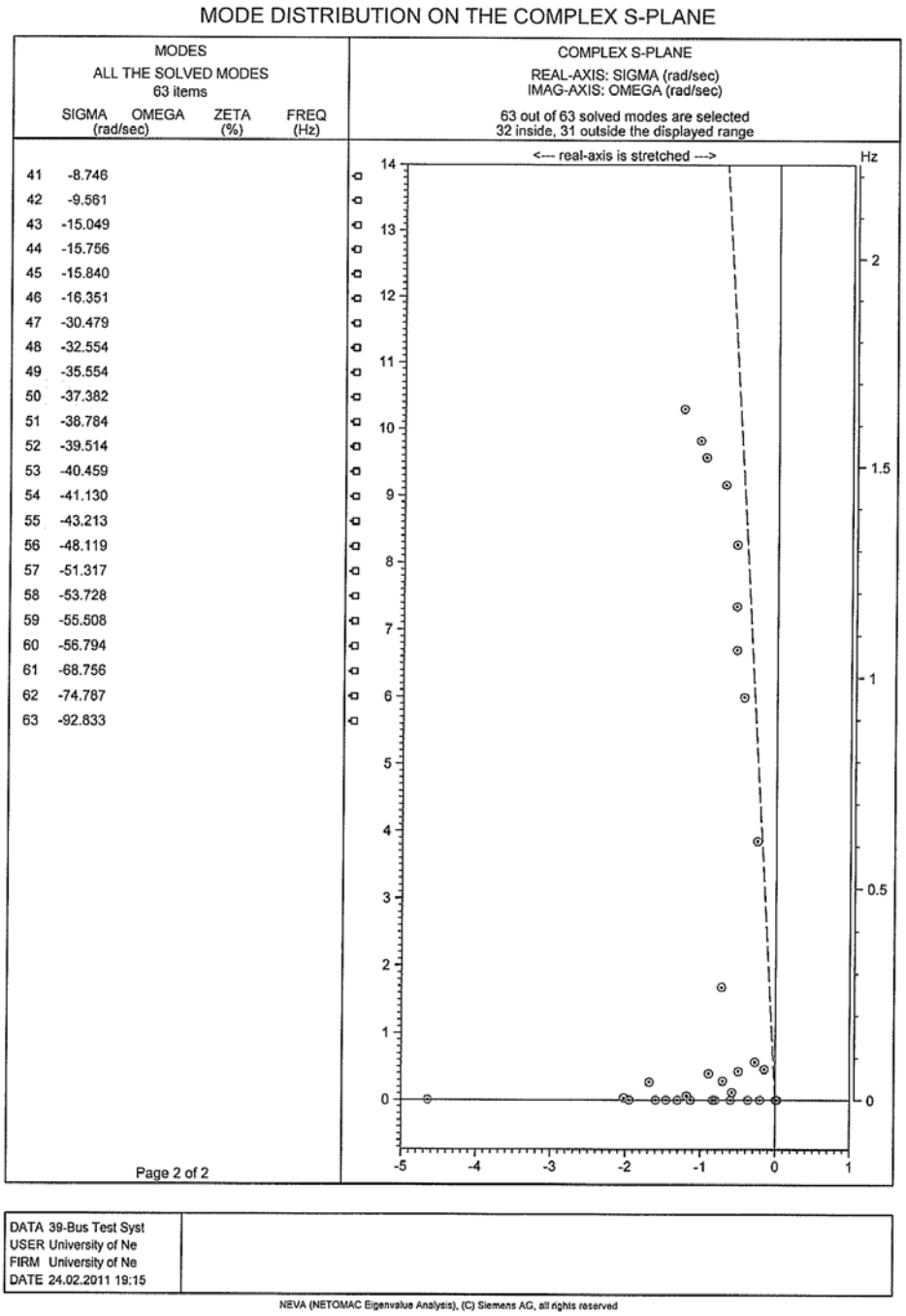

Fig 72: Modal analysis (eigenvalues) of 39 bus test system with shunt capacitor B = -1000 at load bus 23

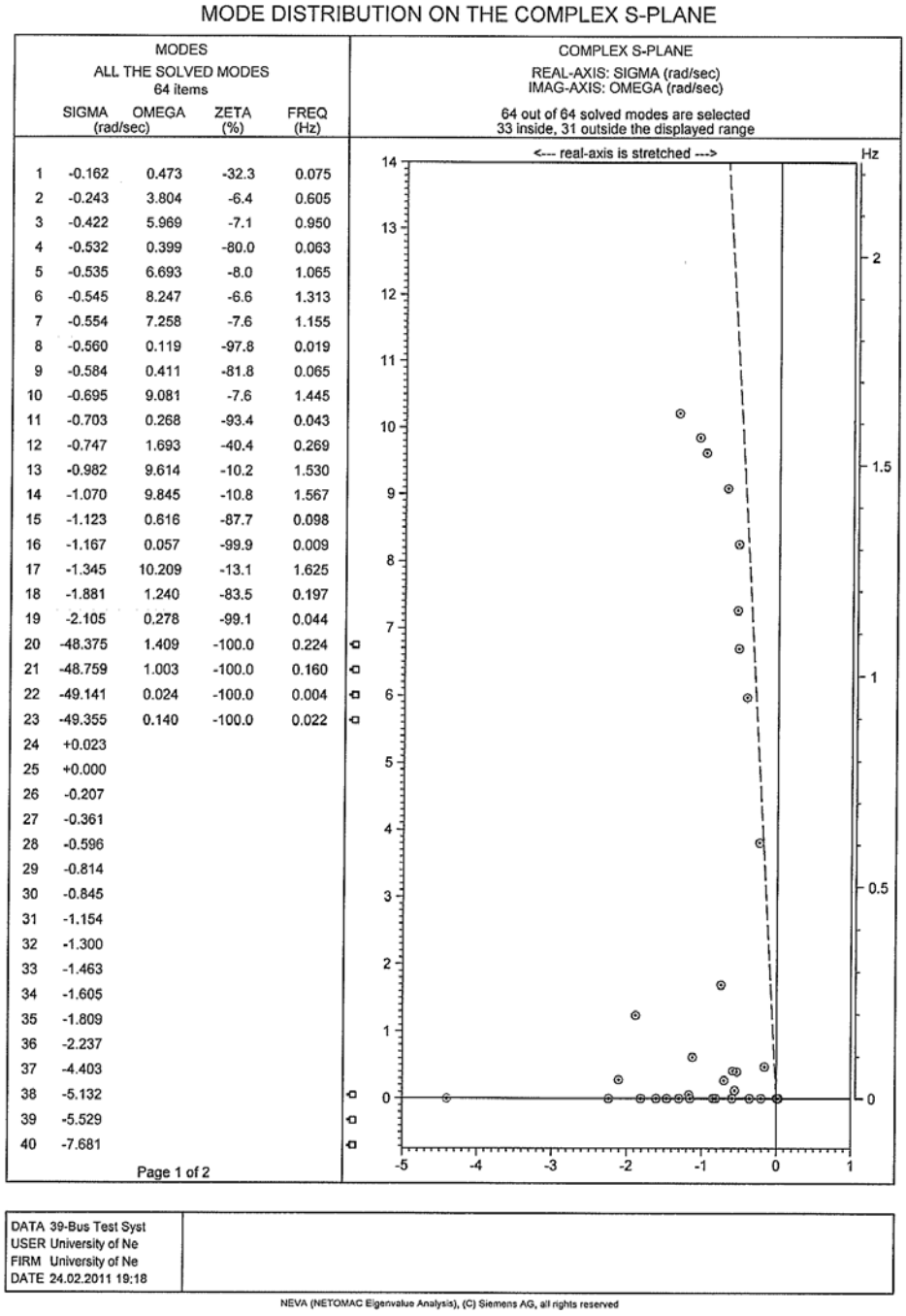

Fig 73: Modal analysis (eigenvalues) of 39 bus test system with shunt capacitor B = -1000 at load bus 24

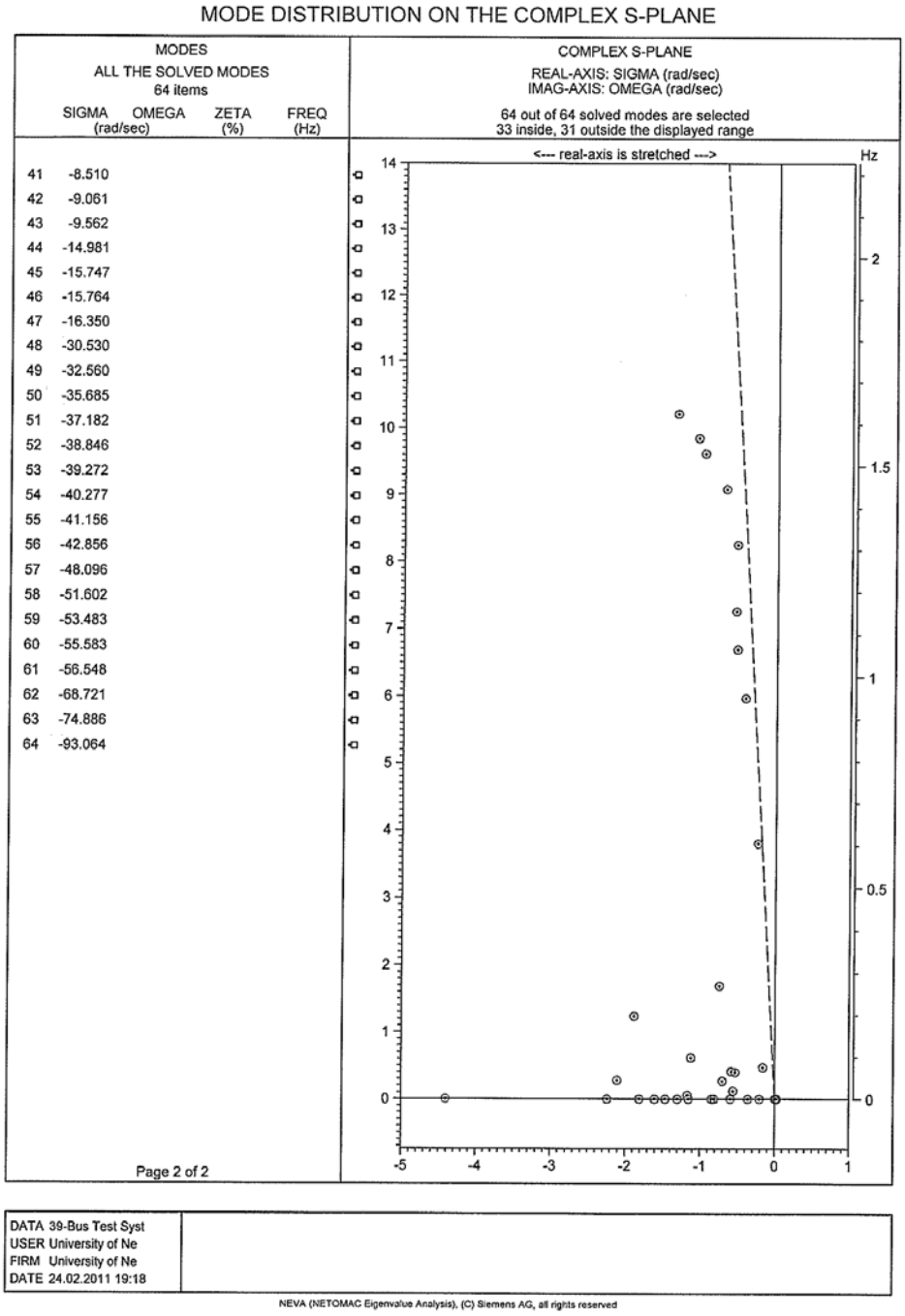

Fig 74: Modal analysis (eigenvalues) of 39 bus test system with shunt capacitor B = -1000 at load bus 24

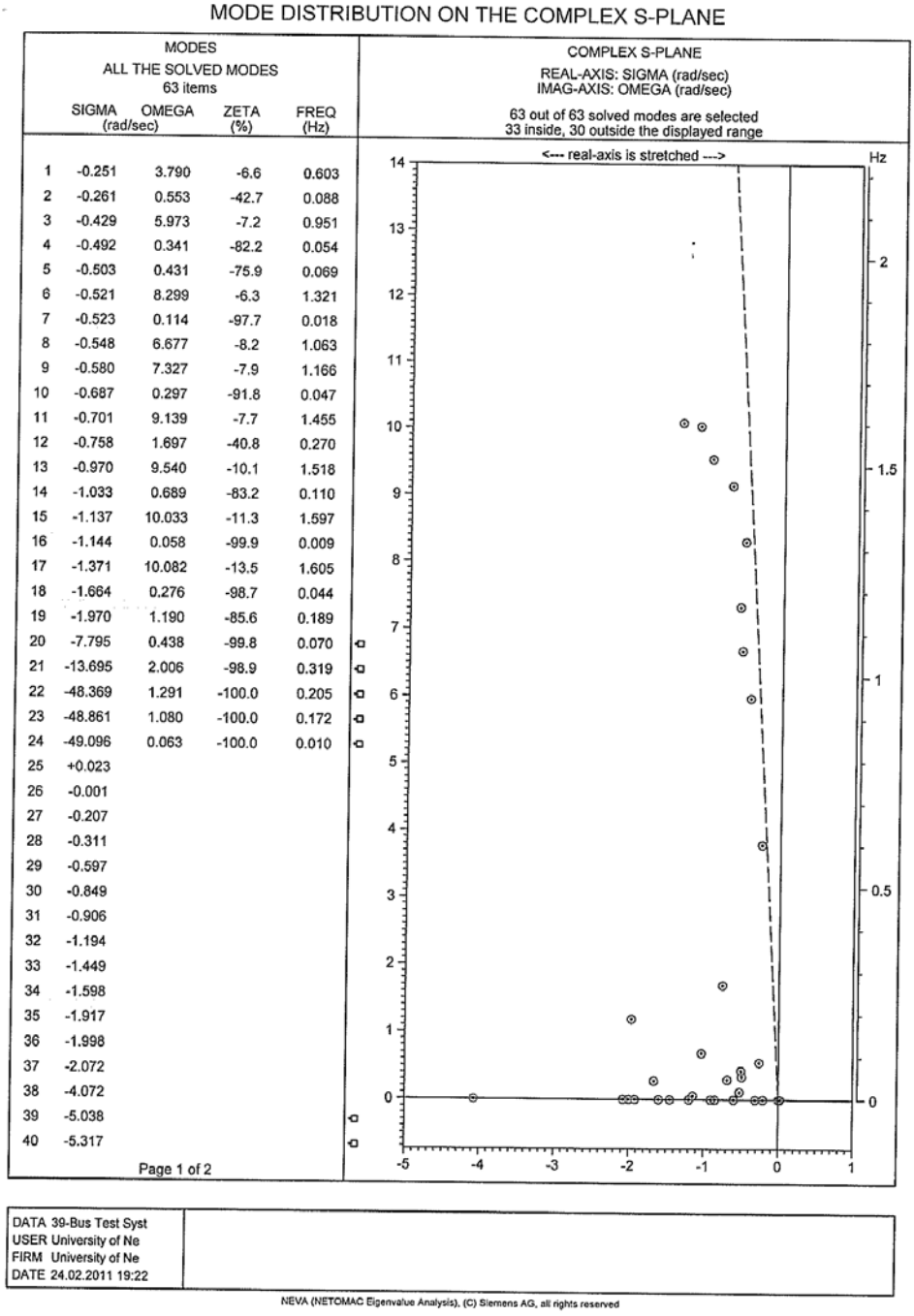

Fig 75: Modal analysis (eigenvalues) of 39 bus test system with shunt capacitor B = -1000 at load bus 25

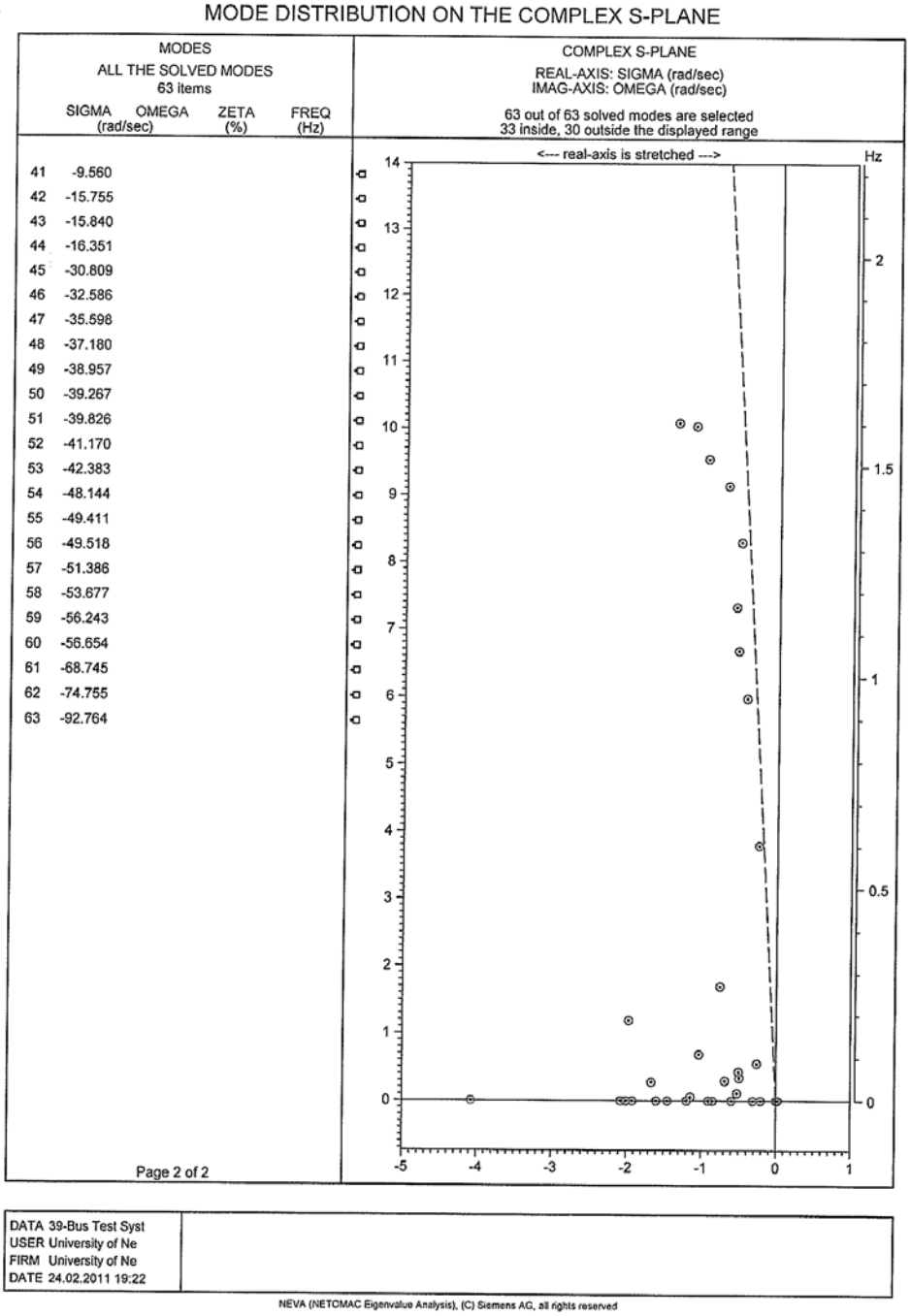

Fig 76: Modal analysis (eigenvalues) of 39 bus test system with shunt capacitor B = -1000 at load bus 25

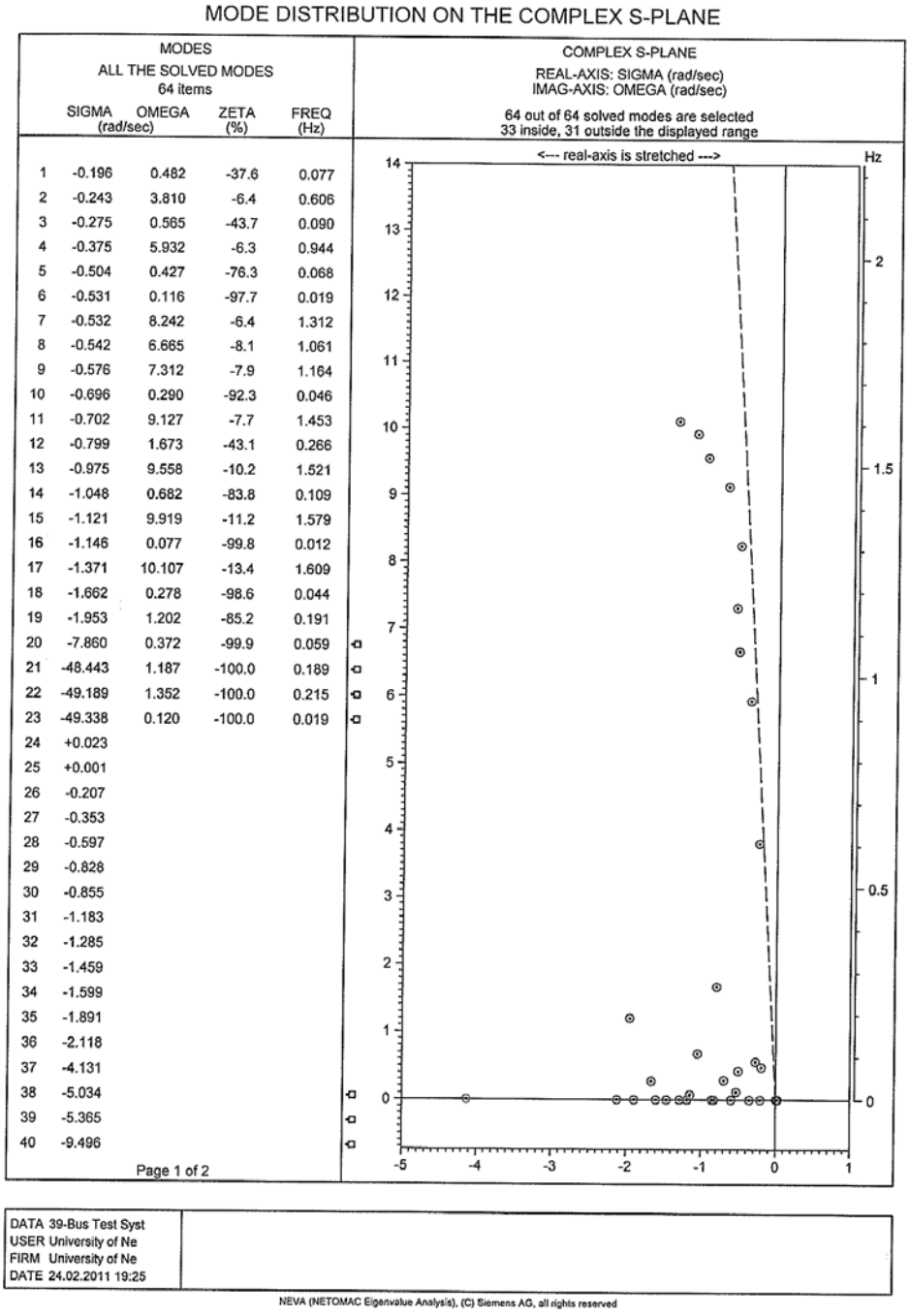

Fig 77: Modal analysis (eigenvalues) of 39 bus test system with shunt capacitor B = -1000 at load bus 26

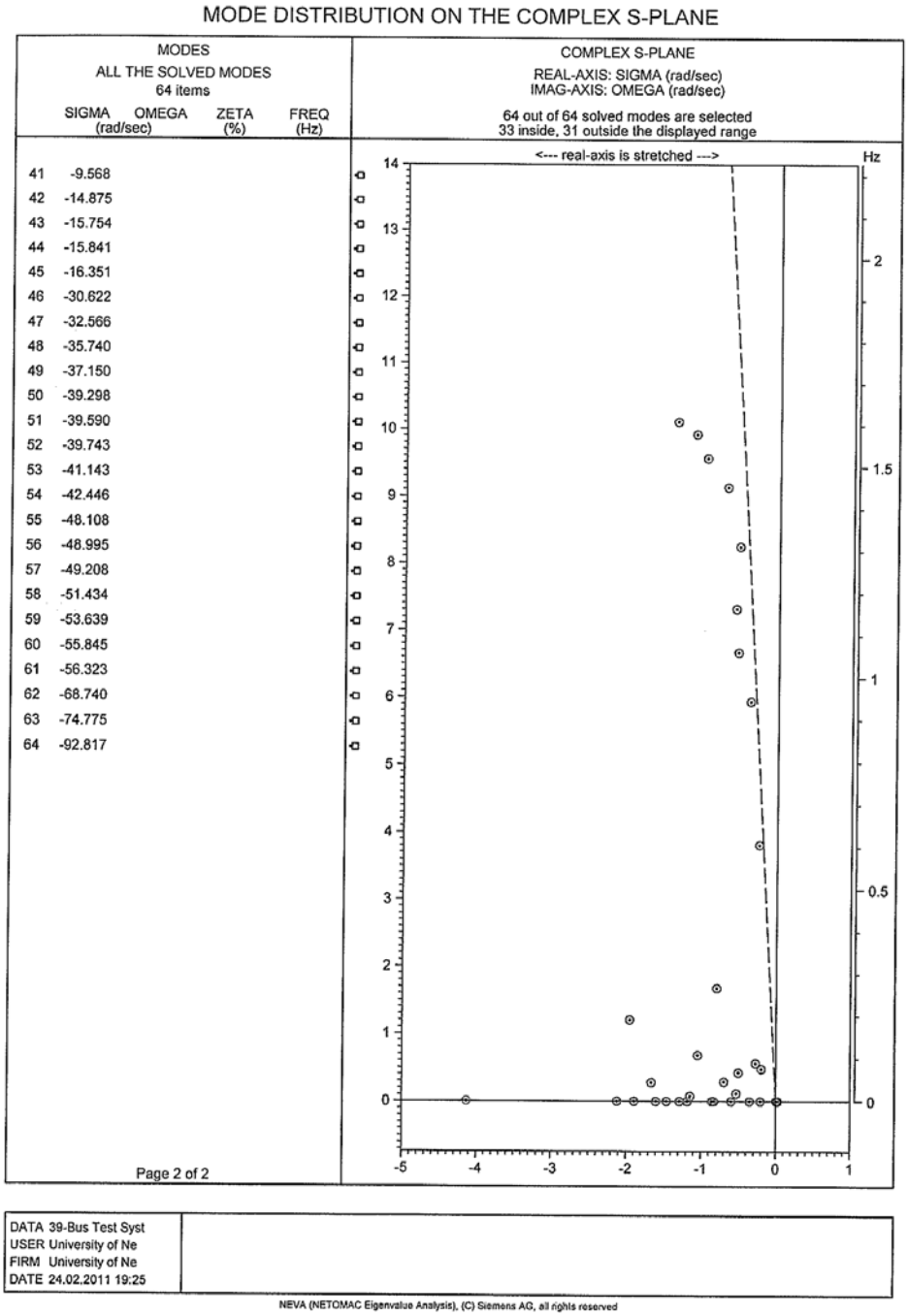

Fig 78: Modal analysis (eigenvalues) of 39 bus test system with shunt capacitor B = -1000 at load bus 26

MODE DISTRIBUTION ON THE COMPLEX S-PLANE

MODES

ALL THE SOLVED MODES
63 items

	SIGMA (rad/sec)	OMEGA (rad/sec)	ZETA (%)	FREQ (Hz)
1	-0.185	0.479	-36.0	0.076
2	-0.243	3.803	-6.4	0.605
3	-0.282	0.569	-44.4	0.091
4	-0.387	5.916	-6.5	0.942
5	-0.515	0.422	-77.3	0.067
6	-0.536	8.241	-6.5	1.312
7	-0.538	0.118	-97.7	0.019
8	-0.542	6.673	-8.1	1.062
9	-0.572	7.293	-7.8	1.161
10	-0.697	9.097	-7.6	1.448
11	-0.704	0.282	-92.8	0.045
12	-0.780	1.690	-41.9	0.269
13	-0.979	9.577	-10.2	1.524
14	-1.059	0.670	-84.5	0.107
15	-1.108	9.897	-11.1	1.575
16	-1.145	0.071	-99.8	0.011
17	-1.369	10.131	-13.4	1.612
18	-1.659	0.276	-98.6	0.044
19	-1.941	1.213	-84.8	0.193
20	-7.929	0.252	-99.9	0.040
21	-39.207	0.051	-100.0	0.008
22	-48.484	1.241	-100.0	0.198
23	-48.879	1.275	-100.0	0.203
24	-49.336	0.127	-100.0	0.020
25	+0.023			
26	+0.000			
27	-0.207			
28	-0.354			
29	-0.596			
30	-0.826			
31	-0.854			
32	-1.182			
33	-1.290			
34	-1.461			
35	-1.603			
36	-1.848			
37	-2.189			
38	-4.193			
39	-5.049			
40	-5.403			

Page 1 of 2

COMPLEX S-PLANE

REAL-AXIS: SIGMA (rad/sec)
IMAG-AXIS: OMEGA (rad/sec)

63 out of 63 solved modes are selected
33 inside, 30 outside the displayed range

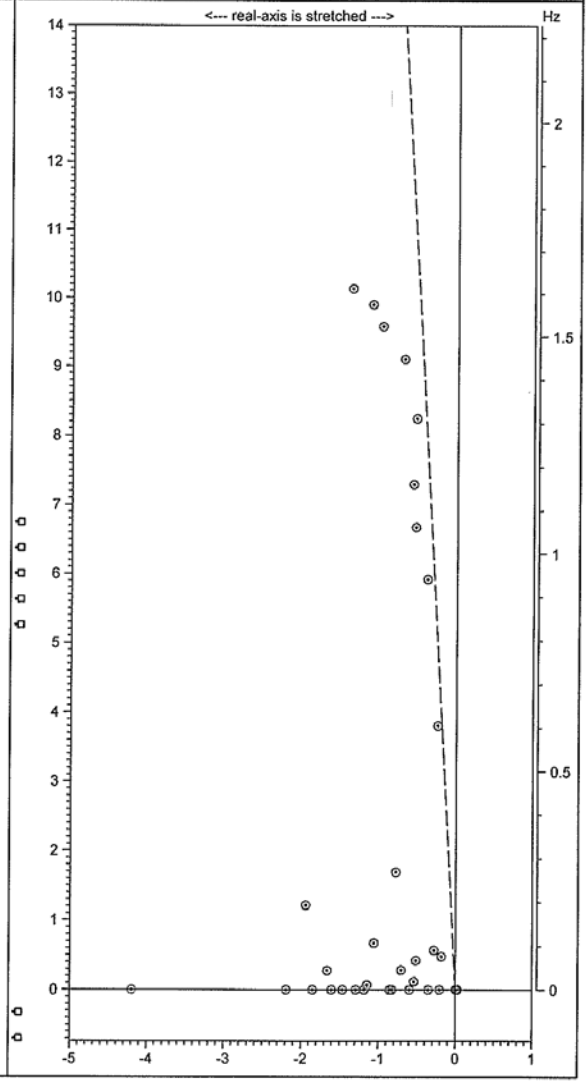

DATA 39-Bus Test Syst
USER University of Ne
FIRM University of Ne
DATE 24.02.2011 19:29

Fig 79: Modal analysis (eigenvalues) of 39 bus test system with shunt capacitor B = -1000 at load bus 27

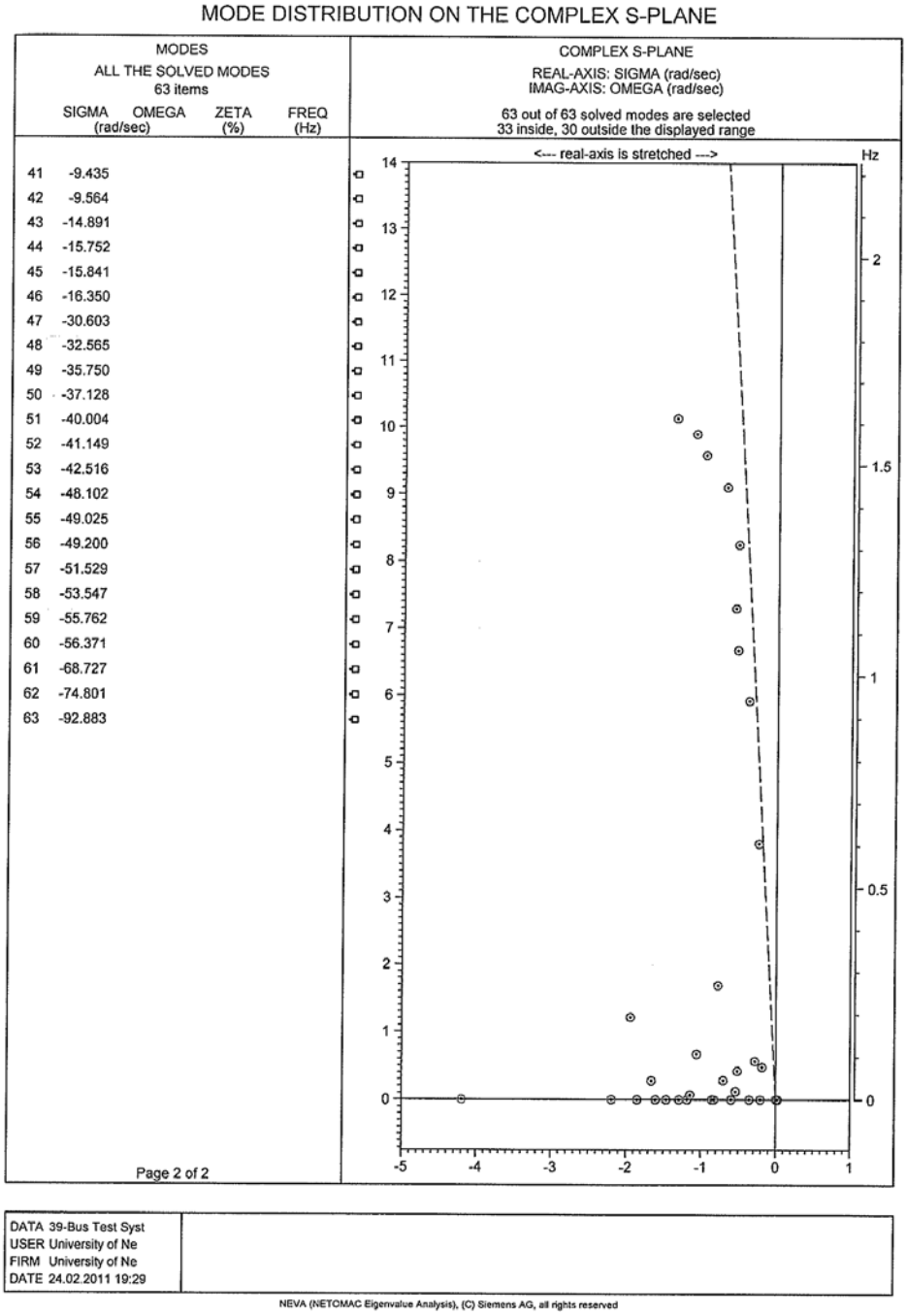

Fig 80: Modal analysis (eigenvalues) of 39 bus test system with shunt capacitor B = -1000 at load bus 27

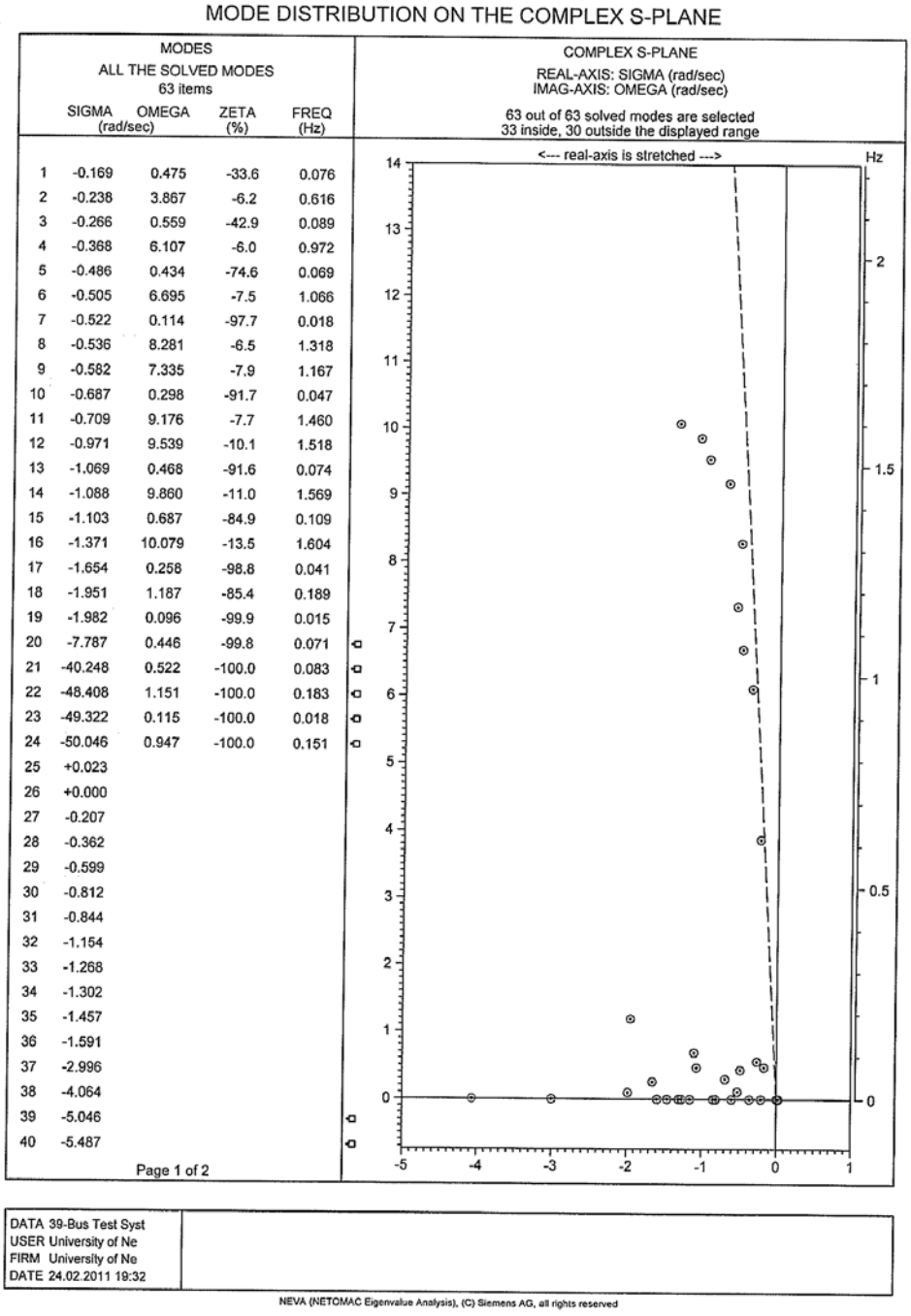

Fig 81: Modal analysis (eigenvalues) of 39 bus test system with shunt capacitor B = -1000 at load bus 28

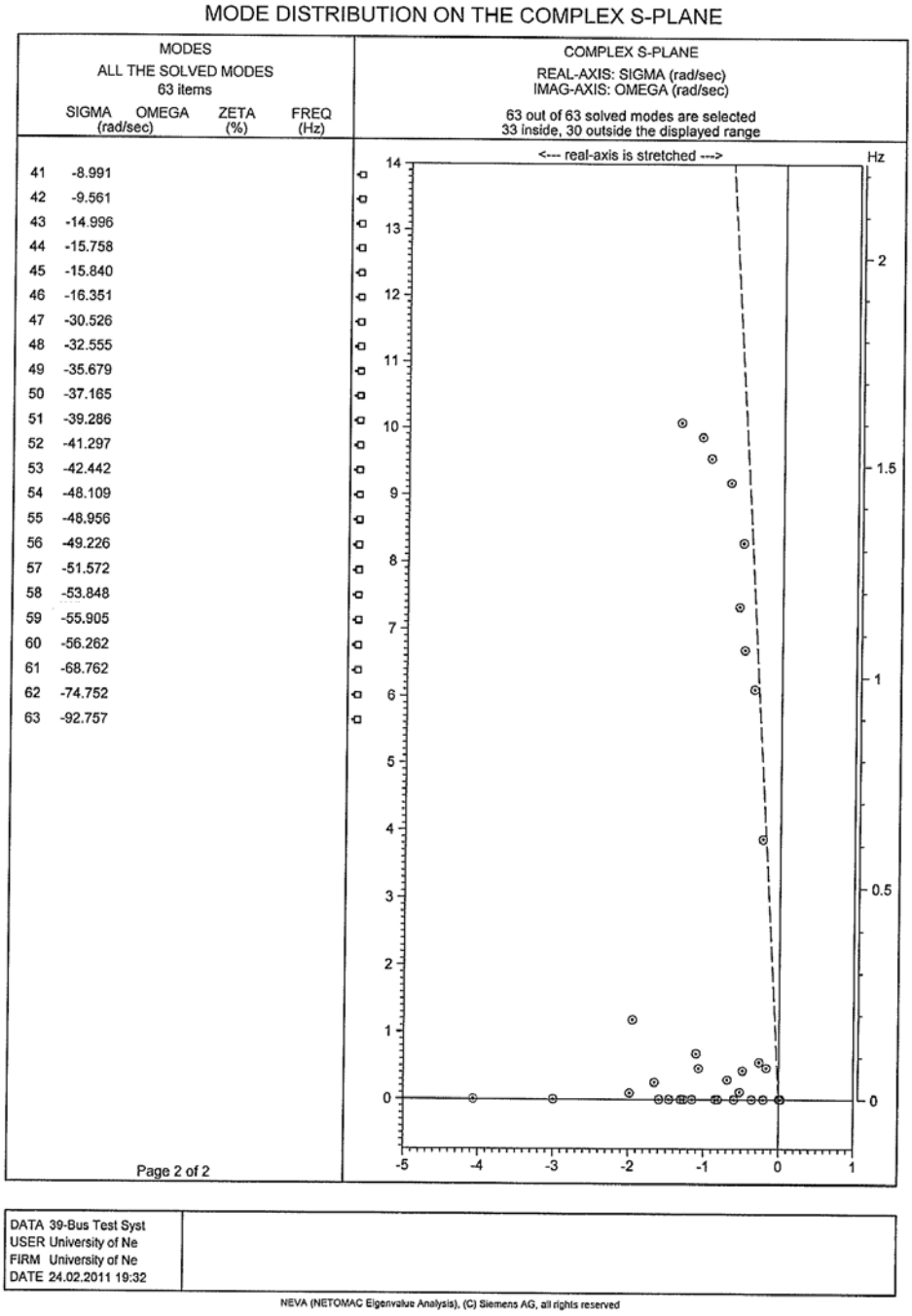

Fig 82: Modal analysis (eigenvalues) of 39 bus test system with shunt capacitor B = -1000 at load bus 28

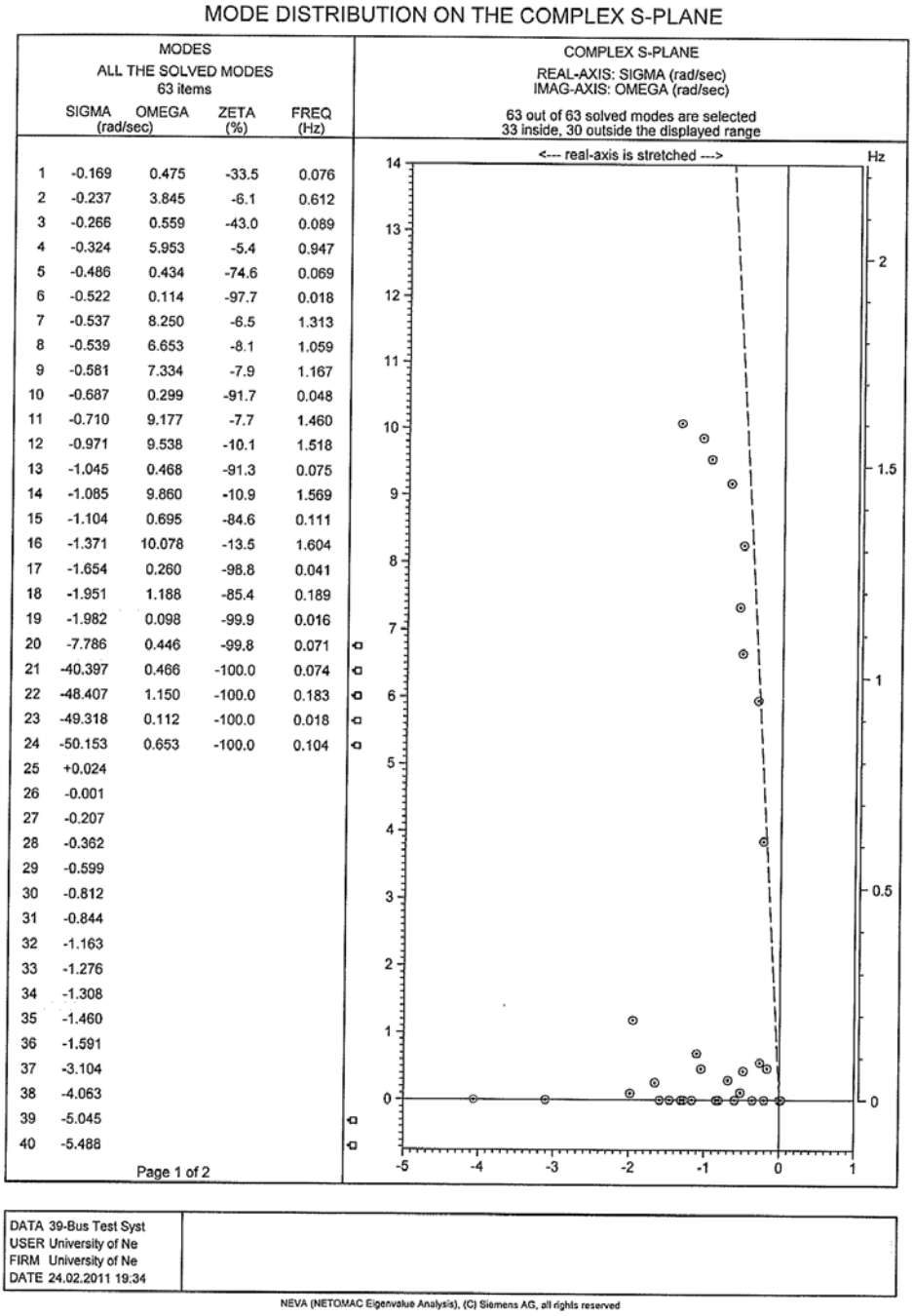

Fig 83: Modal analysis (eigenvalues) of 39 bus test system with shunt capacitor B = -1000 at load bus 29

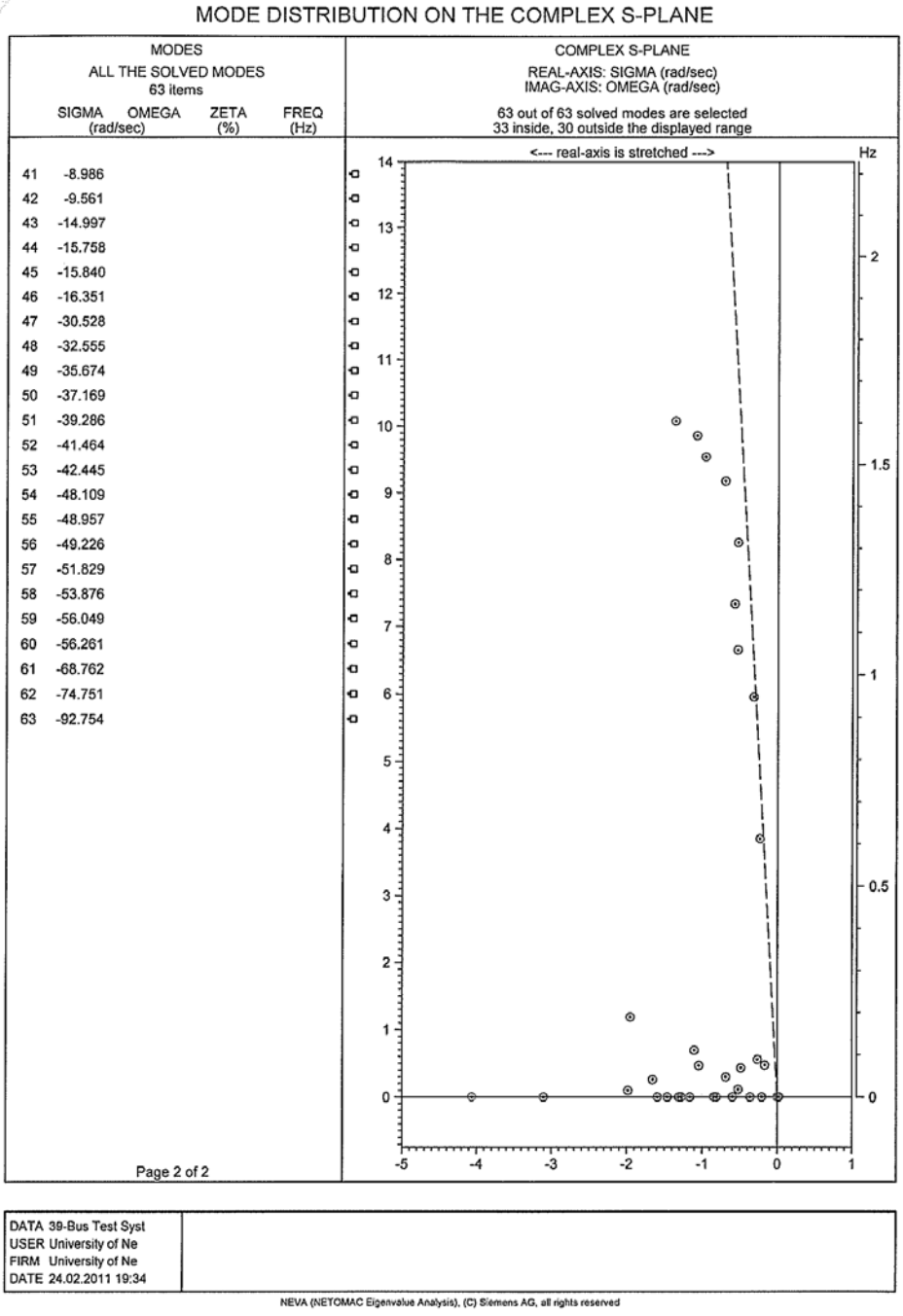

Fig 84: Modal analysis (eigenvalues) of 39 bus test system with shunt capacitor B = -1000 at load bus 29

MODE DISTRIBUTION ON THE COMPLEX S-PLANE

MODES
ALL THE SOLVED MODES
63 items

	SIGMA (rad/sec)	OMEGA (rad/sec)	ZETA (%)	FREQ (Hz)
1	-0.138	0.460	-28.8	0.073
2	-0.252	0.550	-41.6	0.088
3	-0.258	3.854	-6.7	0.613
4	-0.462	6.002	-7.7	0.955
5	-0.471	0.438	-73.2	0.070
6	-0.513	0.110	-97.8	0.018
7	-0.558	6.691	-8.3	1.065
8	-0.562	8.273	-6.8	1.317
9	-0.588	7.351	-8.0	1.170
10	-0.677	0.307	-91.1	0.049
11	-0.719	9.173	-7.8	1.460
12	-0.720	1.699	-39.0	0.270
13	-0.968	9.519	-10.1	1.515
14	-1.010	0.703	-82.1	0.112
15	-1.026	9.799	-10.4	1.560
16	-1.211	0.080	-99.8	0.013
17	-1.370	10.051	-13.5	1.600
18	-1.669	0.273	-98.7	0.043
19	-1.973	0.162	-99.7	0.026
20	-1.989	1.172	-86.2	0.186
21	-7.712	0.485	-99.8	0.077
22	-48.276	1.348	-100.0	0.215
23	-48.703	1.000	-100.0	0.159
24	-49.347	0.147	-100.0	0.023
25	+0.025			
26	-0.001			
27	-0.222			
28	-0.372			
29	-0.595			
30	-0.796			
31	-0.829			
32	-1.086			
33	-1.309			
34	-1.539			
35	-1.650			
36	-3.997			
37	-5.057			
38	-5.677			
39	-8.494			
40	-9.561			

Page 1 of 2

COMPLEX S-PLANE
REAL-AXIS: SIGMA (rad/sec)
IMAG-AXIS: OMEGA (rad/sec)
63 out of 63 solved modes are selected
32 inside, 31 outside the displayed range

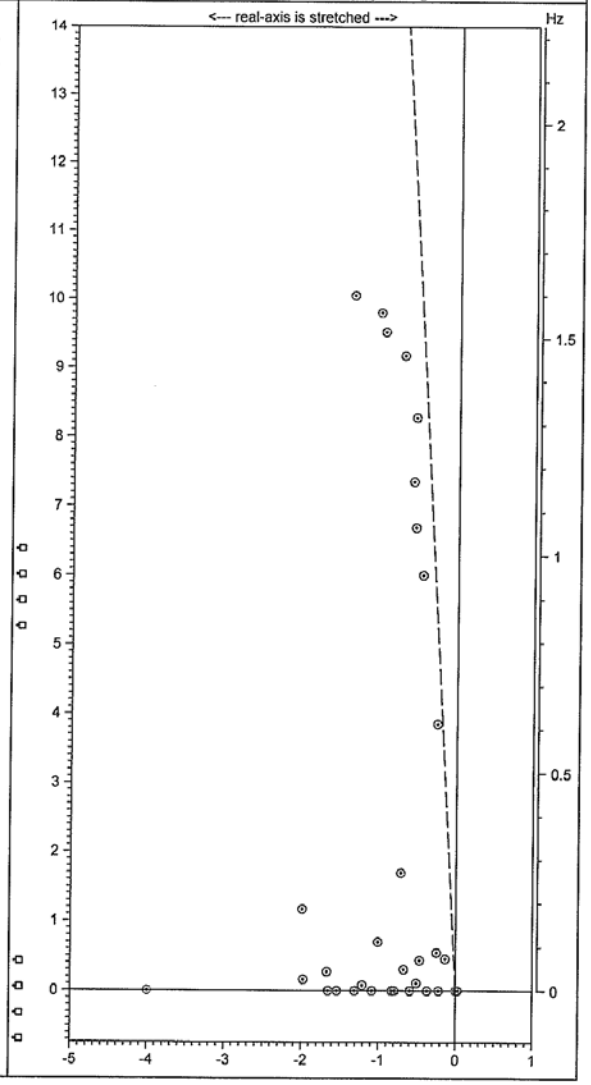

DATA 39-Bus Test Syst
USER University of Ne
FIRM University of Ne
DATE 24.02.2011 19:41

Fig 85: Modal analysis (eigenvalues) of 39 bus test system with shunt capacitor B = -1000 at load bus 39

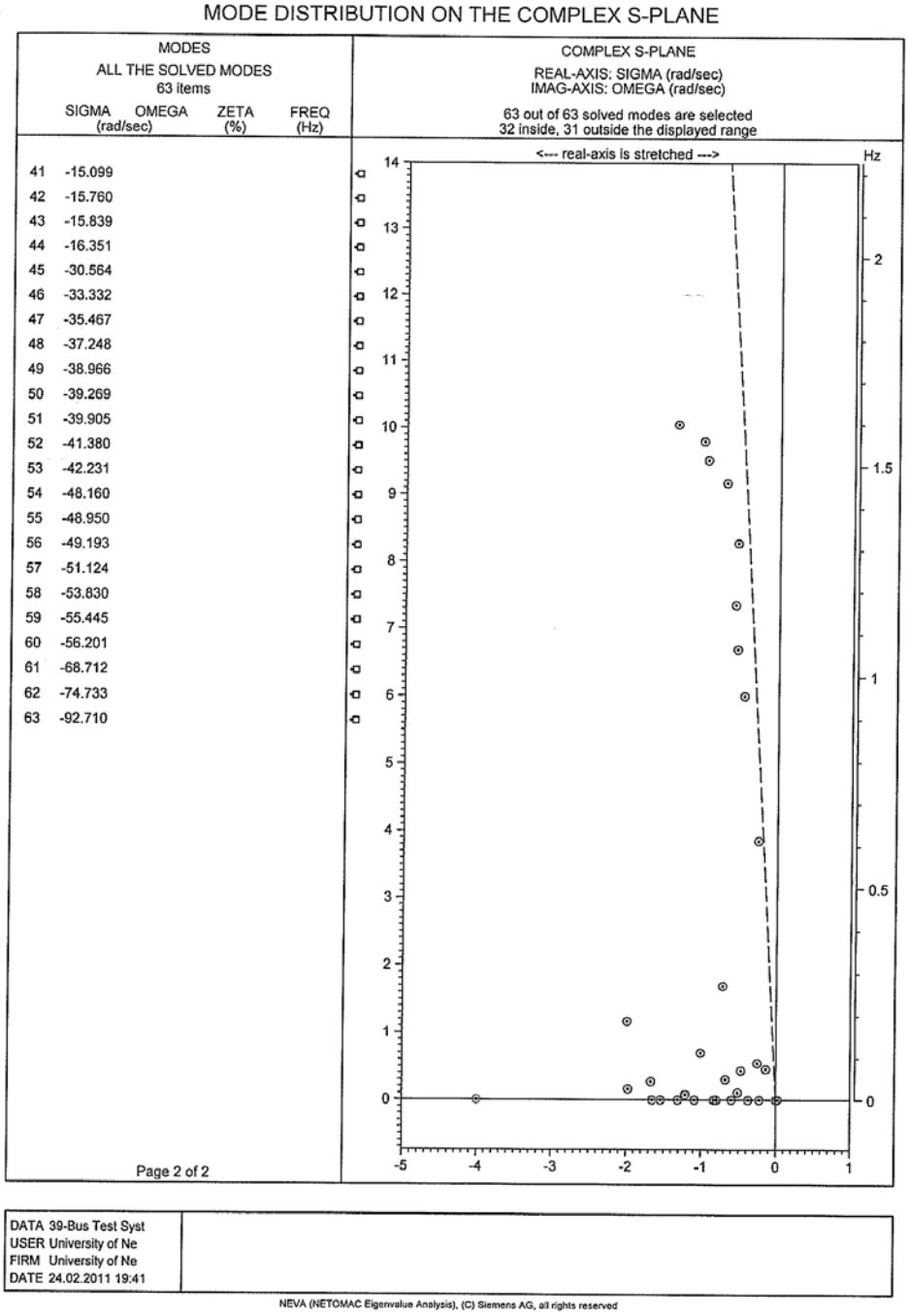

Fig 86: Modal analysis (eigenvalues) of 39 bus test system with shunt capacitor B = -1000 at load bus 39

Vita

Rogers Whitlock Jr received his Bachelor of Engineering from Southern University and A&M College in 2004. Rogers worked as an electrical engineer, associate project manager and firefighter before joining LOOP in 2010 as an electric power engineer. Rogers has been pursuing his Master's of engineering at UNO since 2008 and is doing research in the area of Power Systems Engineering with a concentration on Modal Analysis and Participation Factor Metrics. Rogers expects to graduate with his Masters in Engineering from the University of New Orleans in December 2011